TRANSCRIPTIONAL REGULATION OF GENES ASSOCIATED WITH DRUG
RESISTANCE AND GROWTH OF PANCREATIC CANCER CELLS BY MUCIN 1

by

Sritama Nath

A dissertation submitted to the faculty of
The University of North Carolina at Charlotte
in partial fulfillment of the requirements
for the degree of Doctor of Philosophy in
Biology

Charlotte

2013

<div style="margin-left:50%">

Approved by:

_____
Dr. Pinku Mukherjee

_____
Dr. Didier Dréau

_____
Dr. Valery Grdzelishvili

_____
Dr. Daniel Nelson

_____
Dr. Jennifer Weller

</div>

ABSTRACT

SRITAMA NATH. Transcriptional regulation of genes associated with drug resistance and growth of pancreatic cancer cells by Mucin1 (Under the direction of DR. PINKU MUKHERJEE)

Pancreatic ductal adenocarcinoma (PDA) is the 4th leading cause of cancer-related deaths in the US. An understanding of the molecular pathogenesis of PDA is of utmost importance to be able to improve the current or design new targeted therapies for treatment of PDA. MUC1 (CD227), a membrane tethered mucin glycoprotein is overexpressed in >60% of human pancreatic cancers and 80% of PDA and is associated with poor prognosis, enhanced metastasis, and chemoresistance in PDA. The objective of thesis was to delineate the mechanism by which MUC1 induces drug resistance, and promotes invasion and proliferation in PDA.

We report here for the first time that MUC1 contributes to drug resistance in pancreatic cancer (PC) via upregulating the expression of ABC transporters that reduces intracellular drug concentration inside the cancer cells. We found that MUC1 high PC cells exhibit increased resistance to chemotherapeutic drugs (gemcitabine and etoposide) in comparison to cells that express low levels of MUC1. This chemo resistance is attributed to the enhanced expression of multidrug resistance (MDR) genes including ABCC1, ABCC3, ABCC5 and ABCB1. In particular, levels of MRP1 protein, encoded by the ABCC1 gene is significantly higher in the MUC1-high PDA cells. In human PDA cell lines, MUC1 upregulates MRP1 via an Akt dependent pathway, whereas, in mouse cells, MUC1 mediated MRP1 upregulation is via an Akt independent mechanism. However, in both mouse and human cell lines, the cytoplasmic tail motif of MUC1 associates directly

with the promoter region of the Abcc1/ABCC1 gene, indicating a possible role of MUC1 as a transcriptional regulator of this gene. This is the first report to show that MUC1 can directly regulate the expression of MDR genes in PDA cells and thus confer drug resistance.

We also report that human and mouse PDA cell lines expressing high levels of endogenous MUC1 also express high levels of Cox-2 compared to MUC1 null cells. Further, in both mouse and human cell lines, MUC1 upregulates expression of Cox-2/COX-2 gene via an NF-kB dependent mechanism. In MUC1 positive PDA cell lines, MUC1 and NF-kB binds to the 5'UTR of Cox-2/COX-2 gene around the NFkB response element (within 500bp upstream of TSS), which is not observed in MUC1 null PDA cells. The increased expression of Cox-2 gives the MUC1 positive PDA cell lines a growth and/or invasive advantage.

Lastly, we report that MUC1 modulates TGF-β signaling axis causing TGF-β1 to act as a tumor promoter in MUC1 high cells and acting as a tumor suppressor in MUC1 null cells. The difference in TGF-β1 functioning could be partly attributed to difference in the expression profile of the TGF-βRI and TGF-βRII and activation of the downstream signaling cascades.

ACKNOWLEDGEMENTS

I would like to thank my advisor, Dr. Pinku Mukherjee for her relentless support, and encouragement during my doctoral thesis work. I am thankful to her for giving me the opportunity to be a part of her lab and also her unwavering faith in my abilities. I deeply appreciate her mentorship, for letting me pursue my research interests independently, yet providing intellectual help and guidance during the most challenging times. I would like to thank Dr. Didier Dréau, Dr. Valery Grdzelishvili, Dr. Daniel Nelson and Dr. Jennifer Weller for serving on my committee and providing me with support and feedback along the way. I would specially like to thank the past and present members of the Mukherjee lab, Dr. Jorge Schettini, Dr. Lopamudra Das Roy, Dr. Jennifer Curry, Dr. Mahnaz Sahraei, Priyanka Grover, Dr. Dahlia Besmer, Amritha Kidiyoor, Ahmed Mohammad and Emily Ashkin for their friendship and their valuable contribution to my PhD thesis work. I would also like to thank my dearest friends - Dr. Bhawana Bariar, Dr. Kaveh Daneshvar, Dr. Abid Khan, and Dr. Rita Bagwe for their endless support, encouragement and making graduate school a fun experience. I would like to thank my father Dr. Ranjit Kumar Nath, my mother Manjusri Nath, and my husband Biswajit Mazumder for their unconditional love and support. Without them I would not have been able to get this far. Lastly, I would like to thank UNCC Graduate School for the Graduate Assistant Support Plan which provided funding for my graduate education.

TABLE OF CONTENTS

LIST OF FIGURES

LIST OF TABLES

LIST OF ABBREVIATIONS

aa   amino acid

Ab   antibody

ABC   ATP binding cassette

ABCC1   ATP binding cassette C1

ABCC2   ATP binding cassette C2

ABCG2   ATP binding cassette G2

AML   acute myeloid leukemia

ANOVA   analysis of variance

Arg   arginine

BSA   bovine serum albumin

c-JUN   a protein encoded by JUN gene

COX   cyclooxygenase

COX-1   cyclooxygenase-1

COX-2   cyclooxygenase-2

cpm   counts per minute

CT   cytoplasmic tail

CT2   antibody directed against the cytoplasmic tail of muc1

ChIP   Chromatin Immunoprecipitation

CRE   cyclic AMP response element

DAB   3,3'-diaminobenzidine tetrahydrochloride hydrate

DCIS   Ductal carcinoma in-situ

DMEM   dulbecco's modified eagles medium

DMSO	dimethyl sulfoxide
DNA	deoxyribonucleic acid
EC	extracellular
ECL	enhanced chemiluminescence
EGF	epidermal growth factor
ELISA	Enzyme-linked immunosorbent assay
EMT	epithelial to mesenchymal transition
EP	prostaglandin E receptor
ERK1/2	extracellular signal regulated kinase 1/2
FBS	fetal bovine serum
h	hours
^{3}H	tritium
His	histidine
HIF-1α	hypoxia inducible factor 1α
H&E	hematoxylin and eosin
HBS	HEPES buffered saline
HMFG2	anti-milk fat globule 2 monoclonal antibody
HPDE	human pancreatic duct epithelial cell line
HRP	horse radish peroxidase
IACUC	institutional animal care and use committee
ICC	immunocytochemistry
IDO	indoleamine 2,3 dioxygenase
IFN	interferon

Ig   immunoglobulin

IHC   immunohistochemistry

Indo   indomethacin

IP   intraperitoneal

IPMN   intraductal papillary mucinous neoplasms

KC   Cre-LSL-KRAS^{G12D} mouse model of PDA

KCKO   PDA mice lacking MUC1/Muc1

KCM   PDA mice expressing MUC1

M   matrix protein

MAPK   mitogen activated protein kinase

MBD   membrane binding domain

MCN   mucinous cystic neoplasms

MDSCs   myeloid derived suppressor cells

MDR   multidrug resistance

MEM   Minimum Essential Medium

MEK   mitogen activated Erk kinase

mg   milligrams

min   minutes

MMP-9   matrix metalloproteinase

MMTV   mouse mammary tumor virus

mRNA   messenger RNA

MTAG   middle T antigen

MTT   3-(4,5-dimethyl-2-thiazolyl)-2,5-diphenyl-2H-tetrazolium bromide

MRP1   multidrug resistance protein-1

MRP2   multidrug resistance protein-2

MRP3   multidrug resistance protein-3

MRP5   multidrug resistance protein-5

MUC1   human mucin-1

MUC2   Mucin-2

MUC3   Mucin -3

MUC5   Mucin -5

MUC7   Mucin -7

Muc1   mouse mucin-1

MUC1.Tg   human MUC1 transgenic

MXR   mitoxantrone resistance protein

NBD   nuclear binding domain

NEO   transfected with neomycin empty vector

NIH   national institute of health

NFkB p65   nuclear factor kB protein 65

Nkrf   NFkB repressing factor

nm   nanlmolar

NT   nucleotide transporters

OD   optical density

P38MAPK   mitogen activated protein kinase protein 38

PanIN   pancreatic intraepithelial neoplasia

PBS   phosphate buffered saline

PCR	polymerase chain reaction
PDA	pancreatic ductal adenocarcinoma
PDGF	platelet derived growth factor
PFA	paraformaldehyde
Pgp	P-glycoprotein
PGE_2	prostoglandin E_2
PGEM	prostogladin E_2 metabolite
PI3K	phosphatidyl inositol 3 kinase
PI	phosphatidyl inositol
PIP2	phosphatidyl inositol 2 phosphate
PIP3	phosphatidyl inositol 3 phosphate
POX	peroxidase
PTS	proline/threonine/serine
Ptgs2	murine prostaglandin synthase 2
PTGS2	human prostaglandin synthase 2
Pro	proline
PVDF	polyvinylidene difluoride
PyVMT	polyoma virus middle T antigen
rm-	recombinant mouse
RNA	ribonucleic acid
RNase	ribonuclease
RT	room temperature
RT-PCR	reverse transcription polymerase chain reaction

RTK	receptor tyrosine kinase
SEA	sea urchin Enterokinase domain
SEC	secretory
Ser	serine
SDS-PAGE	sodium dodecyl sulfate polyacrylamide gel electrophoresis
SEM	standard error of the mean
SFM	serum free medium
SH2	Src homology -2
siRNA	silencing RNA
TGFβ	transforming growth factor-β
TGFβRI	transforming growth factor-β receptor I
TGFβRII	transforming growth factor-β receptor II
TM	transmembrane
TMD	transmembrane domain
TR	tandem repeat
Thr	threonine
U	units
UTR	untranslated region
μg	micrograms
VEGF	vascular endothelial growth factor
VNTR	variable number of tandem repeats
wk	week
wt	wild-type

Y   tyrosine

Y0   seven tyrosines of MUC1 CT mutated to phenylalanine

Val   valine

CHAPTER1: INTRODUCTION

1.1. Pancreas Structure and Function

Pancreas is a glandular organ which is located deep within the abdominal cavity, just below the stomach. Anatomically it is divided broadly into three regions – head, body and tail of pancreas. The head of the pancreas is situated close to the duodenum, the centrally located large body is located just below the stomach and the tail portion is located furthest from the duodenum (Figure 1.1). It is a unique organ, as it has both exocrine and endocrine glandular functions. The exocrine part of pancreas is made up of acinar cells, which secretes digestive enzymes which assist in the breakdown of carbohydrates, proteins, and lipids. The endocrine part of the pancreas is composed of cell clusters called the islet of Langerhans, which secretes hormones related to metabolism. The islet of Langerhans is made up of four main types of cells, alpha, beta, gamma (PP) and delta cells. Each of these cell types performs distinct functions. The α cells secrete glucagon, the β cells secrete insulin, the delta cells secrete somatostatin and the PP cells secrete pancreatic polypeptide, all of which are important in glucose metabolism and regulating blood glucose concentration.

The digestive enzymes and hormones secreted by pancreas are transported via the pancreatic duct, which either empties into bile duct to form the common bile duct or directly empties into the duodenum. The pancreatic ducts are lined by ductal epithelial cells which open into sac-like-structures of acinar cells (Figure 1.2).

1.2. Pancreatic Cancer

Pancreatic Cancer (PC) is a debilitating disease and is the fourth leading cause of cancer related deaths in the United States. According to SEER cancer statistics review, in 2013, an estimated 45,220 men and women will be diagnosed with pancreatic cancer and an estimated 38,460 patients will die from the disease [1], [2]. Both men and women are equally affected by this disease. The 5 year survival rate is around 3% and the median survival rate is less than 6 months [3], [4]. Despite tremendous advancement in the field of medicine and biological sciences, the mortality rate of pancreatic cancer has improved marginally over the last 40 years. This indicates that a better understanding of the incidence and progression of pancreatic cancer is much needed in order to help fight the disease.

1.3. Pancreatic Ductal Adenocarcinoma (PDA) Cellular Origin and Genetic Mutations

Greater than 95% of pancreatic cancers arise in the epithelial ductal cells of the pancreas and is designated pancreatic ductal adenocarcinoma (PDA). PDA is the most common type of pancreatic cancer and investigators use the term pancreatic cancer and PDA synonymously. It is commonly believed that PDA arises from genetic mutations in the ductal epithelial cells that line the pancreatic ducts (Figure 1.2) [3], [5]. However, there is evidence which suggests that transdifferentiated acinar cells may also contribute to PDA. The genetic mutation in K-ras is believed to be the 'early' oncogenic event that leads to the initiation and development of PDA. In addition , amplification of HER-2/Neu gene is observed in 16% of PDA patients and 9% of PDA patients are born with germline mutation in BRCA2 gene [6], [7]. As the disease progresses, the lesions in the duct accumulate more genetic mutations – such as alterations in p16, p53 and DPC4

genes [3] [5]. However, it is still not clear how these signature genetic mutations contribute to the initiation or the progression of the disease. Global genomic analysis on 24 pancreatic cancer samples indicated that the great majority of PDA cells carry on an average 63 genetic alterations, which causes dysregulation of a set of 12 core signaling pathways (Table 1.1, Fig 1.3.) [8].

1.4. Progression of PDA

Based on the pathological studies and genetic analysis of the lesions, three different preneoplastic lesions of the duct have been identified that acts as precursors of PDA. These lesions are pancreatic intraepithelial neoplasia (PanIN), intraductal papillary mucinous neoplasm (IPMN) and mucinous cystic neoplasm (MCN). Among these lesions, the PanIN lesions are most frequent and contribute to 85% of PDA. Another less frequent form of pancreatic cancer is endocrine carcinoma (PECA) or endocrine tumors which accounts for less than 2% of pancreatic malignancies. PanINs are graded into four categories based on the severity of dysplasia (1A, 1B, 2, and 3). In majority of cases, low-grade PanINs (PanINs-1A, PanINs-1B, PanINs-2) may be found in individuals without any clinical manifestation of the disease. In contrast, PanINs-3 (also referred to as in-situ carcinoma) [9] is very rarely seen in the pancreas of individuals without PDA (Figure 1.4). The normal ductal epithelial cells have a cuboidal appearance, are attached to the basement membrane and maintain polarity. In PanIN-1, cells appear elongated and they overexpress mucin. In PanIN-2, moderate nuclear atypia occurs and the cells lose polarity and detach from the basement membrane. In PanIN -3, severe nuclear atypia is observed and cluster of cells bud off into the lumen of ducts. In PanIN-4, invasive carcinoma cells start infiltrating the neighboring healthy tissue [3].

1.5. Pathology of Pancreatic Cancer

Pancreatic cancer is characterized by poorly defined edges and intense non-neoplastic desmoplastic stroma (Figure 1.5). The dense stroma provides a niche for the tumor cells to proliferate and progress into invasive metastatic cells. In addition, pancreatic cancer contains pancreatic stellate cells that are crucial for the formation, reabsorption and turnover of the stroma. Within the tumor microenvironment, autocrine and paracrine secretion of growth factors such as platelet-derived growth factor (PDGF), transforming growth factor β (TGF-β) and cytokines results in continuous interaction between the stromal and the cancer cells. In response to growth factors, the pancreatic stellate cells produce collagen fibers that form the dense stroma. Another salient feature of pancreatic cancer is poor vascularization which leads to tumor hypoxia. The role of angiogenesis in pancreatic cancer remains controversial. Although early data suggested that pancreatic cancer is angiogenesis-dependent, as are most solid tumors, treatment with inhibitors of angiogenesis has failed in patients with pancreatic cancer. Due to its dense stroma and low vascularization, pancreatic cancer is resistant to most conventional cancer therapies. However, a recent study in a mouse model showed that targeting the stromal hedgehog pathway increases tumor vascularization, resulting in increased delivery of chemotherapeutic agents to pancreatic tumors [10].

1.6. Risk Factors Associated with Pancreatic Cancer

Pancreatic cancer rarely occurs before the age of 40 [3]. In year 2006 - 2010, 2.1% of the patients diagnosed with pancreatic cancer were in the age group of 35 to 44 years, whereas, 26% of the pancreatic cancer patients belonged to the age group of 55 to 64 years. The majority of the cancer patients were of 65 years age and above. [2]. This data indicated that the risk of developing pancreatic cancer increases sharply after the age

of 50. The average age of patients diagnosed with pancreatic cancer is 71 years of age [2]. Several risk factors have been identified that is thought to play a key role in the development of the disease. Patients with a history of chronic pancreatitis, diabetes and chronic cirrhosis, are at a high risk of developing pancreatic cancer. Epidemiological studies have linked tobacco use as a major risk factor for developing pancreatic cancer [5]. Tobacco users have 2.5 to 3.6% increased likelihood of developing pancreatic cancer. Other mild risk factors include moderate intake of alcohol, caffeine, a high fat and high cholesterol diet [11], [12]. The most important risk factor of pancreatic cancer is a family history of the disease. Individuals who had primary family members being diagnosed with pancreatic cancer have a 2.3 fold higher predisposition to developing this disease [11].

1.7. Symptoms, Diagnosis and Treatments

Pancreatic cancer is one of the most lethal malignancies due to its aggressive growth and rapid development of distant metastases. Pancreatic cancer is usually asymptomatic until the disease progresses to late metastatic stage. In metastatic pancreatic cancer, the disease spreads predominantly to the liver and peritoneal cavity. Vague abdominal discomfort, nausea, dull deep upper abdominal pain, back pain and weight loss are some of the common symptoms of pancreatic cancer. Rarely, tumors in the pancreas cause duodenal obstruction or gastrointestinal bleeding [12]. Since the symptoms of pancreatic cancer are similar to the symptoms of a wide array of other diseases, the diagnosis of pancreatic cancer is often delayed until the disease has progressed to late metastatic stage. The delay in diagnosis accounts for the high mortality rate associated with pancreatic cancer.

The most widely accepted pancreatic cancer marker is CA 19-9 (a carbohydrate antigen on mucin glycoproteins) which is routinely used for monitoring the progression of the disease or recurrence of the tumor. However, due to its high non-specificity, the use of CA 19-9 for early diagnosis of pancreatic cancer is limited in clinics. A study showed that use of ICAM-1and osteoprotegerin along with CA 19-9 greatly improves the efficacy and sensitivity of the diagnostic test for pancreatic cancer [13]. CEA (carcinoembryonic antigen), CA 50, CA 242, DUPAN2, MUCIN1, MUCIN2 and MUC5AC, elastase 1 and Span-1 are some the markers that have added to the growing list of pancreatic cancer markers for their diagnostic purposes [14], [15].

Surgery is the only curative option for treatment of pancreatic cancer. The 2 year survival rate following surgery is only 20-40% and recurrence of tumor with aggressive phenotype occurs in 50% of the patients post-surgery [16]. However, majority of the pancreatic cancer patients present with grossly unresectable tumors and only a small percentage of pancreatic cancer patients (5-25%) are eligible for surgery. Hence, chemotherapy is the critical component of treatment regimen in combination with radiotherapy [12]. With the current treatment modality the median survival ranges between 9 months to 10 months. For over a decade, gemcitabine is the treatment of choice [17], [18]. Multiple new agents with diverse mechanisms of action, such as oxaliplatin, bevacizumab, cisplatin in combination with gemcitabine have been tested in randomized phase III clinical trials, with no improvement in outcome[19], [20], [21], [22]. Erlotinib (an epidermal growth factor receptor inhibitor) is the only agent which given in combination with gemcitabine produced a statistically significant improvement of survival in comparison to gemcitabine alone [18]. As of last week, FDA approved Abraxane (paclitaxel bound to albumin) for the treatment of patients with late stage

pancreatic cancer. Patients treated with Abraxane plus gemcitabine lived on average 1.8 months longer than patients who were treated with gemcitabine only [23].

1.8. Mucins: Classification, Structure and Function

Mucins are a class of modular proteins characterized by the presence of mucin domain (also called PTS domain) rich in proline/serine/ threonine amino acids [24]. Mucins are typically found on the apical surface of the glandular or luminal epithelial cells. They are high molecular weight proteins; composed of long peptide chain called 'apomucin' which is extensively modified by O-glycosylation [25]. Based on their location on the cell surface, and their biochemical structure, mucins are broadly classified into two categories: gel forming (secreted) mucins and the membrane anchored or transmembrane mucins. Altogether there are 20 members in the mucin family of proteins (Table 1. 2) [26].

1.8.1. Secreted Mucins

MUC2, MUC5AC, MUC5B, MUC6, MUC7 and MUC19 belong to the family of secreted mucins. The main function of the secreted mucins is to oligomerize and form protective mucinous gel that lubricates airways or protects the underlying epithelia from desiccation, changes in pH, pollutants, microbes etc [27], [28]. All secreted mucins contain serine/threonine rich PTS or mucin domain that is extensively O- glycosylated (Figure 1.6 A). It also contains von Willebrandt factor domain (vWF-D) and C-terminal cysteine knot domains, which allow the mucin monomers to oligomerize and form mucinous gel. MUC7 and MUC9 are smaller secreted mucins that neither oligomerize nor form gels. Most of the intestinal and airway mucins are of secreted form, with the exception of MUC1, which is a membrane bound mucin [29].

1.8.2. Membrane Bound Mucins

MUC1, MUC3A/3B, MUC4, MUC12, MUC16, MUC17, MUC21 and MUC22 are members of the membrane bound mucins [30]. The hallmark of membrane tethered mucins, is their heavily glycosylated, large extracellular domain which extends up to a remarkable distance 1500 nm from the cell surface [24]. The large number of carbohydrate side chains on the extracellular domain gives the transmembrane mucins their classic bottle-brush appearance.

Membrane bound mucins are single pass, type I transmembrane proteins, which have plethora of biological functions ranging from acting as anti-adhesive molecule to signal transduction molecule. By definition, membrane bound mucins bear serine/ threonine rich PTS domain, Sea urchin sperm protein Enterokinase (SEA) domain, a membrane spanning hydrophobic transmembrane domain (TMD) and a cytoplasmic domain (CD) or cytoplasmic tail (CT) (Figure 1.6B). The PTS, SEA domain mainly comprises the extracellular domain of the membrane tethered mucin. The PTS domain is encoded by a large intronless and highly polymorphic gene of more than 10kb size. As a result the sequence and the length of this domain vary greatly among different members of the membrane anchored mucins. Hence, this region is also called as variable number tandem repeat (VNTR) region (Figure1.7). The polymorphism of VNTR region of the membrane bound mucins add a great variety to their biological role [31] [25], [29]. VNTR region comprises of multiple copies of a sequence motif of 20 amino acids, which makes up the peptide core. In mature mucins large branches of sugar chains are added to the hydroxyl group of the serine and threonine residues of VNTR (Figure 1.6A) [24].

The conserved SEA domain acts as a cleavage site, where mucins undergo autoproteolysis within GSVVV site of SEA domain. MUC1, MUC3, MUC4, MUC16

and MUC17 bear the conserved SEA domain [31]. The autoproteolysis can occur within the cytosol or outside the cell membrane. It is thought that conformational strain induces the autoproteolysis of mucins. Additionally studies have shown that ADAM 17 (also known as TACE) and MMP1 can trigger shedding of MUC1 in response to TNF stimulation [32].

The cytoplasmic tail of mucins is also poorly conserved among different members of the membrane tethered mucins. (Table 1.3) [25]. Studies have shown that most of the membrane bound mucins such as MUC1, MUC3 and MUC4 have signaling ability, which mostly lies within the cytoplasmic domain (tail). The cytoplasmic tail of MUC1 and MUC3 has been extensively studied. This will be discussed in detail under the section, structure of mucin 1.

1.8.3. Glycosylation of Mucins

Following synthesis, the apomucins are extensively modified co-translationally or post translationally to yield the mature functional mucins. The VNTR is mostly O-glycosylated and to a lesser extent is N- glycosylated. O-glycosylation status correlates with some biological properties of mucins, whereas, N-Glycosylation is vital for their folding, sorting, and secretion.

In the sequence of addition of sugar moieties to the apomucin, N- glycosylation occurs first, which is a co-translational event. The mannose rich oligosaccharide is transferred to an acceptor asparagine residue in the tripeptide Asn-Xaa-Ser/Thr, motif on VNTR. The reaction is catalyzed by a number of enzymes belonging to N-acetylgalactoseaminyltransferase (GalNAcT) family [26][33]. The mannose-rich N-glycans undergo further modification and truncation in the Golgi apparatus [34]. About 40% of the amino acid in the VNTR comprises of serine (Ser) and threonine (Thr)

residues. In the glogi apparatus, step by step O-glycosylation occurs, where Galactose, N-acetylgalactoosamine (GalNAc), fucose, and/or sialic acid are added to the hydroxyl group of Ser and Thr residues of VNTR by GalNAc transferases [25], [35]. The sugar moieties greatly influence the overall charge, molecular weight and biological functions of the mucins [32]. In addition, glycosylation stabilizes mucins at the cell surface by preventing them from undergoing clathrin mediated endocytosis and also shields them from the proteolytic attack of the environmental enzymes[36][37][37] .

The membrane anchored mucins are eventually transported from ER lumen to the cell surface where it undergoes a series of recycling events. During recycling of the mucin through the trans-Golgi network, its sialylation increases and further changes occur in its O-glycosylation status [38]. During transit from ER lumen to the cell surface, secreted mucins oligomerize through disulfide bridges and are subsequently packaged into secretory granules. Membrane tethered mucins, are transported via trans-golgi network to the cells surface, where they are transiently expressed, until they are trafficked back to trans-golgi network to undergo further glycosylation cycles. Through the process of continued sialylation, the O-glycans of mucins gain maturation, as a consequence of which, the glycosylation pattern of secreted mucins is different from the membrane tethered mucins [38].

1.8.4. Functions of Mucins in Normal Epithelial Cells

The mucins mainly provide physiochemical protection from several adverse environmental conditions. The secreted mucins form mucinous gel around the apical surface of the epithelial cells, which protects them from dessication, changes in pH, entry of microbes etc. It is also thought that mucins act as stress sensor molecules. In normal conditions, mucins sequester growth factors, chemokines and inflammatory cytokines,

such as EGF, TGF-α, IL-1, TNF-α, IL-4, IL-6, IL-9 and IL-13. However, during breach of the physicochemical barrier, release of the mucin ectodomains causes release of the sequestered factors which now sends off warning signal by triggering inflammation. It is also thought that conformational changes or changes in the ligand status caused by the release of mucin ectodomain triggers activation of the signaling axis of mucins (Figure 1.8) [39].

1.9. Structure of Mucin 1 (MUC1)

Mucin 1 (MUC1), a polymorphic, type I transmembrane glycoprotein is normally expressed at the apical surface of the glandular or luminal epithelial cells and to some lesser extent in hematopoietic cells [40][41]. MUC1 is mostly found in the pulmonary tracts, intestinal linings, mammary glands, pancreas and female reproductive tract. It is also referred to as episialin, PEM, H23Ag, EMA, CA15–3, MCA [42]. The gene encoding MUC1 is located on the long arm (q) of chromosome 1 at position 21, a region which is frequently altered in breast cancer cells [43]. The MUC1 gene is encoded as a single polypeptide chain. Immediately after translation, conformational stress causes breakage of the MUC1 polypeptide chain into two subunits of varying sizes – the longer N terminal and the shorter C-terminal subunits (Figure 1.9). The autoproteolysis occurs at GSVVV site which lies within the SEA domain between the N-terminal and C-terminal subunits [24], [44] (Figure 1.10). The two subunits remain non-covalently associated through hydrogen bonds and are exported to the surface of the cell. The exact functional significance of the autoproteolysis still remains to be elucidated. It is believed that autoproteolysis allows rapid shedding of the extracellular domain of MUC1 in response to stress, which forms a protective barrier around the epithelial cells to protect the cells from environmental insults.

The N-terminal subunit of MUC1 is mainly extracellular and it comprises of PTS domain and SEA domain. The 20 amino acids repeats in the VNTR vary from 40-60 in numbers depending upon allelic polymorphism. Unlike human MUC1, the mouse Muc1 does not have variable number tandem repeat. The N-terminal consists of 16 tandem repeats of 20-21 amino acids [45]. The serine and threonine residues of VNTR are extensively modified by O-glycosylation, along with moderate N- glycosylation on five sites C-terminal to the VNTR region [40]. Glycosylation of MUC1 occurs in the Golgi complex and contributes 50-90% of the total weight of the protein. MUC1 expressed by different tissues have similar peptide core, but they differ in the number of tandem repeats and in the glycosylation pattern. Tissue specific glycosylation pattern of MUC1 depends upon the expression profile of the glycosyltransferases in those tissues [24]. Thus, MUC1 can weigh between 250-500KDa based on the presence of the number of repeats and the extent of glycosylation. In normal epithelial cells, MUC1 is heavily glycosylated and the peptide core is masked by the sugar moieties. But in cancer cells, MUC1 is undersglycosylated, which reveals the peptide core [46]. The unmasked peptide backbone of tumor associated MUC1 behaves as a strong immnodominant peptide.

In contrast to the long N-terminal domain, the C-terminal domain of MUC1 is rather short. The C-terminal subunit mainly comprises of 53 amino acids long SEA domain, 28 amino acids long single pass transmembrane (TM) domain and 72 amino acids long cytoplasmic tail (CT). The N-terminal and C-terminal subunit are linked by non-covalent bonds at the GSVVV motif. The cytoplasmic tail of MUC1 weighs around 23 - 25KDa, which is further cleaved by TACE/ADAM17 or MT1/MMP to generate a shorter peptide with a molecular mass of 15-17KDa (Figure 1.11) [47]. The cytoplasmic tail of MUC1 contains a CQC motif. MUC1 monomers associate at CQC motif to

generate functional homodimers, which translocates to the nucleus and participates in regulation of gene expression. The cytoplasmic tail of MUC1 contains phosphorylated tyrosine and serine residues, which acts as docking sites for certain signaling molecules and thus participates in cell signaling cascades (Figure 1.12). The TM domain and six of the seven tyrosine residues of MUC1 CT are highly conserved (88% and 100% identical respectively) among different species of mammals suggesting important functional roles [24]. Phosphorylated tyrosine 20 and tyrosine 60 of the cytoplasmic tail of MUC1 binds to adaptor protein complex 2 and Grb2, which facilitates clathrin mediated endocytosis of MUC1. Studies have shown that Cys-palmitoylation of the CQC motif is necessary for reentry of MUC1 in the secretory pathway [48][49]. During subsequent recycling, MUC1 glycosylation undergoes remodeling from Core 2 to core-1O-glycan [50].

1.10. Alternative Splice Variants of MUC1

In addition to full length membrane tethered MUC1; there have been undisputable reports about presence of MUC1 isoforms, which are preferentially expressed in tissue specific manner. Alternative splicing event generates truncated variants of MUC1 mRNA that lacks either the extracellular or cytoplasmic domain of MUC1. Till date 9 isoforms of MUC1 have been reported. MUC1 Y contains all the domains except the VNTR region [51]. It is expressed in high levels in breast, ovarian and prostate cancer cells [52], [53]. MUC1/X and MUC1/Z similarly lacks the VNTR region, but are 18 amino acids longer than MUC1/Y splice variant [40]. MUC1/SEC, which lacks the hydrophobic TM domain and the cytoplasmic domain, is secreted from cell and acts as a binding partner for MUC1/Y. Interaction of MUC1/SEC with MUC1Y results in the phosphorylation of tyrosine residues of MUC1/Y. Presently; there is a lack of clear understanding of the functional significance of the various splice variants of MUC1.

1.11. Expression of Mucins in Normal Pancreas and in Pancreatic Cancer

Normal pancreatic epithelial cells express fully glycosylated form of membrane anchored MUC1 and secreted MUC5B. In addition, moderate expression of MUC2 and MUC6, and rare expression MUC5A and MUC5C are observed in these cells [9]. An aberrantly glycosylated form of MUC1 is overexpressed in ~ 80% of PDA (Figure1.13). In addition, MUC4, which is usually absent in normal pancreas, is expressed by PDA cells at PanIN 1 lesion and its expression gradually increases as the disease progresses. PanIN3 is characterized by strong expression of MUC1, MUC3 and MUC4. There are no reports of MUC17 expression at PanIN stage, but its overexpression is observed in pancreatic tumor cell lines and in tumor samples. MUC5A and MUC5C which are not expressed in healthy pancreas are neoexpressed in PanIN1 lesions (70% of cases) and its expression reaches 85% in adenocarcinoma. MUC6 expression peaks in PanIN1A (74%) and then decreases during carcinogenetic progression (35% of PDA). Thus, the expression profile of mucins alter at different stages of PDA [40].

Over the recent years, a large body of evidence has been gathered that indicates the role of membrane tethered mucins, especially MUC1, MUC4 and MUC16 in the progression of cancer. In clinics, MUC1 (CA15-3) and MUC16 (CA125) are used as biomarkers for detection of breast and ovarian cancers [24], [54]. Among the membrane tethered mucins, MUC1 is the most thoroughly studied mucin in context of cancer progression. A clear relationship has been established between changes in the expression and glycosylation pattern of MUC1, and the progression of cancer; especially in breast, lung, colon, pancreas and prostate cancer.

1.12. Regulation of MUC1 Gene Expression

Over expression of MUC1 in cancer cells is caused due to an increase in the gene dosage and an increase in the level of transcription of MUC1 gene [55]. Pro-inflammatory cytokines, interferons, prolactin, steroid hormones, TNF-α and PMA stimulate MUC1 gene expression via activation of STAT transcription factors [56]. MUC1 gene promoter contains several cis-elements such as Sp1, AP1-4, NF-1, NFκB, an E-box, GC boxes, and estrogen and progesterone receptor sites [40].

1.13. Role of MUC1 in Cancer

Research over the last decade has brought tremendous insights into the structure, function and role of MUC1 in the pathogenesis of cancer. Tumor associated MUC1 differs from MUC1 expressed in normal cells, both in their biochemical features and cellular distribution. In normal glandular or luminal epithelial cells, MUC1 is expressed at normal levels and is confined to the apical surface of the cells. But in carcinoma cells, MUC1 is overexpressed and loss of cell polarity causes MUC1 to be distributed all over the cell surface and also in the cytoplasm [40]. Lack of cell polarity in cancer cells also causes re-distribution of growth factors all over the cell surface, which otherwise in normal epithelial cells remain confined to the basal surface (Figure 1.14). Growth factors situated in close proximity of MUC1 phosphorylates 18 potential motifs (serine and tyrosine residues) on MUC1 CT and there by activates it. The phosphorylated MUC1 CT acts as docking site for binding other kinases and components of cell signaling cascades, such as Erk1/2, P13K/Akt, Wnt and are likely to regulate the activation status of these pathways. Hence, MUC1 positive cancer cells of pancreas, breast, lung and colon origin, commonly display hyperactivation of these pathways [57] [58][59][60]. In addition, MUC1 CT interacts with several transcription factors and redirects them to their target

genes. Several studies have indicated that MUC1 plays a critical role in the transcriptional regulation of genes that are related to invasion, metastasis, angiogenesis, proliferation, apoptosis, drug resistance, inflammation and immune regulation [28], [57], [61], [62], [63], [64], [65] [66]. Studies on mouse models of human pancreatic and breast cancer provides evidence that supports the importance of MUC1 in the progression of cancer. Muc1$^{-/-}$ mice expressing high levels of polyomavirus middle T antigen in the mammary gland spontaneously develop breast cancer, but they display a profound delay in the progression and metastatic spread of breast cancer to lungs in comparison to Muc1$^{+/+}$ mice [67]. A similar study performed in a mouse model of PDA that spontaneously develop pancreatic cancer showed that mice null for Muc1 (KCKO) show delayed tumor progression and metastasis compared to mice expressing mouse Muc1(KC) or human MUC1(KCM) [58].

1.13.1. Role of MUC1 in Tumor Growth

Early studies in various tumor cell lines revealed that MUC1 plays a crucial role in tumor growth and survival. MUC1 induces production of growth factors such as CTGF and PDGF-A, PDGF-B, which promotes activation of MAPK and PI3K/Akt pathways in MUC1 positive cells and thereby potentiate proliferation and survival of tumor cells [58], [61], [68]. Upon EGF stimulation, MUC1 directly associates with EGFR, translocate to the nucleus and binds to the promoter of CCND1 and MYBL2 gene, which allows the expression of G1/S phase genes [69]. Another study showed that upon PDGF-A stimulation, activated MUC1 associates with HIF-1α and upregulates the expression of PDGF-A, leading to increased proliferation and invasion of PDA cells [63]. These observations are recapitulated nicely in a study on mouse model of human PDA [58].

1.13.2. Role of MUC1 in Invasion and Metastasis

During the progression of cancer from carcinoma in-situ to metastatic disease, the tumor cells acquire invasive and metastatic potential. Invasion causes destruction of the tissues, and prevents normal organ functioning, whereas metastasis allows systemic dissemination of malignant cells and formation of secondary tumors. Cancer patients presenting locally advanced or metastatic disease are difficult to treat as surgical resection of tumors is not enough for cure. Thus, metastasis is the most life threatening aspects of cancer and accounts for 95% of death in pancreatic cancer patients [4], [70].

Invasion is an early and prerequisite step to metastasis. Invasion comprises of a cohort of biochemical events that allow the cancer cells to detach from the basement membrane, degrade the surrounding matrix and invade into the neighboring tissues or enter bloodstream [71]. Recently, a new concept emerged called EMT – epithelial to mesenchymal transition, to support the biological process by which cancer cells acquire invasive potential. In normal epithelial tissue, intracellular adhesion junctions, such as adherens, tight junctions and desmosomes maintain the integrity of epithelial cell layers, cell polarity and spatially confine the signaling molecules. Tight junctions, positioned apically define the segregation between the apical and basolateral surfaces of the epithelial cells. Whereas, adheren junctions, located directly below the tight junctions maintain cell to cell contact via cadherin molecules. During EMT the junctional complexes are weakened, followed by loss of apico-basal polarity and contact with basement membrane, finally leading to acquisition of invasive properties (Figure 1.15).

Classical cadherin junctions constitute a basic complex formed by the association of cadherin molecules with α-, β- and p120 catenins. β-catenin bridges the gap between cell surface and the actin cytoskeleton through α-catenin, which gives β-catenin the

ability to induce changes in the cytoskeletal architecture in response to extracellular signals or perturbed junctional assembly [46]. In normal epithelial cells, MUC1 is localized to the apical surface, adheren junctions to the lateral surface and growth factors to the basal surface of the cells. However, stress induced loss of apico-basal polarity of cancer cells causes MUC1 to be redistributed all over the surface of cancer cells. As a result, MUC1 is found in close vicinity of adheren junctions and growth factors [24]. Studies have shown that the cytoplasmic tail of MUC1 associates with β-catenin, translocates to the nucleus and repress expression of the E-CADHERIN gene and upregulates expression of the EMT inducers- Snail, Slug, Vimentin and Twist [62] [72]. As a consequence, the adheren junctions are destabilized and profound cytoskeleton rearrangement occurs, which makes the cancer cells to lose cell- cell contact and invade the basement membrane (Figure 1.9). PDGF-BB stimulation promotes nuclear localization of MUC1-β catenin transcriptional complex, which results in increased invasiveness of PDA cells [73]. Studies evaluating the relationship between MUC1 overexpression and metastasis or prognosis on clinical samples have shown that MUC1 overexpression leads to metastasis and poor prognosis of pancreas, gall bladder and colon cancer [74], [75], [76].

After the tumor cells have left the site of primary tumor and are in circulation, the migrating cancer cell binds to endothelial cells, extravasate and form secondary tumors at distant sites. The peptide core of underglycosylated MUC1 expressed on tumor cells, acts as ligands to cell adhesion molecules such as I-CAM, E-selectin and SIGLECS (sialic acid binding immunoglobulin superfamily lectins) expressed on endothelial cells, and thereby aids the tumor cells to reestablish secondary tumors (Figure 1.16) [39].

1.13.3. Role of MUC1 in Angiogenesis

Unregulated cellular proliferation leads to formation of cellular mass that extend beyond the normal vasculature. This leads to deprivation of nutrients and oxygen within the tumor mass. However, the proliferating tumor cells, adapt to survive amidst low nutrient and oxygen environment (hypoxia) by promoting formation of new blood vessels within the tumor. Hypoxia-inducible factor 1α (HIF-1α), an oxygen sensing molecule is the key mediator of cellular responses under oxidative stress (hypoxia). HIF-1α is constitutively expressed and is stable for less than 5 minutes under normaxic conditions. The stability of HIF-1α is dependent upon the intracellular abundance of prolyl hydroxylase (PHD) and its activity. At normaxic conditions (O_2 more than 5%), PHD hydroxylates HIF-1α at Pro-402 and Pro-564 and marks it for ubiquitination and subsequent proteosomal degradation. During oxidative stress, the elevated ROS level attenuates PHD activity and thereby increases stability of HIF-1α [77]. There are around 70 genes that are under transcriptional regulation of HIF-1α [78], [79]. Activated HIF-1α induces expression of pro-angiogenic factors, such as vascular endothelial growth factor-A (VEGF-A) and platelet-derived growth factor-B (PDGF-B), which promotes tube formation in endothelial cells and synthesis of new blood vessels within the tumor [80]. In addition, HIF-1α regulates the expression of enzymes involved in glycolytic pathway, which is the preferred metabolic pathway in   proliferating cancer cells [78].

The signaling and transcriptional role of MUC1 is critical for mediating HIF-1α angiogenesis in cancer. A recent finding demonstrated that, MUC1 overexpression in breast cancer cells promote the synthesis and secretion of vascular endothelial growth factor (VEGF) through the AKT signaling pathway [81]. Recently, we showed that MUC1 in association with HIF-1α drives the expression of PDGF-A in PDA cells.

MUC1 gene itself is under regulation of HIF-1α. In pancreatic cancer and renal carcinoma cells, HIF-1α binds to the promoter of the MUC1 gene and drives its expression. MUC1 in turn drives transcriptionally upregulates the expression of CTGF gene by binding to its promoter through β-catenin and p53 [64]. MUC1 induced pro-angiogenic factors not only stimulates angiogenesis but also promotes migratory and invasive properties of cancer cells [63], [82], [83].

1.13.4. Role of MUC1 in Resistance to Apoptosis

Apoptosis or programmed cell death is a key mechanism by which physiological growth is regulated and tissue homeostasis is maintained. Most of the anti-cancer treatments such as chemotherapy, radiotherapy, gene therapy and immunotherapy work through induction of apoptosis in cancer cells. However, most of the cancer cells have defects in the apoptotic pathway and therefore do not respond well to these anti-cancer treatments. MUC1 is one such molecule that aids cancer cells to evade cell death via blocking activation of intrinsic apoptotic pathway. In rat fibroblasts 3Y1, overexpression of MUC1 interferes with activation of apoptosis via selectively upregulating the expression of anti-apoptotic protein Bcl-xL and inactivating the pro-apoptotic protein Bad via phosphophorylating it [68]. Reactive oxygen species activates apoptotic pathways in hypoxic cells. However, it has been reported that MUC1 decreases intracellular ROS concentration by upregulating expression of catalase. Another study in colon cancer cell reported that MUC1 induced decrease in intracellular ROS concentration reduces PHD-3 activity and thereby suppress HIF-1α stability. Thus, MUC1 blocks hypoxia induced cell death in colon cancer cells [84].
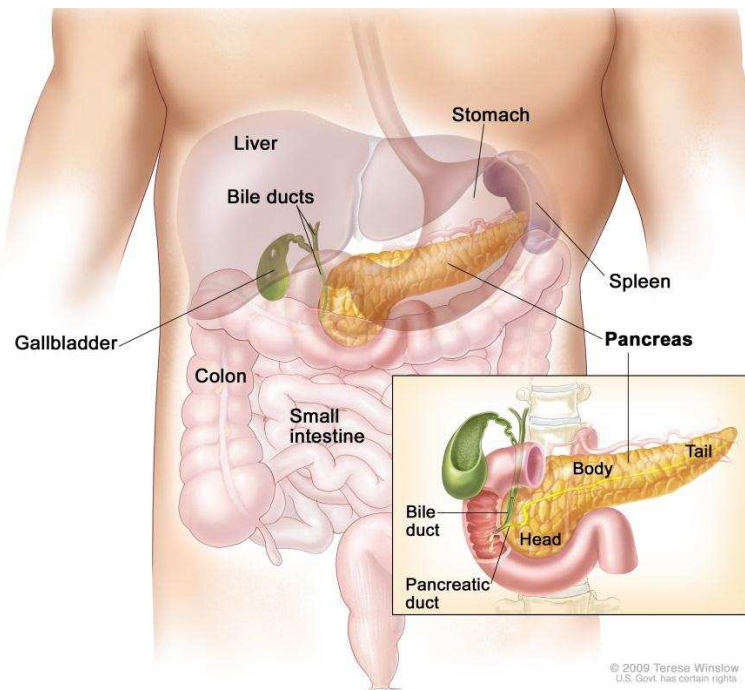
Figure 1.1.Anatomical position of pancreas within the human body. [85]
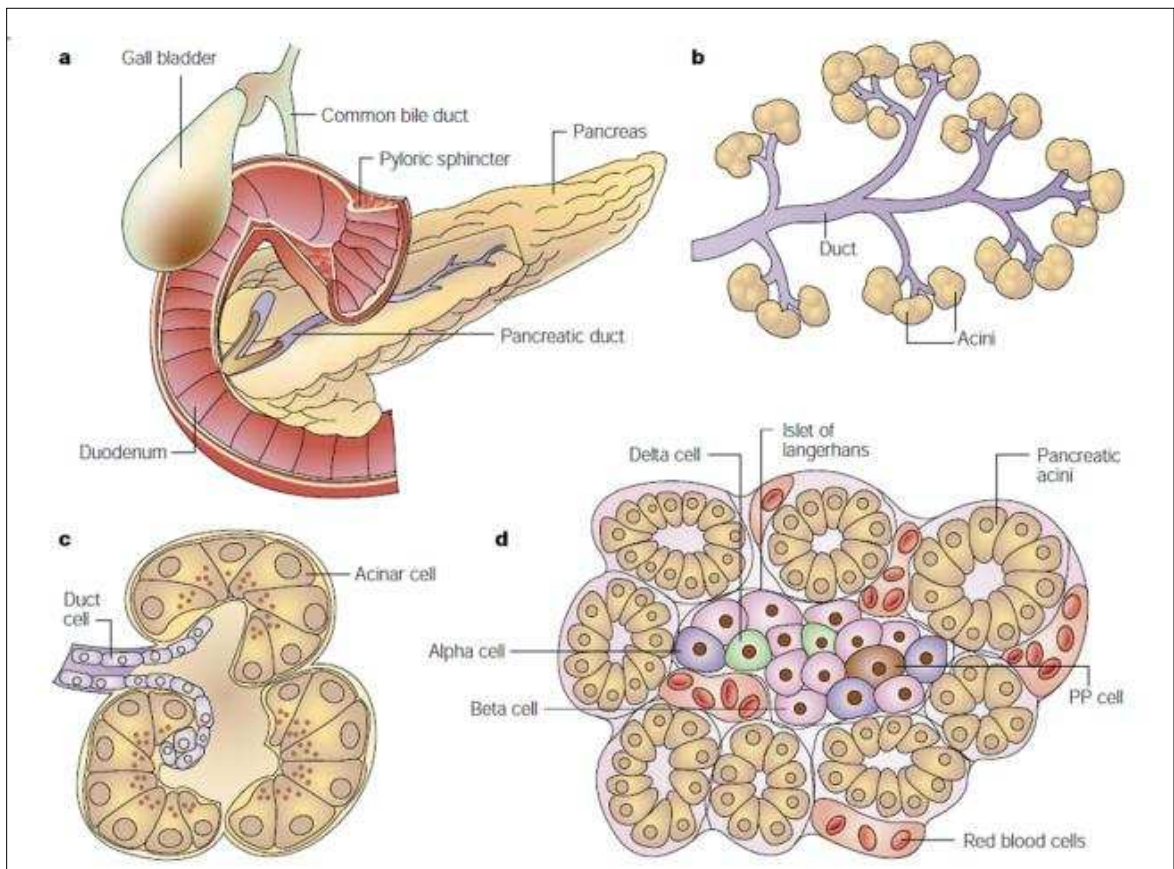
Figure 1.2. Pancreas structure and the pancreatic cancer: (a) The pancreatic ducts empties either directly into the duodenum or through common bile duct. (b), (c) The pancreatic duct opens to sac like structures formed by acinar cells. (d) The Islets of Langerhans are found interspersed within acinar cells. Islets of Langerhans are made up of alpha, beta, gamma (PP) and delta cells. Figure adapted from [3].
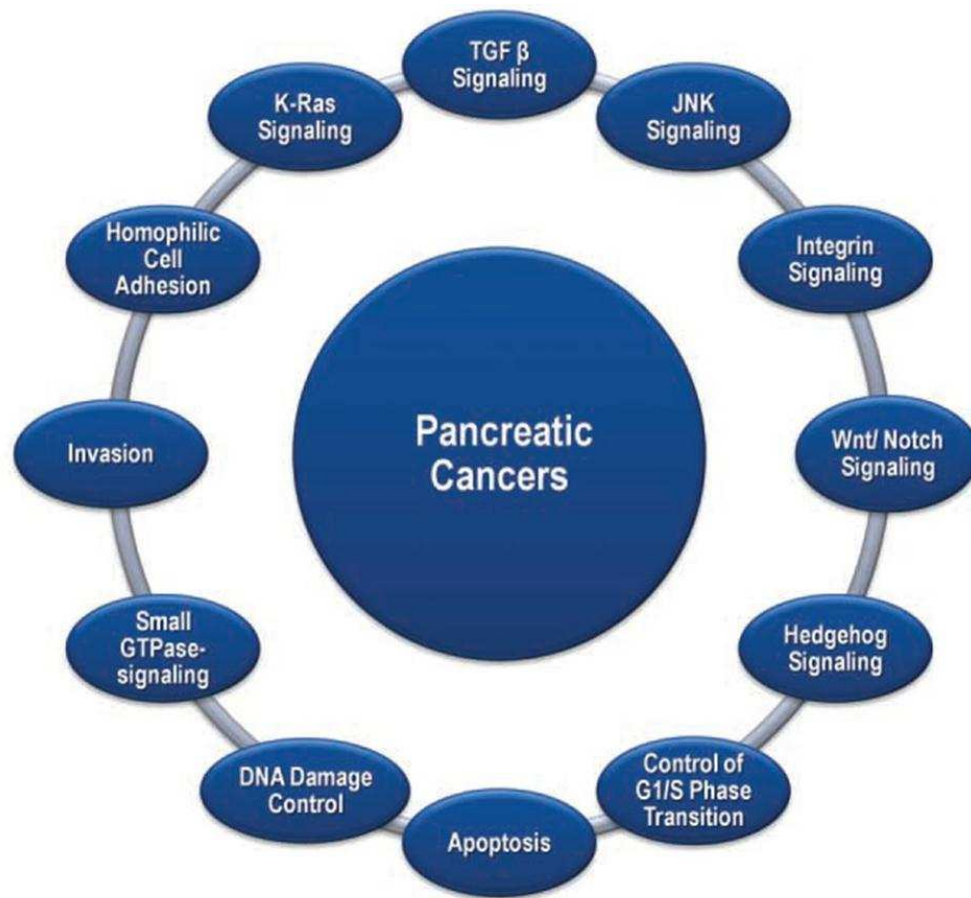
Figure 1.3. Core signaling pathways mutated in PC: The chart displays12 core signaling pathways, whose component genes are genetically modified in most pancreatic cancers [8].

Table 1.1. A complete listing of the gene sets defining these signaling pathways and processes that are mutated [8].

Regulatory process or pathway	Number of genetically altered genes detected	Fraction of tumors with genetic alteration of at least one of the genes	Representative altered genes
Apoptosis	9	100%	CASP10, VCP, CAD, HIP1
DNA damage control	9	83%	ERCC4, ERCC6, EP300, RANBP2, TP53
Regulation of G$_1$/S phase transition	19	100%	CDKN2A, FBXW7, CHD1, APC2
Hedgehog signaling	19	100%	TBX5, SOX3, LRP2, GLI1, GLI3, BOC, BMPR2, CREBBP
Homophilic cell adhesion	30	79%	CDH1, CDH10, CDH2, CDH7, FAT, PCDH15, PCDH17, PCDH18, PCDH9, PCDHB16, PCDHB2, PCDHGA1, PCDHGA11, PCDHGC4
Integrin signaling	24	67%	ITGA4, ITGA9, ITGA11, LAMA1, LAMA4, LAMA5, FN1, ILK
c-Jun N-terminal kinase signaling	9	96%	MAP4K3, TNF, ATF2, NFATC3
KRAS signaling	5	100%	KRAS, MAP2K4, RASGRP3
Regulation of invasion	46	92%	ADAM11, ADAM12, ADAM19, ADAM5220, ADAMTS15, DPP6, MEP1A, PCSK6, APG4A, PRSS23
Small GTPase–dependent signaling (other than KRAS)	33	79%	AGHGEF7, ARHGEF9, CDC42BPA, DEPDC2, PLCB3, PLCB4, RP1, PLXNB1, PRKCG
TGF-β signaling	37	100%	TGFBR2, BMPR2, SMAD4, SMAD3
Wnt/Notch signaling	29	100%	MYC, PPP2R3A, WNT9A, MAP2,TSC2, GATA6, TCF4
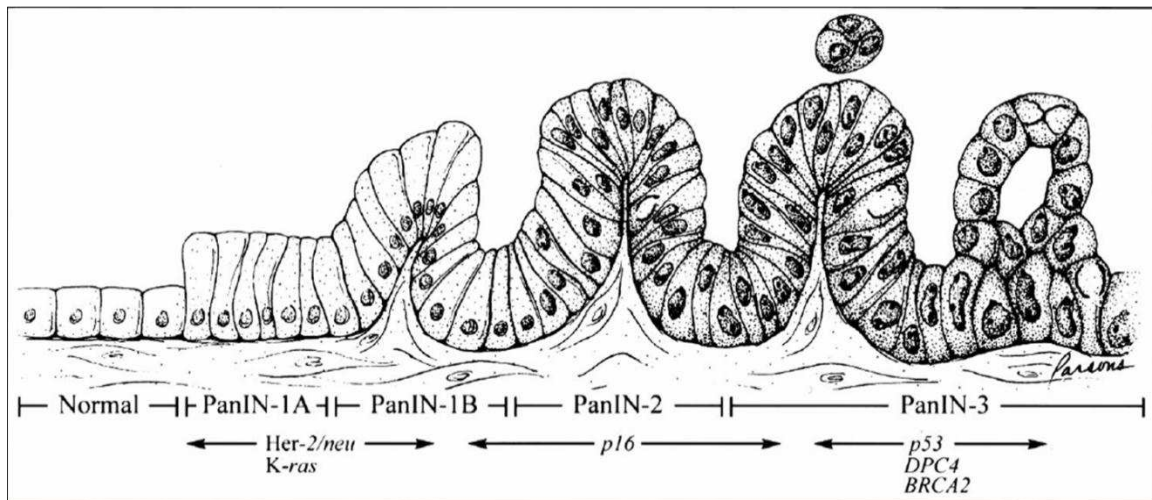
Figure 1.4. Progression model for pancreatic cancer: The normal pancreatic ductal epithelial cells undergo phenotypic changes and progresses into invasive cancer cells. Based on the cytological atypia of the lesions, PanINs are graded into three categories - PanIN 1A, PanIN 1B, PanIN 2 and PanIN 3. The signature genetic mutations that are commonly observed in the PanIN lesions are point mutation in K-ras gene, and homozygous deletion of p16, p53, DPC4 and BRCA2 genes. Figure adapted from [5].
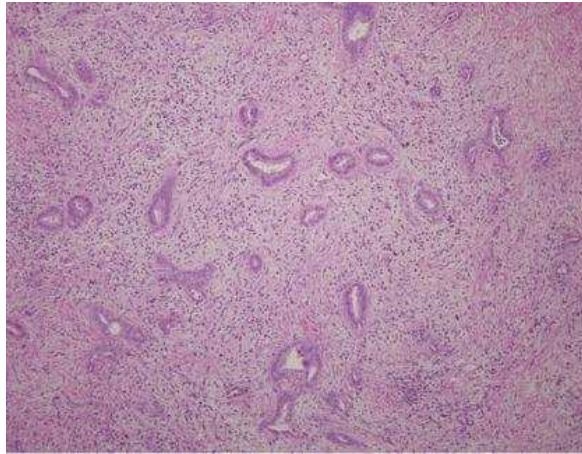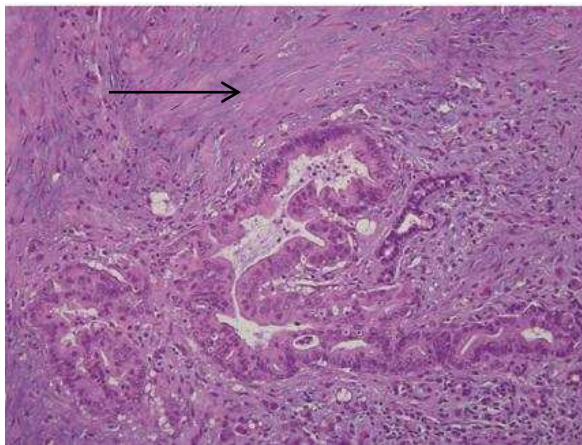
Figure 1.5. Hematoxylin and eosin staining of PanIN lesions and stromal cells in human PDA specimens: (a) Adenocarcinoma marked by haphazard arrangement of the glands and the associated non-neoplastic desmoplastic stroma.(b) At higher magnification - the desmoplastic stroma (black solid arrow) and the marked pleomorphism in the cancerous duct [11].

Table 1.2: Members of the mucin family of proteins and their cellular location. Table adapted from [26].

Human mucin	Approved name
MUC1	Mucin 1, cell surface associated
MUC2	Mucin 2, oligomeric mucus/gel-forming
MUC3/17	Mucin 17, cell surface associated
MUC3A	Mucin 3A, cell surface associated
MUC3B	Mucin 3B, cell surface associated
MUC4	Mucin 4, cell surface associated
MUC5AC	Mucin 5AC, oligomeric mucus/gel-forming
MUC5B	Mucin 5B, oligomeric mucus/gel-forming
MUC6	Mucin 6, oligomeric mucus/gel-forming
MUC7	Mucin 7, secreted
MUC8	Mucin 8
MUC9	Oviductal glycoprotein 1, 120 kDa (mucin 9, oviductin)
MUC10	Record discontinued
MUC11	Withdrawn and substituted by MUC12
MUC12	Mucin 12, cell surface associated
MUC13	Mucin 13, cell surface associated
MUC14	EMCN, endomucin
MUC15	Mucin 15, cell surface associated
MUC16	Mucin 16, cell surface associated
MUC18	MCAM, melanoma cell adhesion molecule
MUC19	Mucin 19, oligomeric
MUC20	Mucin 20, cell surface associated
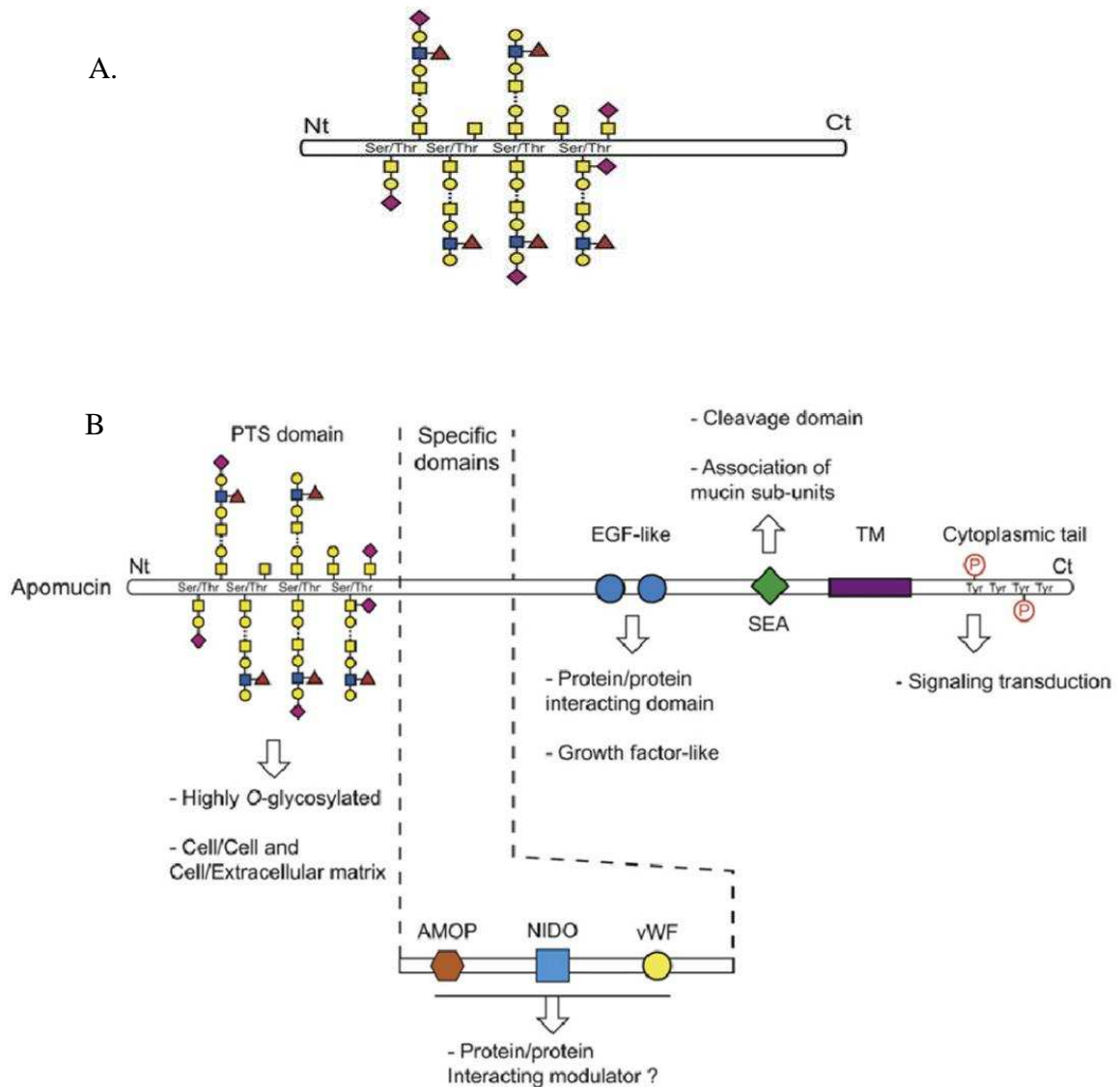
Figure 1.6. Schematic representation of the general structure of mucins: A. Secreted mucins contain Ser/Thr rich PTS domainand cytoplasmic tail.B. All membrane anchored mucin containing conserved PTS domain (VNTR), EGF like domin, enterokinase, and agrin (SEA) domain, transmembrane domain (TMD) and cytoplasmic tail. MUC4 exclusively contains the AMOP, NIDO and vWF domains but lacks SEA domain. The apoprotein is extensily O-glycosylated in both secreted and membrane anchored mucins[25].
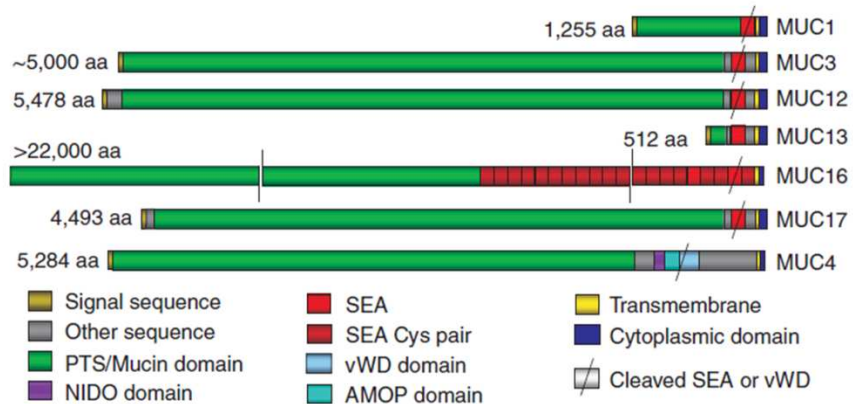
Figure 1.7. Schematic representation of the viable length of PTS domain among different types of human membrane bound mucins. The PTS domain is highly polymorphic among the different members of the membrane bound mucins as indicated by the green bar. MUC4 lacks SEA domain but contains von-Williebrand (vWF-D) domain [31].

Table 1.3. Sequence of the cytoplasmic tail of the various members of membrane bound mucins: The cytoplasmic tails of membrane tethered mucins are poorly conserved. The size and sequence vary greatly between the various members of the mucins. The tyrosine residue(s) in the cytoplasmic tail of mucins is (are) phosphorylated, which acts a potential docking site for cell signaling molecules [47].

Sequence and functions of the cytoplasmic tails of membrane-bound mucins.

Apomucin	Cytoplasmic tail sequence	Protein binding-domains and phosphorylated tyrosines
MUC1	CQCRRKNYGQLDIFPARDTY HPMSEYPTYHTHGRYVPPSS TDRSPYEKVSAGNGGSSLSYT NPAVAATSANL	7 Tyr SH2 domain c-Src, Lyn, Lck, ZAP70, c-Abl, Grb2, IKK, HSP70, HSP90, b-catenin, GSK3, FGFR3
MUC3	AVRSGWWGGQRRGRSWD QDRKWFETWDEEVVGTFSN WGFEDDGTDKDTNFHVALE NVDTTMKVHIKRPEMTSSSV	SH2 domain
MUC4	LRFWGCSGARFSYFLNSAEALP	1 Tyr
MUC12	SQRKRHREQYDVPQEWRKEG TPGIFQKTAIWEDQNLRESRFG LENAYNNFRPTLETVDSGTELH IQRPEMVASTV	2 Tyr
MUC13	VTARSNNKTKHIEEENLIDEDF QNLKLRSTGFTNLGAEGSVFPK VRITASRDSQMQNPYSRHSSM PRPDY	2 Tyr PKC
MUC15	GKRKTDSFSHRRLYDDRNEPVL RLDNAPEPYDVSFGNSSYYNPT LNDSAMPESEENARDGIPMDD IPPLRTSV	4 Tyr
MUC16	VTTRRRKKEGEYNVQQQCPG YYQSHLDLEDLQ	3 Tyr moesin
MUC17	SIYSNFQPSLRHIDPETKIRIQRP QVMTTSF	1 Tyr PDZK1
MUC20	ENGGFLLLRLSVASPEDLTDPRV AERLMQQLHRELHAHAPHFQV SLLRVRRG	c-Met
MUC21	RNSLSLRNTFNTAVYHPHGLNH GLGPGPGGNHGAPHRPRWSPN WFWRRPVSSIAMEMSGRNSGP	1 Tyr
MUC22	SFCLRNLFFPLRYCGIYYPHGHSH SLGLDLNLGLGSGTFHSLGNALV HGGELEMGHGGTHGFGYGVGH GLSHIHGDGYGVNHGGHYGHG GGH	6 Tyr
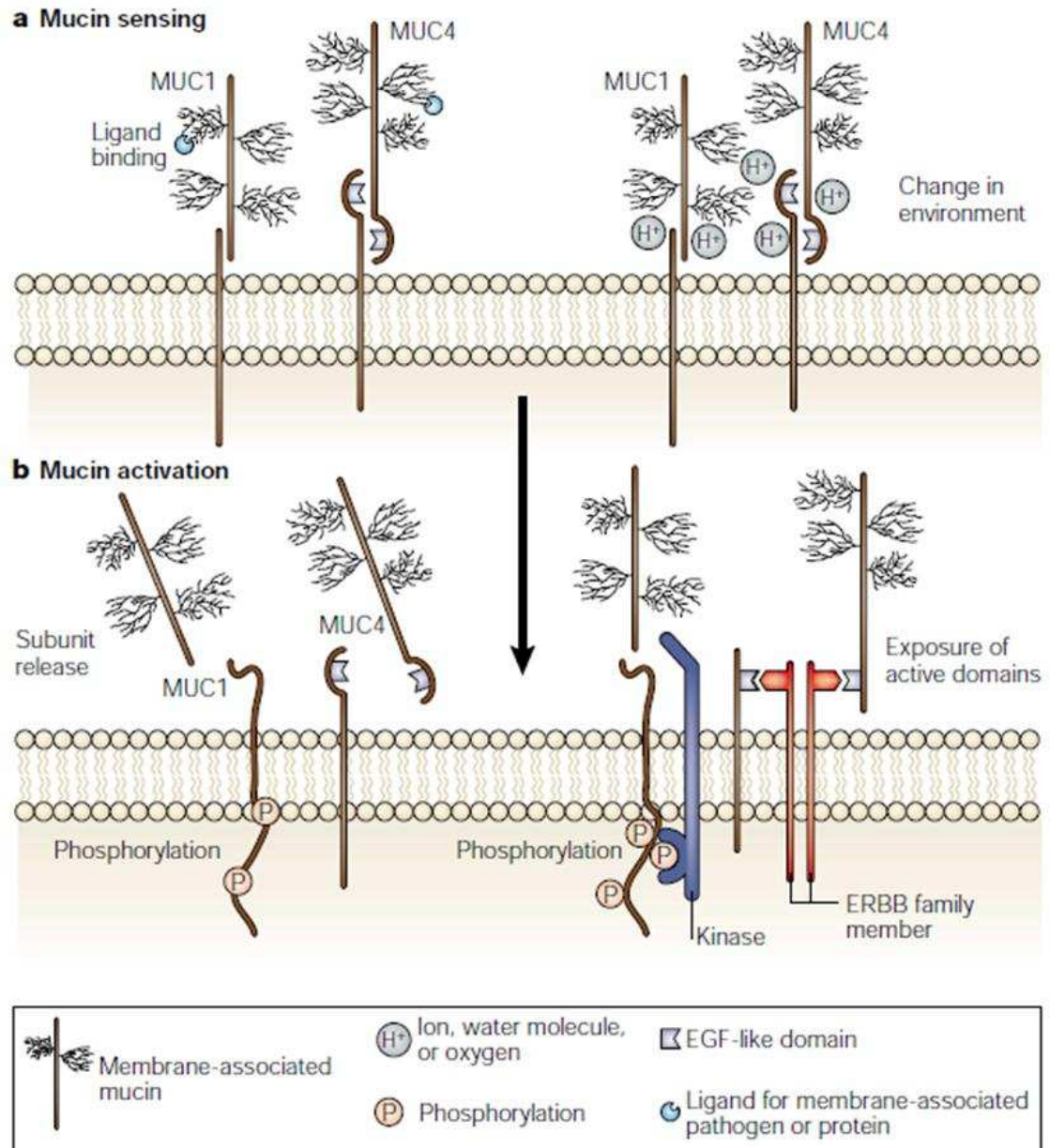
Figure 1.8. Membrane associated mucins act as receptors or sensors of the environment. (a) Membrane anchored mucins act as ligands for lectins, selectins, bacteria and other adhesion molecules. It also detects changes in the pH of the environment. (b) Mucin ectodomain is release in response to external stimuli such as changes in pH. Upon activation, the C-terminal subunit of mucins undergoes conformational changes, phosphorylation of the cytoplasmic tail and recruits signaling molecules [39].
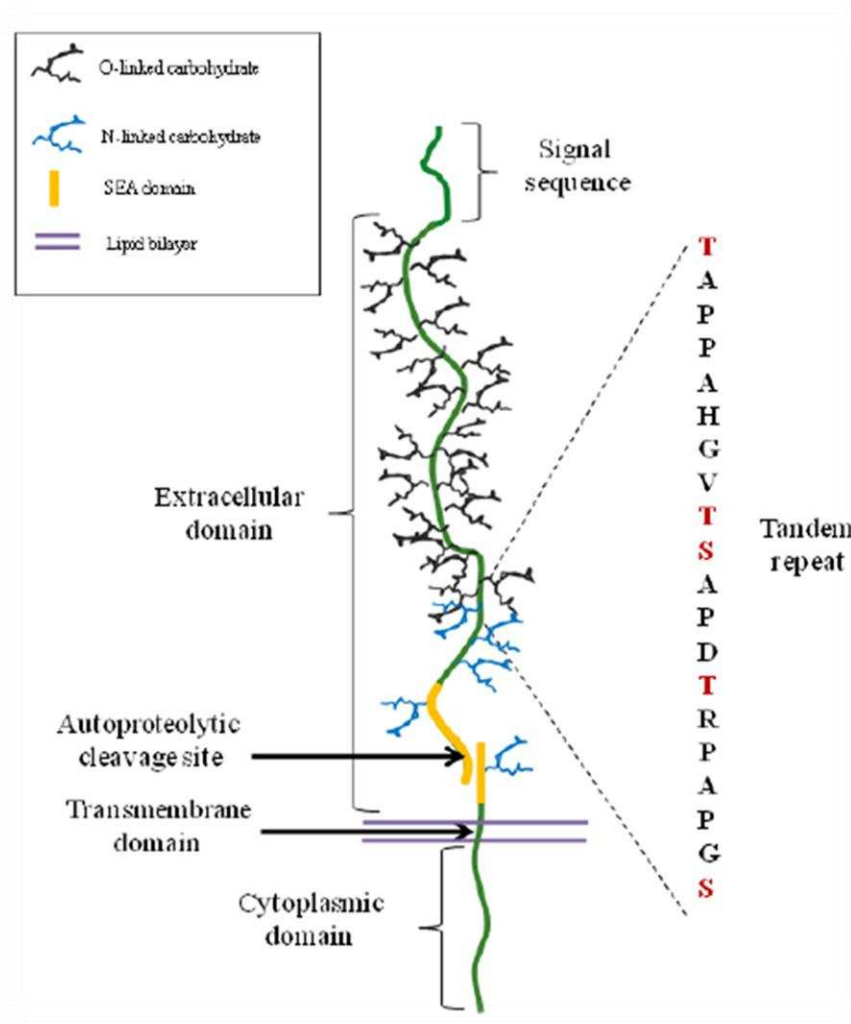
Figure 1.9. Schematic representation of the structure of MUC1: MUC1 is a heterodimer consisting of the N-terminal and C-terminal subunits. The N-terminal subunit comprises the VNTR of 20 amino acids that are extensively O-glycosylated at serine and threonine residues and sparingly glycosylated at the arginine residues. The C terminal domain consists of a 53 amino acid long extracellular domain, 28 amino acid long transmembrane domain and the 72 amino acid long cytoplasmic tail. Immediately after translation, the MUC1 protein undergoes autoproteolysis at GVVV site to generate the N-terminal and C-terminal subunits. The autoproteolytic cleavage site lies with the SEA domain of the subunits. Figure adapted from the PhD thesis of Ashlyn Bernier.
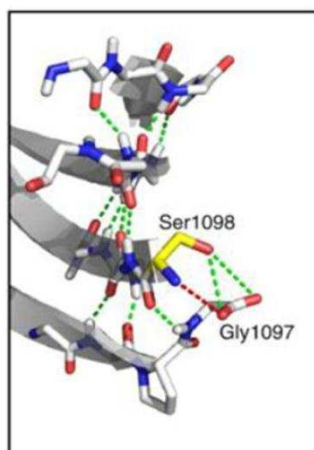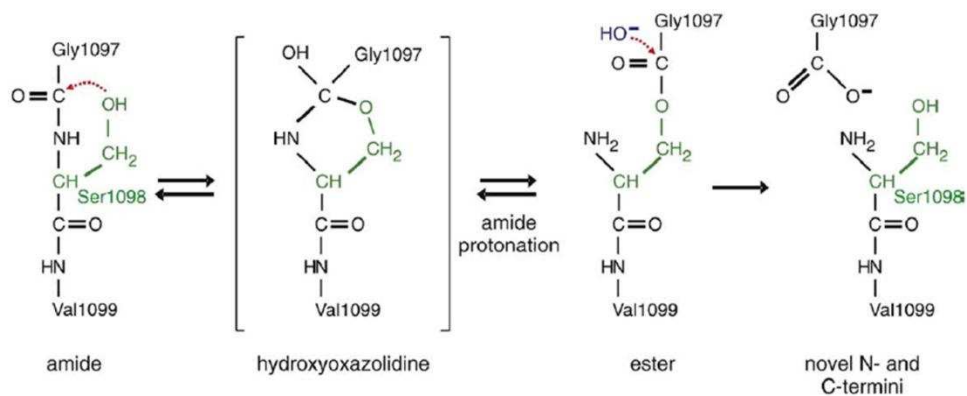
Figure 1.10. Autoproteolytic cleavage of MUC1: Cleavage at the GSVVV site generates two subunits of MUC1 – the N-terminal and C-terminal subunits. The conformational strain causes the hydroxyl group of Ser1098 to attack the carbonyl group of Gly1097. The two subunits are held together by hydrogen bonds. Figure has been adapted from [86]
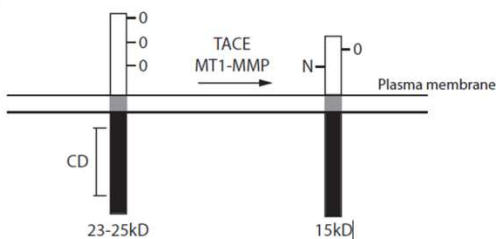
Figure 1.11. MUC1 cleavage by sheddase: The extracellular region of MUC1 is cleaved by ADAM17 (TACE) or MMP1 to generate shorter peptide fragments (15-17KDa)[47] .
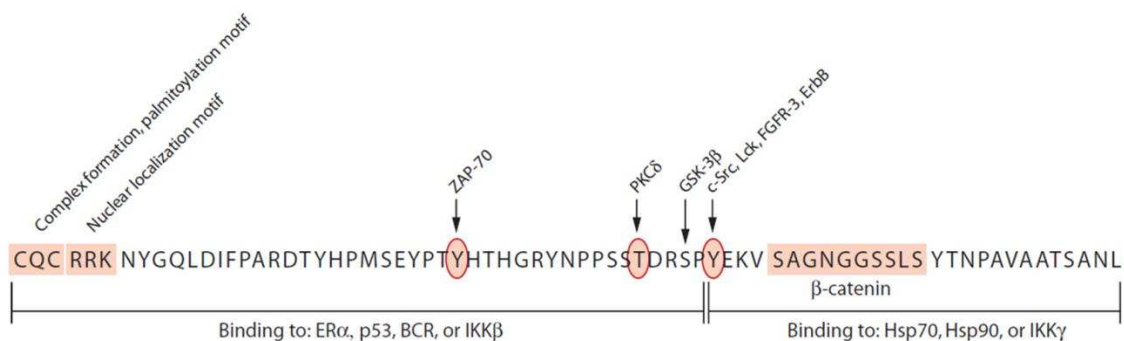
Figure 1.12. Protein binding and phosphorylation sites on the cytoplasmic tail of MUC1: The cytoplasmic tail of MUC1 contains tyrosine (7) and serine residues that are phosphorylated. The phosphorylated residues physically interact with other signaling molecules and thus can modulate cell signaling cascades. The MUC1 monomers dimerizes around the CQC motif in the cytoplasmic tail Figure adapted from [47].
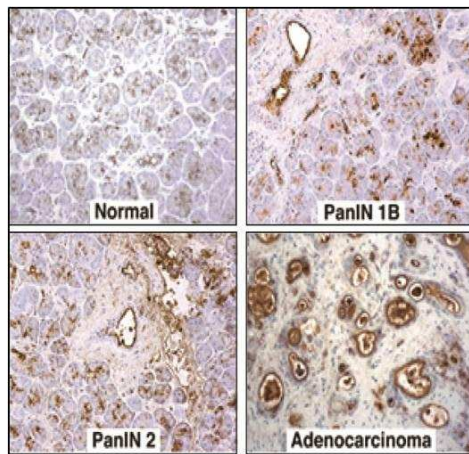
Figure 1.13. MUC1 expression in PanIN lesions of human PDA. Immunohistochemical staining of MUC1 in normal pancreas and PanIN lesions using CT2 antibody which detects the cytoplasmic tail of MUC1. The expression of MUC1 protein increases with the progression of PanIN lesions.
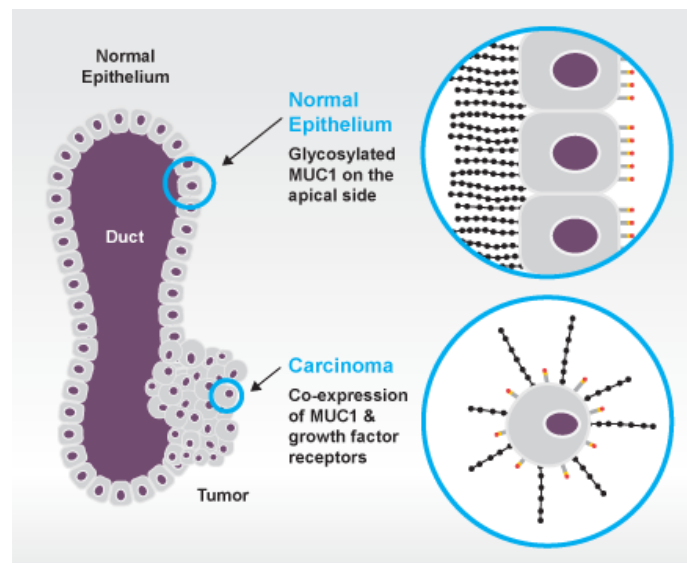
Figure 1.14 Loss of polarity of MUC1 in cancer cells: In normal epithelial cells, MUC1 is confined to the apical surface of the cells and growth factors to the basal surface. However, in cancer, the tumor cells lose apico-basal polarity, for which MUC1 is found all over the surface of the tumor cells often in close proximity of the growth factors [87].

36
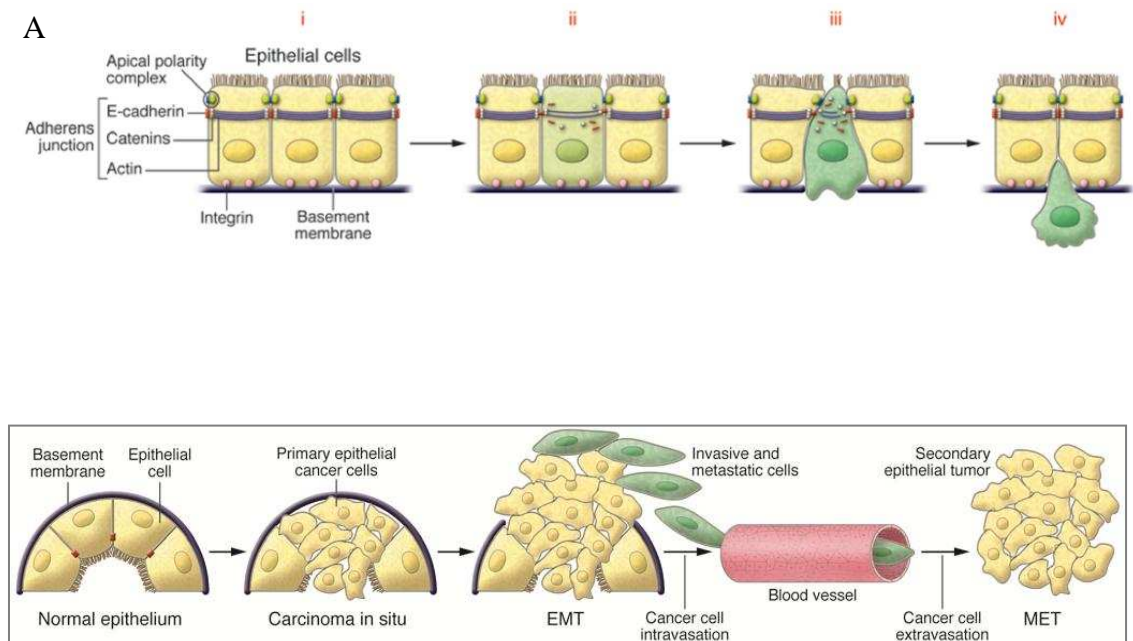
Figure 1.15. Multistep process of metastasis which occurs through EMT-MET transition: In a healthy tissue, the normal epithelial cells are attached to the basement membrane. In carcinoma in-situ, the transformed cells exhibit increased proliferation, loss of polarity followed by acquisition of invasive and metastatic properties. The cancer cells enter circulation, disseminate through bloodstream and exit the bloodstream at a remote site, where they form micro or macro metastases. Figures adapted from [71], [88].
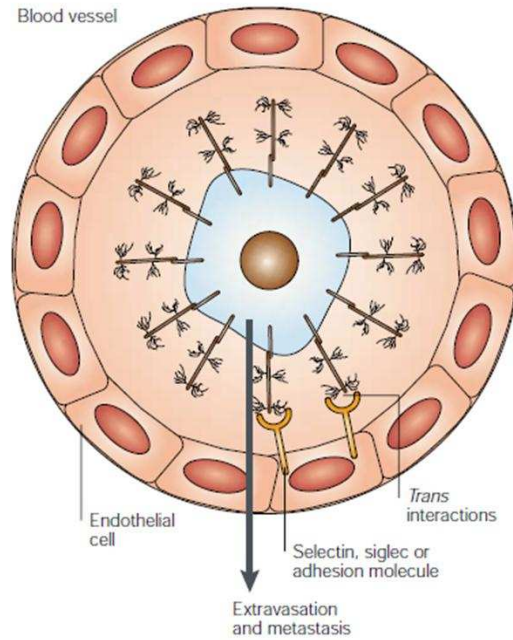
Figure 1.16. Adhesion of cancer cells via interaction of MUC1 with cell adhesion molecules on the endothelial cells: Tumor cells aberrantly express high levels of underglycosylated MUC1, exposing the peptide core, which acts as ligands for several cell adhesion molecules such as I-CAM, E-selectin and SIGLECS (sialic acid binding immunoglobulin superfamily lectins). Figure adapted from [39]

CHAPTER 2: MUC1 INDUCES DRUG RESISTANCE IN PANCREATIC CANCER CELLS VIA UPREGULATION OF MULTIDRUG RESISTANCE GENES.

2.1. Introduction

Chemoresistance:

Chemoresistance not only affects PC but also affects various types of tumors such as acute myeloid leukemia (AML), ovarian, colon, pancreatic, breast and lung cancer. The tumor consists of mixed cell population, where some of the malignant cells are sensitive and some are resistant to chemotherapeutic drugs. During chemotherapeutic treatment, the drug sensitive cells are effectively eradicated, leaving behind the drug resistant population, which is accountable for the relapse of the disease in cancer patients.

Drug resistance can be classified into two categories: de novo resistance or acquired resistance (Figure 2.1). Cancer patients that exhibit de novo resistance do not respond to chemotherapy from the start. However, in acquired resistance, the cancer cells initially respond to a chemotherapeutic drug but eventually acquire resistance to it. The cells might also show cross-resistance to other structurally and mechanistically unrelated drugs - a phenomenon commonly known as Multi Drug Resistance (MDR) [89]. Due to acquisition of MDR, treatment regimens that combine multiple agents with different targets are no longer effective [89], [90], [91]. The efficacy of chemotherapy is compromised in pancreatic cancer due to its inherent chemoresistant nature of the disease. Resistance to drugs in cancer cells is caused primarily due to two reasons:

Interference with the apoptotic pathway - A lot of anti-cancer drugs work through inducing apoptosis in cancer cells. However, most of the most cancer cells have deregulated apoptotic pathway and the anti-cancer drugs fail to induce apoptosis effectively. Thus decreased apoptosis can lead to chemoresistance.

Efflux of drugs from the cancer cells – Another common mechanism by which cancer cells evade killing by drugs is via upregulation of ATP dependent membrane efflux pumps or ATP-binding cassette (ABC) transporters. These transporters or pumps efflux anticancer drugs and reduces the accumulation of drugs inside the cancer cells, thus allowing the cancer cells to evade the toxic effects of the drugs (Figure 2.2) [92], [93]. This type of resistance is mostly seen against amphipathic drugs such as vinkaalkaloids, anthracyclins, which enter the cell through passive diffusion. Since the movement of these molecules cannot be restricted, organisms starting from bacteria to humans have developed methods to overcome the toxic effects of the xenobiotics by reducing their intracellular concentration [94].

ABC transporters – Structure, function and expression:

The ABC superfamily comprises of structurally and highly functionally diverse group of proteins that are crucial for all living cells for transport of a variety of substrates such as organic ions, lipids, oligosaccharide, oligopeptides, proteins, vitamins, metals etc. Till this date 49 ABC transporters have been identified, and they are designated A through G.

The basic unit of an ABC transporter consists of four core domains – two transmembrane domains (TMD) and two nucleotide binding domains (NBD) (Figure 2.3). The hydrophobic α-helices of TMD span the plasma membrane multiple times and are required for the insertion of the protein into the lipid bilayer. The TMDs form

hydrophilic aqueous pore through which solutes are transported across the plasma membrane. The aqueous pore has a large opening which faces the extracellular part of the membrane. In addition, TMD harbors the substrate binding site, that usually can bind a wide range of substrates. Table 2.1 lists the various types of ABC pumps and their substrates. The NBD is hydrophilic, and is peripherally situated towards the cytoplasmic face of the membrane. The NBD domain consists of the core 215 amino acids which bind ATP and use the energy of ATP catalysis to drive the export of substrates across the cell membrane [89], [95]. The NBD domain is highly conserved and the members of ABC family of proteins are defined by the presence of this domain.

MRP1 and its structurally and functionally similar counterpart P-gp are the two most extensively studied ABC transporters. They share similar substrate specificity and they both efflux a wide variety of anticancer drugs such as etoposide, daunorubicin, doxorubicin, epirubicin etc. MRP1 is also called as glutathione drug conjugate pumps or GS-X pumps because it transports a wide range of substrates that are conjugated to negatively charged hydrophilic ligands such glutathione, glucuronic acid and sulfates [89], [94]. Structurally ABCB1 differs from P-gp around the TMD. P-gp contains two transmembrane domains (TMD) and two nucleotide binding domains (NBD). In contrast ABCC1 contains three TMD and two NBD (Figure2.4) [96] [97].

Upregulation of Mdr1 (or ABCB1/Abcb1) gene, encodeing for P-gp and ABCC/Abcc (1-9) genes encoding for the MRP family of multidrug transporters are frequently observed in cancer cells. The increases in expression of the ABC pumps are thought to be responsible for increased chemoresistance in cancer cells. In particular, ABCB1 (P-glycoprotein), ABCC1 (MRP1), ABCC2 (MRP2) and ABCG2 (BCRP, MXR) actively extrude several types of anti-cancer drugs from cancer cells, thereby

conferring drug resistance to those agents [89]. A study involving tumors from 45 pancreatic cancer patients was conducted to analyze the expression of two types of ABC transporters P-gp and MRP1. It was found that 93.3% of the patients included in the study either or expressed high levels of both P-gp and MRP1 and only a very small fraction of patients (6.7%) expressed neither P-gp nor MRP1[98]. In contrast, another study involving 31 pancreatic tumor and 6 normal pancreas samples analyzed for MRP1-9 and BCRP expression reported that only MRP3 gene is significantly upregulated in pancreatic tumors and the mRNA levels match the tumor stage and grading [99]. Analysis of human PDA cell lines BxPC3, AsPC1, PANC-1 and Capan-1 cell lines shows high expression of MRP1 but little P-gp, suggesting that intrinsic drug resistance may be caused by MRP-1 and not P-gp. This observation has been further confirmed by studies on PDA cell lines that shows 97% of the PDA cell lines express MRP1 [100].

PI3K and Chemoresistance:

Another common mechanism by which cancer cells acquire drug resistance is through enhanced activation of the pro-survival pathways PI3K/Akt and Erk1/2 , which interferes with apoptosis of cancer cells. PI3K constitute a family of lipid kinases that has the catalyzes the phosphorylation of hydroxyl group of phosphatidylinositols (PIs) at their 3-position to form PI(4,5)P2 to PI(3,4,5)P3. The effect of PIP3 is mediated through its specific interaction with PDK1 and Akt/PKB, which are critical mediators of PI3K signaling cascade (Figure 2.4) [101].

PI3K are heterodimers, consisting of the regulatory subunit p85 and the catalytic subunit p110. Binding of the p85 subunit to the phosphotyrosine consensus motif on receptor tyrosine kinases (RTK) or G-protein coupled receptors, leads to allosteric activation of the catalytic subunit. Studies have shown that p85 binds to the consensus

sequence of MUC1 CT (phosphor tyrosine at YHPM motif of MUC1 CT) via its SH2 domain. Upon binding to the consensus sequence motif, p85 is activated, which in turn activates the catalytic subunit p110 [59], [68]. Hence PI3K pathway is often observed in MUC1 high cancer cells. Studies have shown that MUC1 overexpression in breast, colon and thyroid cancer cells exhibit overactivated Erk1/2 and PI3K pathways, which is linked to their unresponsiveness to chemotoxic agents [68], [102]. Recently a link has been shown between activation of activation of PI3K/Akt pathway and upregulation of ABCC1 gene expression in prostate cancer cells [103].

Pancreatic cancer is one of the most difficult malignancies to treat because of its aggressive and drug resistant nature. An understanding of the mechanism of drug resistance in PC is needed for developing strategies that would improve the outcome of chemotherapy. Thus, the goal of the present study was to first determine if MUC1-overexpression in PDA cells makes them resistant to chemotherapeutic drugs and second to delineate the mechanism by which MUC1-associated resistance occurs. We report that MUC1 regulates the mdr gene expression via both Akt dependent and independent pathways, which confers the MDR phenotype to PDA cells. This is the first report that demonstrates a direct relationship between expression of MUC1 and mdr genes, in particular ABCC1 in pancreatic cancer.

2.2. Materials and Methods

Cell culture and Establishment of Stable Cell Lines Expressing MUC1:

BxPC3 (American Type Culture Collection, Manassas, VA, USA) is a human PDA cell line that express very little endogenous MUC1. For retroviral infection, GP2-293 packaging cells (stably expressing the gag and pol proteins) were co-transfected with the full length MUC1 construct or an empty vector expressing the VSV-G envelope

protein as previously described [62], [63]. Cells were treated with 0.5 mg/ml of G418, beginning 48 h post infection. Three independent infections of the constructs were carried out with similar results. Expression of the constructs was stable throughout the span of experiments. Cells infected with vector alone were used as control and designated Neo. For MUC1-infected cells, MUC1-positive cells were sorted using the FACS Aria (BD Biosciences, San Jose, CA, USA). For Neo-infected cells, MUC1-negative cells were sorted. Capan-1 is a human PDA cell line that expresses high levels of endogenous MUC1.

Mouse model and Mouse Cell Lines:

In our laboratory, mice that develop spontaneous pancreatic ductal adenocarcinoma (PDA) were generated by mating the P48-Cre with the LSL-KRAS^{G12D} mice [104]. PDA mice were further mated to the MUC1.Tg mice (that express human MUC1) to generate PDA.MUC1 mice or to the Muc1 knockout mice to generate PDA.MUC1KO mice [58], [105]. All these mice were on the C57/B6 background. Cell lines were generated from the primary tumors of PDA.MUC1 and PDA.Muc1 KO mice and were designated as KCM and KCKO respectively.

MTT assay and H^3-Thymidine Incorporation Assays:

10×10^3 cells were plated in quadruplicate in normal growth medium in 96-well plates and were permitted to grow for 18 hours. Cells were left untreated or treated with etoposide (Sigma-Aldrich) and gemcitabine (Sigma –Aldrich) for 24 hours. Next, MTT (Biotium) solution was added (10 ul/well) to cells, incubated for additional 3-4 hours. In the final step, media was removed, formazan was dissolved in DMSO (200ul/well) and the absorbance was read on an ELISA plate reader.

For H^3-thymidine assay, 5 X 10^3 cells were plated and treated as described above. 24 hours post drug treatment, H^3-thymidine (Perkin Elmer, USA) was added in fresh medium (1 µCi/well) and cells were permitted to grow for another 24 hours. At this time, cells were washed to remove excess radioactivity, trypsinized, and harvested onto a filter plate, which was then read on a TopCount plate reader. The data has been represented as % difference in H^3 – thymidine uptake, which represents the % decrease in proliferation or % in growth arrest. The following formula was used for calculations:

% difference in H^3 thymidine uptake = ((cpm untreated – cpm treated)/ cpm untreated*100)

Transient Knockdown Using siRNA:

The method is previously described in [63]. In brief, cells were seeded in a 6 well plate and were allowed to reach 40% confluency. The cells were then transfected with 100nm of MUC1 siRNA (Smart genome pool) or 100 nm of Akt siRNA (Santa Cruz and Cell Signaling). Cells of the control group were treated with 100nm of scrambled siRNA (Dharmacon, Thermo Fischer Scientific, CO, USA, Santa Cruz and Cell Signaling). Lipofectamine (Invitrogen, San Diego, CA, USA) was used for the delivery of siRNA into the cells over a period of 5-6 hours in serum free Opti-MEM. 48 hours post transfection, MUC1 and Akt expression were evaluated by western blot. For MTT assay, 36hours post siRNA treatment; cells were trypsinized, re-plated in a 96 well plate and treated with or without the drugs. MTT assay was performed 24 hours post drug treatment. The viability of each treatment group without drug treatment (i.e. WT alone, control siRNA alone and Akt siRNA alone) was considered as 100%. The viability following drug treatment on each of these treatment groups was calculated as follows:

% viability of drug treated WT cells = (O.D. of drug treated WT cells/O.D. of WT cells)*100

% viability of drug + control (or Akt) siRNA treated cells = (O.D. of drug + control (or Akt) siRNA treated cells/O.D. of control (or Akt) siRNA treated cells)*100

Preparation of Nuclear Extract:

Cells were grown in 10cm plate. When the cells reached around 80% confluency, they were scraped off the plate and nuclear extraction kit (EMD Millipore) was used to isolate the nuclear and cytosolic fractions.

Western Blots:

Equal quantities of cell lysates were loaded on SDS–PAGE gels. MUC1 antibodies were a gift from Dr. Sandra Gendler. pAkt and Akt antibodies were purchased from Cell Signaling Technology (Danvers, MA, USA), MRP-1, Lamin A/C and β-actin were purchased from Santa Cruz (CA, USA) and MEK1 was purchased from Abcam (Boston, USA). The antibodies were used according to manufacturer's recommendations.

Semi-Quantitative RT-PCR:

Total RNA was extracted from cells by TRIzol (Invitrogen) according to the manufacturer's protocol. 1–2 μg of the extracted RNA was used as template for RT-PCR reaction (Access quick RT-PCR kit, Promega, Madison, WI, USA). Sequence of the primers is available upon request.

Immunohistochemistry:

Cells ($1X10^6$ cells per mouse) were implanted subcutaneously in nude mice and 30 days later, tumors were collected for IHC and protein lysate [62]. In brief, paraffin embedded blocks of formalin fixed tumor sections were made by the Histology Core at Mayo Clinic. 4 micron thick sections were prepared for immunohistochemical staining.

MRP1 expression in the tumor was determined using anti-MRP1 antibody (1:50 dilution, Santa Cruz) followed by appropriate secondary antibody (1:100 dilution, Dako). Slides were examined under light microscope and pictures were taken at 20X.

Chromatin Immunoprecipitation (ChIP):

Cells grown to near 80% confluence, were cross-linked with formaldehyde (Sigma) at room temperature for 10 min. Cross-linked chromatin prepared with a commercial ChIP assay kit (EZ-Magna ChIP; Millipore) was immunoprecipitated with 20 μg of normal Armenian hamster IgG (Santa Cruz Biotechnology, CA, USA) and 20 μg of anti-MUC1 CT antibody (CT2). MUC1 CT binding site on ABCC/Abcc1 promoter was amplified by PCR using the input DNA (1%) or DNA isolated from precipitated chromatin as templates and using primers flanking the promoter region 1000 bp upstream (ChIP region I) and 2000bp upstream (ChIP region II) of ABCC1/Abcc1 gene **(Fig. 6B).** ChIP region II was used as a negative control for binding of MUC1 CT to the promoter region. Sequence of the primers is available upon request.

Statistical Analysis:

Statistical analysis was performed with GraphPad software.

2.3. Results

To determine the relative expression of endogenous MUC1 in BxPC3 and Capan-1 cell lines, immunohistochemical analysis of cells grown in chamber slides was performed using an antibody against the tandem repeat of MUC1 (HMFG2). Immunohistochemical staining showed that Capan-1 cells have higher endogenous MUC1 expression as compared with BxPC3 cells (Figure 2.6a). This was confirmed using western blotting assay using antibodies against the tandem repeat (HMFG2) and CT of MUC1 (CT2). Both antibodies showed that Capan-1 cells have higher endogenous

MUC1 compared with BxPC3 cells (Figure 2.6b). Next, we show MUC1 expression in Capan-1 cells following treatment with control and MUC1-specific siRNA (small interfering RNA) by western blot. Complete knockdown of MUC1 is observed in Capan-1 cells post 48-h treatment with MUC1-specific siRNA (Figure 2.6c and supplementary table 2.1). To determine the effect of MUC1 in drug resistance, BxPC3 and Capan-1 cells were treated with etoposide and gemcitabine, and proliferation post treatment was determined using H^3-thymidine incorporation assay. Etoposide is a toposiomerase II inhibitor, whereas gemcitabine is a nucleoside analog. Low MUC1-expressing BxPC3 cells showed greater sensitivity to etoposide and gemcitabine compared with high MUC1-expressing Capan-1 cells. At 25 µM dose of etoposide, we observed a 62.8% growth arrest in BxPC3 cells. In contrast, at the same dose, only 12.14% growth arrest was observed in Capan-1 cells (Figure 2.6d) Similarly, at 500 nM dose of gemcitabine, ~100% growth arrest was observed in BxPC3 cells, compared with only 50% growth arrest in Capan-1 cells (Figure 2.6e). Further, when Capan-1 cells treated with MUC1 siRNA were exposed to 500 nM of gemcitabine, a 31% increase in growth arrest was observed compared with untreated cells or cells transfected with control scrambled siRNA (Figure 2.6f).

For further investigations, mouse PDA primary cells genetically lacking Muc1 (KCKO) and ones expressing human MUC1 (KCM) were included in this study. Upon using the CT2 antibody that recognizes the CT of both mouse and human MUC1, KCM cells showed high expression of MUC1 while KCKO cells showed no detectable levels (Figure 2.7a and supplementary table 2.2). To further validate the effect of MUC1 in drug resistance, KCKO and KCM cells were treated with etoposide and gemcitabine. We found 76% and 88% of growth arrest upon treatment of KCKO cells with 1.25 µM and

2.5 μM of etoposide, respectively. In contrast, only 52% and 57% of growth arrest was observed in KCM cells at 1.25 and 2.5 μM of etoposide, respectively, indicating that KCM cells were more resistant to etoposide (Figure 2.7b left panel). At 5 μM of etoposide, both cell lines irrespective of their MUC1 status were sensitive. Similar resistance of KCM cells to gemcitabine was observed. At 3 nM of gemcitabine, 60% of growth arrest was observed in KCKO cells compared with only 34% of growth arrest in KCM cells. At higher doses, there was no difference in growth arrest between KCKO and KCM cells (Figure 2.7b, right panel). MTT assay was also performed to validate the cytotoxic effects of these drugs on the same cell lines. At 50 μM of etoposide, 48% of cell death was observed in KCKO cells compared with only 27% cell death in KCM cells (Figure 2.7c, left panel). Similarly, at 150 nM of gemcitabine, 53.3% of cell death was observed in KCKO cells compared with only 40% cell death in KCM cells (Figure 2.7c, right panel).

To further confirm that the effect was due to MUC1 expression, we stably expressed full-length MUC1 in BxPC3 cells that have low levels of endogenous MUC1 (BxPC3.MUC1), and as control we transfected BxPC3 cells with empty vector that contains the neomycin resistance gene (BxPC3.Neo). First we show the relative expression of MUC1 in these cells (Figure 2.8a and supplementary table 3). BxPC3 MUC1 cells express high levels of MUC1 while BxPC3 Neo cells have negligible levels. BxPC3 MUC1 cells were significantly resistant to both the genotoxic drugs as compared with the BxPC3 Neo cells. At 25, 50 and 75 μM of etoposide, cells with low MUC1 showed significantly higher growth arrest compared with cells expressing high levels of MUC1 (Figure 2.8b, left panel). Similar results were observed with 6.25–25 nM of gemcitabine (Figure 2.8b, right panel). MTT assay was performed to validate the

cytotoxic effects of etoposide and gemcitabine on both cell lines. At 75 μM of etoposide, 64% of cell death was observed in BxPC3 Neo cells compared with only 39.6% cell death in BxPC3 MUC1 cells (Figure 2.8c, left panel). Similarly, at 50 nM of gemcitabine, 42.7% of cell death was observed in BxPC3 Neo cells compared with only 15.5% cell death in BxPC3 MUC1 cells (Figure 2.8c, right panel). These results suggested that MUC1 confers resistance to gemcitabine and etoposide in PDA cells.

Previously we have published that KCM cells express 8-fold higher P-glycoprotein, 4-fold higher MRP-1, and 2-fold higher MRP-5 protein compared to KCKO cells [58]. Therefore, we first determined the mRNA level of some of these MDR genes. Consistent with those results, we observed significantly high m-RNA levels of the Abcc1, Abcc3, Abcc5, Abcb1a and Abcb1b genes in KCM versus KCKO cells (Figure 2.9a, left panel). Similarly, in BxPC3 MUC1, the m-RNA levels of ABCC1, ABCC3, ABCC5, and ABCB1 gene was significantly higher compared to BxPC3 Neo cells (Figure 2.9a, right panel). To validate this finding, we determined the protein expression of MRP-1 by western blotting and as expected we observed significantly higher expression of MRP-1 in KCM cells compared to KCKO cells and in BxPC3 MUC1 compared to BxPC3 Neo cells (Figure 2.9b).

All of the data so far has been shown in cells grown in vitro. To answer if this is true in vivo, we determined the MRP-1 protein expression in spontaneously occurring PDA.MUC1 (KCM) and PDA.Muc1KO (KCKO) tumors as well as in BxPC3 Neo and MUC1 tumors grown in nude mice. IHC was performed on tumor sections from ~16-week old KCM and ~24-week KCKO mice and a representative section from each tumor type is shown in Figure 2.9 c. Significantly higher expression of MRP-1 protein was observed in KCM as compared to KCKO tumor sections (Figure 2.9 c). MRP1 levels in

the tumor lysates isolated from BxPC3 Neo and BxPC3 MUC1 xenografted tumors were determined by western blotting. BxPC3 MUC1 tumors showed higher MRP-1 expression compared to BxPC3 Neo tumors (Figure 2.9 d). Interestingly, the tumor sample (sample # 3) that had higher MUC1 expression compared to the other MUC1 positive tumor sample (sample #4) also showed higher MRP-1 expression (Supplemental table 5). The data suggests that a positive correlation exits between MUC1 overexpression and upregulation of mdr genes in PDA cells.

Often in tumor cells, reduced sensitivity to chemotherapeutic drugs is due to enhanced activation of the anti-apoptotic or prosurvival pathways, which includes the PI3K/Akt pathway. We first determined the activation status of PI3K/Akt pathway in KCKO, KCM, and BxPC3.Neo and BxPC3.MUC1 cells. Protein lysates from these cell lines were subjected to immunoblotting using anti-phospho-Akt (p-Akt) and Akt antibodies. Significantly higher levels of pAkt was found in MUC1 positive PDA cells (KCM and BxPC3 MUC1) compared to MUC1 low or null PDA cells (KCKO and BxPC3 Neo) (Figure 2.10 a). The levels of total Akt remained same in all cell lines indicating enhanced activation of the PI3K/Akt pathway in KCM and BxPC3 MUC1cells. This finding positively correlates with the results presented previously in MUC1 overexpressing fibroblasts[68].

To test the contribution of Akt on MRP1 expression and drug resistance, we transiently knocked down Akt and evaluated the levels of MRP1 expression by western blot and drug sensitivity by MTT assay. The levels of Akt, MRP1 and MUC1 are shown in Figure 2.10 b - d. Upon Akt knockdown, we observed a 5.4 fold decrease in MRP1 expression in Capan-1 cells and 4.6 fold decrease in MRP1 expression in BxPC3 MUC1 cells (Figure 2.10b, 2.10c, Supplemental table 7 & 8). Furthermore, roughly 40% and

25% increase in cytotoxicity was observed in Akt siRNA treated BxPC3 MUC1 cells upon treatment with 50μM of etoposide and 25nM of gemcitabine respectively (Fig. 2.10E).This data indicated that Akt pathway played an important role in MUC1 induced MRP1 expression and drug resistance in Capan1 and BxPC3 cells.

Interestingly, we also observed a subsequent decrease in MUC1 expression upon downregulation of Akt in Capan-1 and BxPC3 MUC1 cells (Fig 2.10b, 2.10c). When Akt was transiently knocked down in Capan-1 and BxPC3 MUC1 cells, a respective 3.2 fold and 2.5 fold decrease in MUC1 expression was observed (Supplemental table 7 & 8). This data indicates that MUC1 gene is also under regulation of PI3K/Akt pathway. Hence, abrogation of the Akt pathway causes a significant decrease in MUC1 expression, which in turn negatively affects MRP1 expression.

However, we did not see a significant decrease in MUC1 and MRP1 expression in KCM cells upon Akt knockdown (1.2 fold decrease) (Fig 2.10d) (Supplemental table 9). Consequently, we did not detect a significant increase in cytotoxicity in Akt siRNA treated KCM cells upon treatment with etoposide and gemcitabine (data not shown). This data indicates that in KCM cells, MUC1 gene is not strongly regulated by PI3K/Akt pathway. This observation further led to the possibility that in KCM cells, an Akt independent mechanism must be involved in MUC1 induced MRP1 expression and drug resistance. It is of interest that BxPC3 and Capan-1 are human cells while KCM is a mouse cell line.

Several studies have shown that MUC1 CT associates with mediators of signal transduction and transcriptional regulation and thereby modifies the expression of specific target genes [63][64]. In this study, we wanted to investigate the occupancy of MUC1 CT in the promoter region of ABCC1/Abcc1 gene, which can be indicative of

MUC1's role as a modulator of ABCC1/Abcc1 gene expression. First, we demonstrate that MUC1 CT localizes to the nucleus of MUC1 positive PDA cells. Nuclear and cytosolic fractions were extracted from KCKO, KCM, BxPC3 Neo and BxPC3 MUC1 cells and the lysates were immunoblotted to determine the cellular localization of MUC1 CT in these PDA cells. As expected, we found MUC1 CT localizing to the nucleus of KCM cells (left top panel Figure 2.11a) and BxPC3 MUC1 cells (right top panel Figure 2.11a). Lamin A/C and MEK1 served as controls for the extraction process. Lamin A/C is a nuclear protein and is hence is found only in the nuclear fractions (middle panels, Figure 2.11a). MEK1 is a cytosolic protein and is found only in the cytosolic fractions (bottom panels Figure 2.11a).

Next, we evaluated the occupancy of MUC1 CT in the genomic regions of the ABCC1/Abcc1 gene upstream the transcription start site (Figure 2.11b). Sheared DNA was immunoprecipitated using MUC1 CT specific antibody CT2. IgG antibody was used as a control. The immunoprecipitated DNA was amplified by PCR using primers spanning around 1000 bp upstream (ChIP region I) and 2000bp upstream (ChIP region II) of the ABCC/Abcc1 gene transcription start site (Figure 2.11bB). In Capan-1 cells, we observed a strong interaction between MUC1 CT and ChIP region I of ABCC1 gene (6.5 fold enrichment with CT2 antibody relative to IgG) (Figure 2.11c, Supplemental table 10). Similarly, in KCM cells, a strong interaction was observed between MUC1 CT and ChIP region I of Abcc1 gene (3.2 fold enrichment with CT2 antibody relative to IgG) (Figure 2.11c, Supplemental table 11). However, no interaction was observed between MUC1 CT and ChIP region II in Capan-1 and KCM cells (Figure 2.11c). KCKO cells, which are null for MUC1 did not show any interaction between MUC1 CT and ChIP region I and II of Abcc1 gene (Figure 2.11c). This data indicated that the interaction of

MUC1 CT with the promoter region of ABCC1/Abcc1 gene around ChIP region I is specific. However, in BxPC3 MUC1 cells, a very weak interaction between MUC1 CT and ChIP region I of ABCC1 gene was observed (1.1 fold enrichment compared to IgG, Supplemental table 12) (Figure 2.11c). BxPC3 Neo cell also showed weak binding of MUC1 CT around the same gene locus. This is most likely because BxPC3 cells express low levels of endogenous MUC1 and are not null for the same (Figure 2.11c). The interaction between MUC1 CT and ChIP region II was not observed in BxPC3 cells (Figure 2.11b).

2.4. Discussion

The ability of tumor cells to escape the cytotoxic effect of chemotherapeutic agents may result from genetic alterations that affect cell cycle, apoptosis or accumulation of drugs inside the cell. Several studies in breast, colon and thyroid cancers have shown that MUC1 attenuates stress induced or chemotoxic agents induced apoptosis by blocking the release of cytochrome c from mitochondria [68], [102], [106]. In this study, we demonstrate additional mechanisms by which MUC1 enables PDA cells to escape chemotherapeutic drug mediated cell death.

We found that cells expressing full length MUC1 are less sensitive to genotoxic drugs than cells lacking or expressing low levels of MUC1, indicating a direct correlation between MUC1 expression and chemoresistance in PC (Figure 2.6, 2.7 and 2.8). Here, for the first time, we provide evidence that in PDA cells, mdr gene expression is directly correlated with MUC1 expression (Figure 2.9). Previous work has shown that hyperactivation of PI3K/Akt pathway is able to regulate expression of mdr genes, including ABCC1, ABCC3, ABCC5, and ABCB1 genes [103]. Studies have demonstrated that MUC1 oncoprotein induces transformation in rat fibroblasts or desensitizes thyroid

cancer cells to chemotherapy induced apoptosis through activation of Jak/Stat and PI3K/Akt pathways [68][102]. So, we evaluated if MUC1 induced expression of the mdr gene ABCC1/Abcc1 via activating the PI3K/Akt pathway. We found that in a subset of human PDA cells (BxPC3 MUC1 and Capan-1), MUC1 induced MRP1 expression was via Akt pathway with a pattern that suggests increased refractoriness of these cells to genotoxic drugs. Accordingly, abrogation of the PI3K/Akt pathway resulted in increased responsiveness of these cells to etoposide and gemcitabine (Figure 2.10). We also found the evidence for existence of a positive feedback loop between MUC1 expression and PI3K/Akt signaling cascade. PDA cells with high MUC1 expression exhibited hyper activation of the PI3K/Akt pathway which in turn upregulated MUC1 expression in those PDA cells. However, it is beyond the scope of the current study to determine how Akt pathway regulates MUC1 expression. In the future, we would like to investigate the mechanism in further detail. Interestingly, in the mouse PDA cells, KCM, MUC1 induced MRP1 expression was independent of PI3K/Akt pathway even though the pAkt was significantly higher in the KCM versus KCKO cells. This data underscored the possibility of involvement of an alternative mechanism involved in MUC1-induced MRP1 expression (Figure 2.11). Thus, we report for the first time that two alternate mechanisms may be involved in MUC1-induced MRP1 expression in PDA cells (Figure 2.12).

Interestingly, we found a strong association between MUC1 CT and the promoter region of the ABCC1/Abcc1 gene (Figure 2.11). This preliminary data raises a possibility that MUC1 might be part of the transcriptional complex that regulates expression of the ABCC1/Abcc1 gene. The 5' untranslated promoter region of the human ABCC1 gene contain several putative binding sites such as, GC elements (-91 to +103) which binds

Sp1; AP1 sites (-511 to -492) which binds a complex of cJun/cFos and E box elements (-1020 to -2008) which binds N-myc [106], [107], [108]. We found MUC1 CT associating with the promoter region of the ABCC1/Abcc1 gene within ChIP region I. Both mouse and human ChIP region I contain putative AP1, CREB1, GATA1, c-Ets1 and MZF1 binding motifs, as predicted by the transcription factor binding site prediction tools that uses TRANSFAC and JASPAR core databases (data not shown). MUC1 does not have a DNA - responsive domain and studies have shown that it binds to DNA via transcription factors such as NF-kB, cJun, β-catenin and HIF-1α [60], [63], [64]. Thus, in future we intend to investigate in detail what MUC1 CT is doing at the promoter region of ABCC1/Abcc1 gene and also the transcription factor that is involved in MUC1 mediated MRP1 gene expression.

Taken together, our study shows that, in PC cells, MUC1 overexpression leads to chemoresistance, and that MUC1 CT associates directly with the promoter region of the ABCC1/Abcc1 gene. Thus, the data provide new insights into the mechanisms by which MUC1 can interfere with the effectiveness of chemotherapy in PC. As MUC1 acts as a vital component that minimizes the efficacy of chemotherapy, it could be considered as a key molecular target for sensitizing cancer cells to conventional or novel treatments. The CT of MUC1 can be targeted to inhibit its ability to initiate signaling cascades, and also to block its nuclear translocation and subsequent binding to the promoter regions of its target genes. MDR modulators did not gain much popularity in the clinic owing to their ability to regulate more than one transporter and subsequently causing severe side effects in patients. [89]. As an alternative strategy, MUC1 CT can be targeted to downregulate the expression of mdr genes or the activity of these efflux pumps.

2.5. Figures
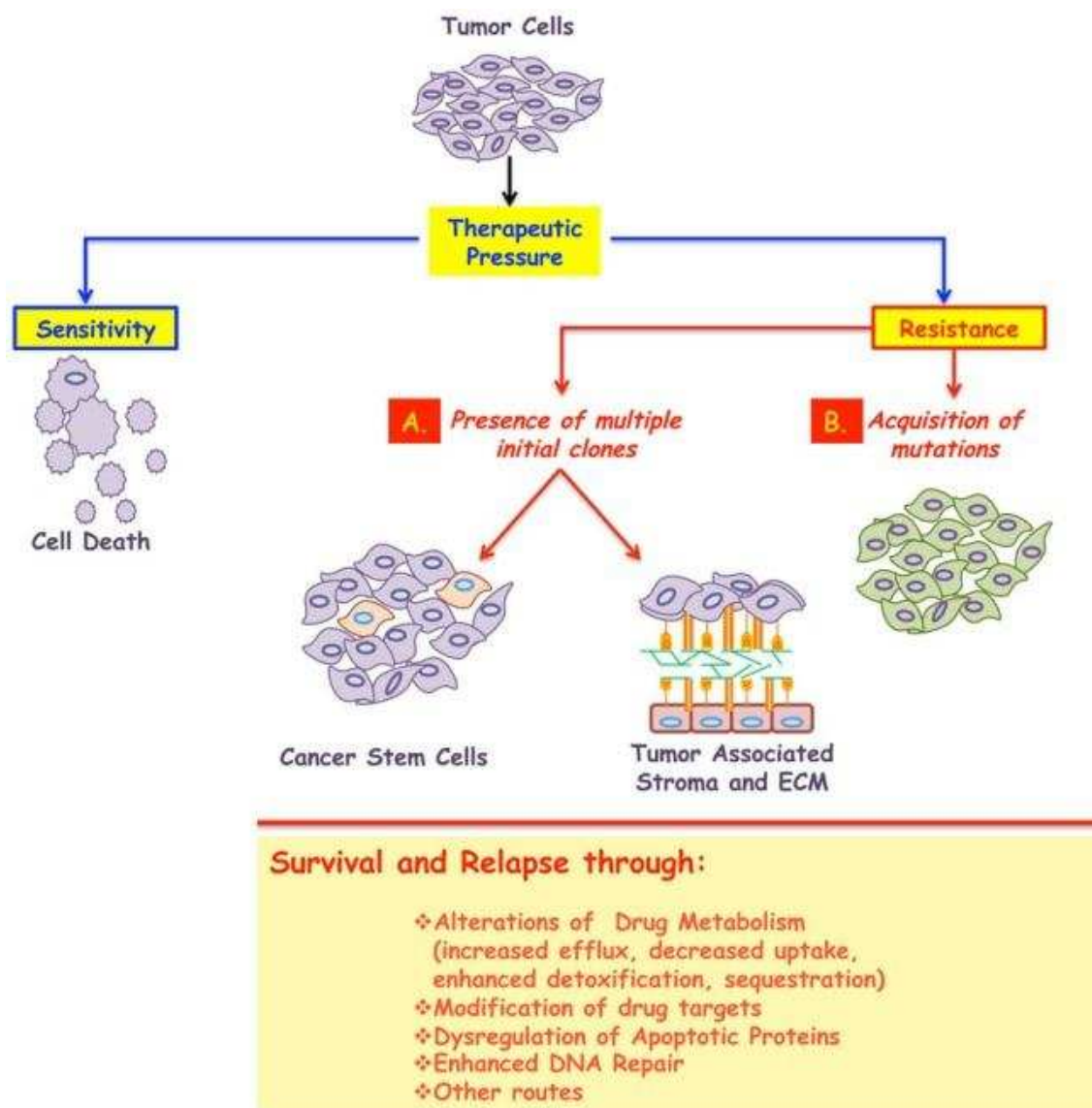
Figure 2.1: Classification of the cancer resistance into two broad types: de-novo or acquired resistance. A. De-novo resistance consists of presence of multiple drug resistant sub population of cancer cells, which emerge as the dominant clone following chemotherapy treatment. These subpopulations of cells possess stem cell like properties and are believed in dormancy, thus escaping the insults of chemotherapy. B. Acquired drug resistance results from alterations in the cancer cell following exposure to chemotherapy. In both cases the surviving cell population are likely not to respond to chemotherapy and will be responsible for the relapse of the disease [109].
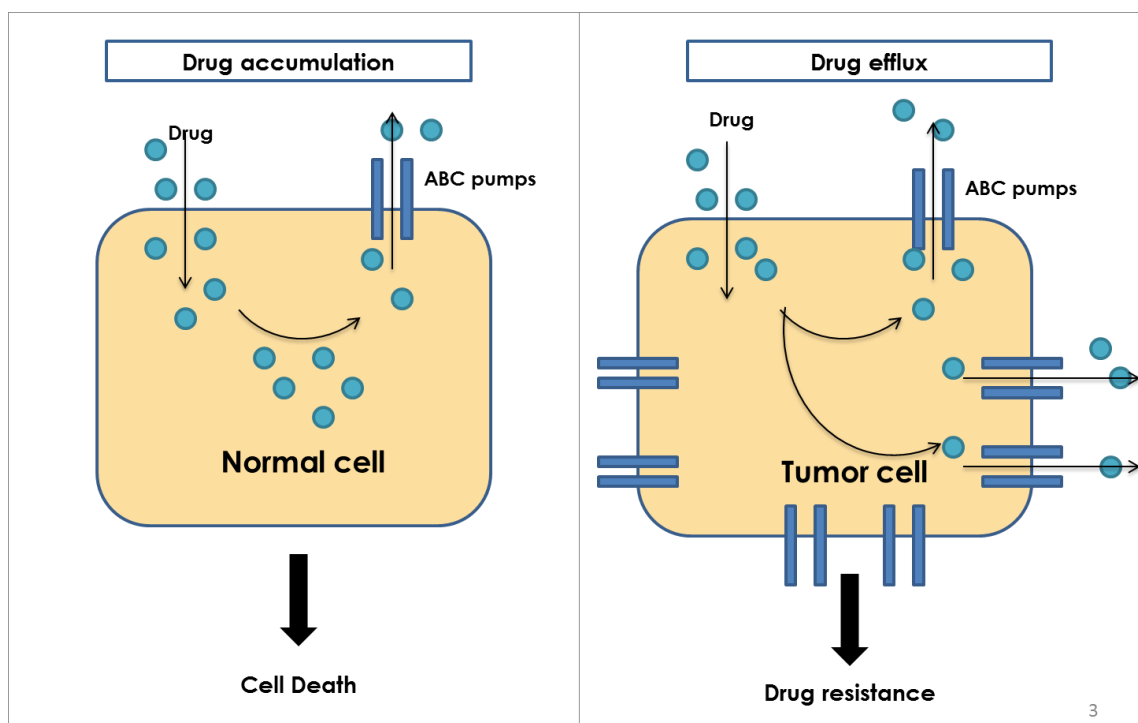
Figure 2.2: Chemoresistance caused by efflux of drugs by ABC transporters: ABC transporters effelux drugs and prevent accumulation of drugs inside the drug resistant cancer cells. The drug sensitive cells are eradicated by the chemotherapeutic drugs.

Table 2.1: The different members of ABC pumps and their substrates [89].

ABCB1 (P-gp)	ABCG2 (BCRP)
Actinomycin D	Daunorubicin
Daunorubicin	Doxorubicin
Docetaxel	Epirubicin
Doxorubicin	Etoposide
Epirubicin	Flavopiridol
Etoposide	Gefitinib
Mitoxantrone	Imatinib
Paclitaxel	Irinotecan, SN38
Teniposide	Methotrexate
Vinblastine	Mitoxantrone
Vincristine	Teniposide
	Tomudex
	Topotecan

ABCC1 (MRP1)	ABCC2 (MRP2)	ABCC3 (MRP3)	ABCC4 (MRP4)	ABCC5 (MRP5)	ABCC6 (MRP6)	ABCC7 (MRP7)
Antimony	Cisplatin	Etoposide	Folate	Folate	Cisplatin	Daunorubicin
Daunorubicin	Daunorubicin	Teniposide	Glucuronides	GSH-conjugates	Daunorubicin	Doxorubicin
Doxorubicin	Doxorubicin	Folate	GSH-conjugates	Leucovorin	Doxorubicin	Epirubicin
Epirubicin	Epirubicin	Glucuronides	Leucovorin	Methotrexate	Epirubicin	Etoposide
Etoposide Teniposide	Etoposide Teniposide	Leucovorin	Methotrexate		Etoposide Teniposide	Teniposide
Folic acid Methotrexate	Glucuronides	Methotrexate	Sulfates		GSH-conjugates	Glucuronides
Glucuronides	GSH-conjugates	Sulfates	Topotecan			GSH-conjugates
Melphalan Arsenite	Methotrexate					Sulfates
Sulfates	Sulfates					Taxans
Taxol	Vinblastine					Vinblastine
Vinblastine	Vincristine					Vincristine
Vincristine						
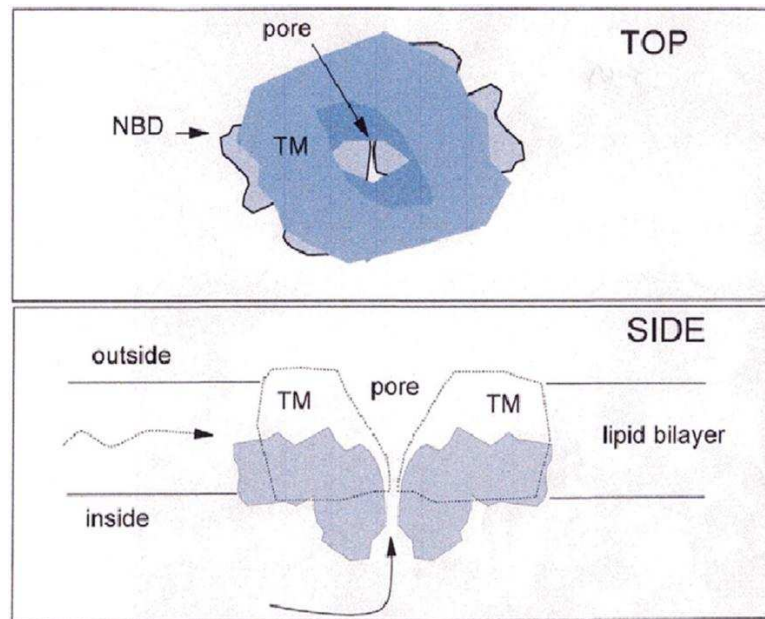
Figure 2.3: Basic structure of ABC transporters: ABC transporters consist of an aqueous pore with a large opening towards the extracellular region. The aqueous pore is made up of transmembrane domains (TMD), which spans the lipid bilayer of cell membrane. The nucleotide binding domain (NBD) which is partly embedded into the lipid bilayer faces the cytosolic part [95].
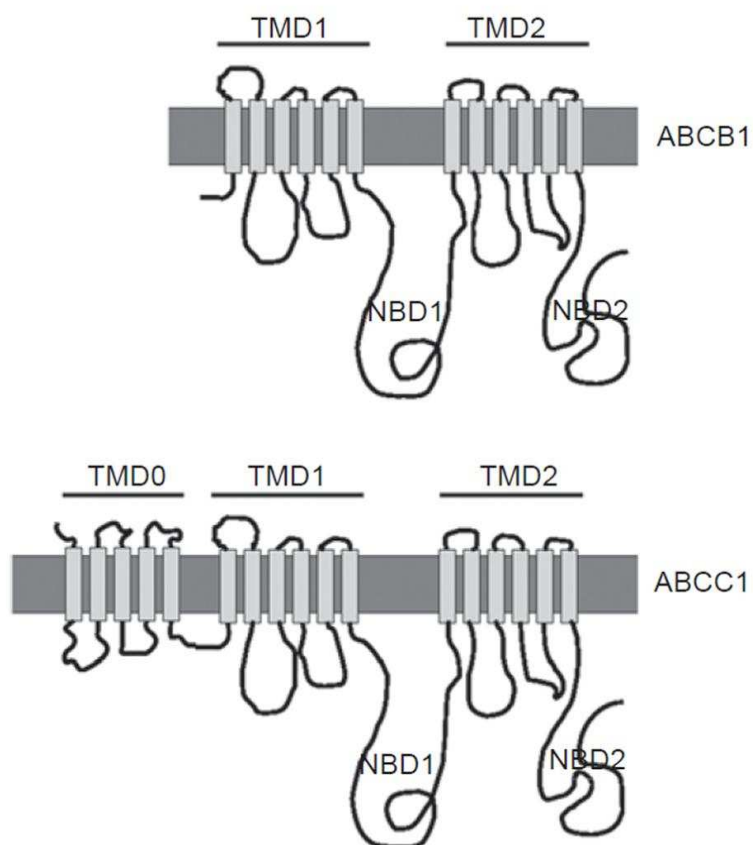
Figure 2.4: Schematic representation of the topological features of the ABC transporters: ABCB1 contains two transmembrane domain (TMD) and two nucleotide binding domain (NBD). In contrast ABCC1 contains three TMD and 2 NBD [96].
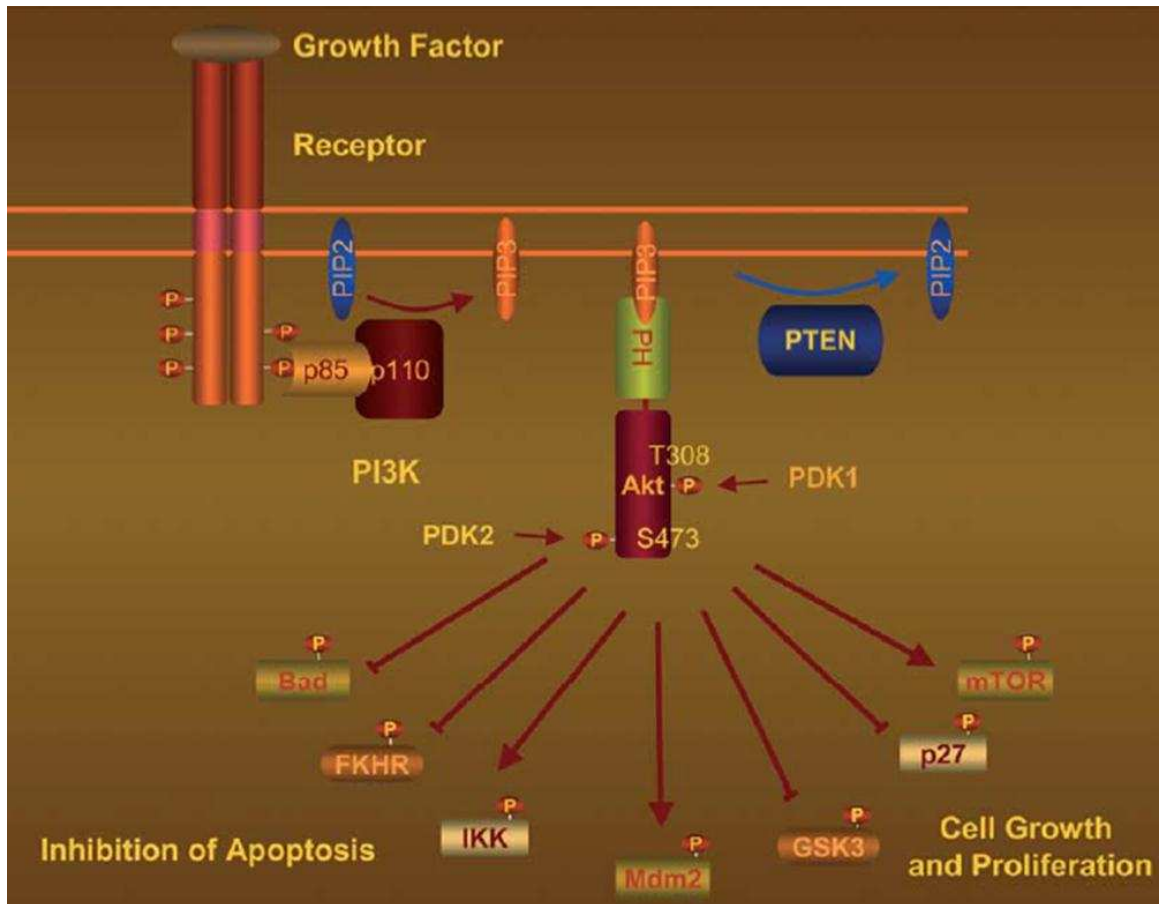
Figure 2.5: Activation of PI3K pathway. [101]
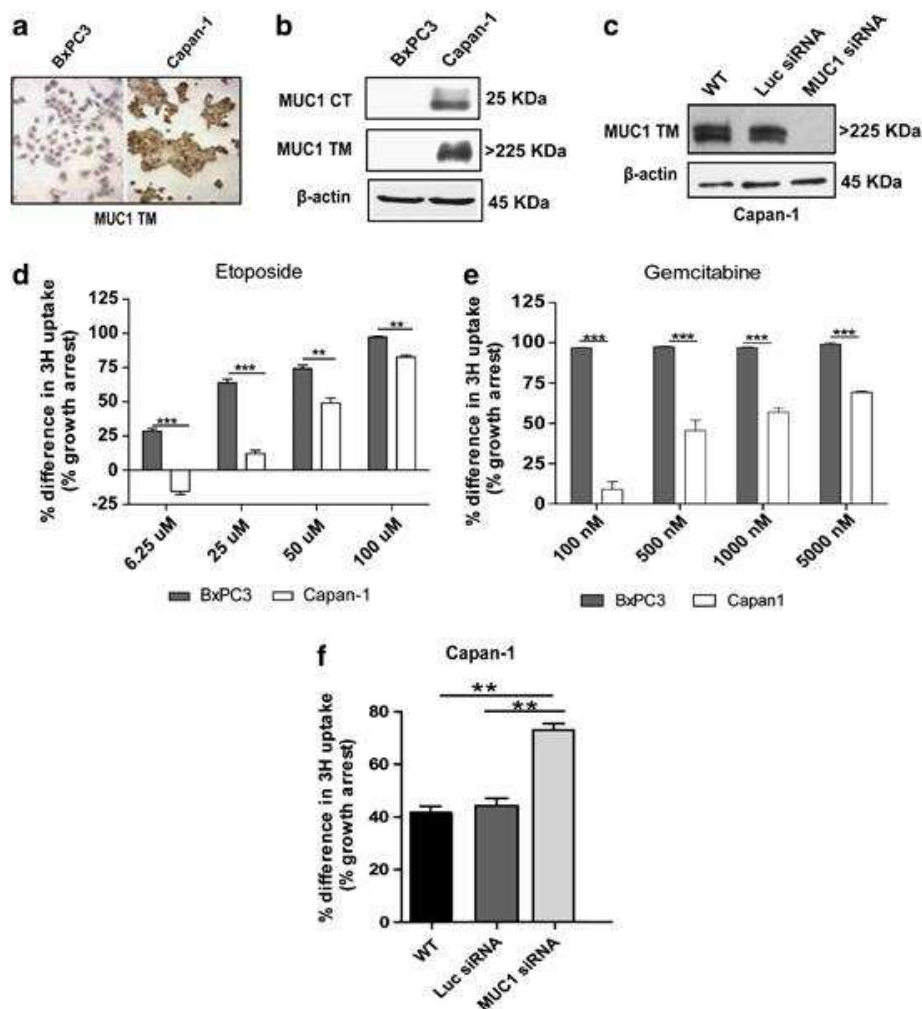
Figure 2.6: MUC1 expression and drug sensitivity of a panel of cancer cells: (a) Staining of endogenous MUC1 expression in BxPC3 and Capan-1 cells using HMFG2 antibody, Capan-1 expresses high levels as depicted by the brown staining whereas BxPC3 cells have negligible levels of MUC1 staining. (b) Western blot analysis of MUC1 expression in BxPC3 and Capan-1 cells by western blot using HMFG2 and CT2 antibody. (c) Western blot analysis of MUC1 expression in Capan-1 cells following treatment with MUC-1 specific siRNA (48 h). (d, e) H^3-thymidine incorporation to measure proliferation in PDA cells following 24 h treatment with etoposide and gemcitabine (n=4). Significantly higher proliferation was observed in Capan-1 cells, which express high levels of MUC1 (***P<0.001). (f) Percent difference in H^3-thymidine uptake in control siRNA and MUC1 siRNA treated cells as a function of Capan-1 WT cells. Cells were treated for 24 h with 500 nM of gemcitabine (n=4). Cells treated with MUC1 siRNA showed significantly reduced proliferation in response to gemcitabine as compared with untreated or control siRNA treated cells (**P<0.05).
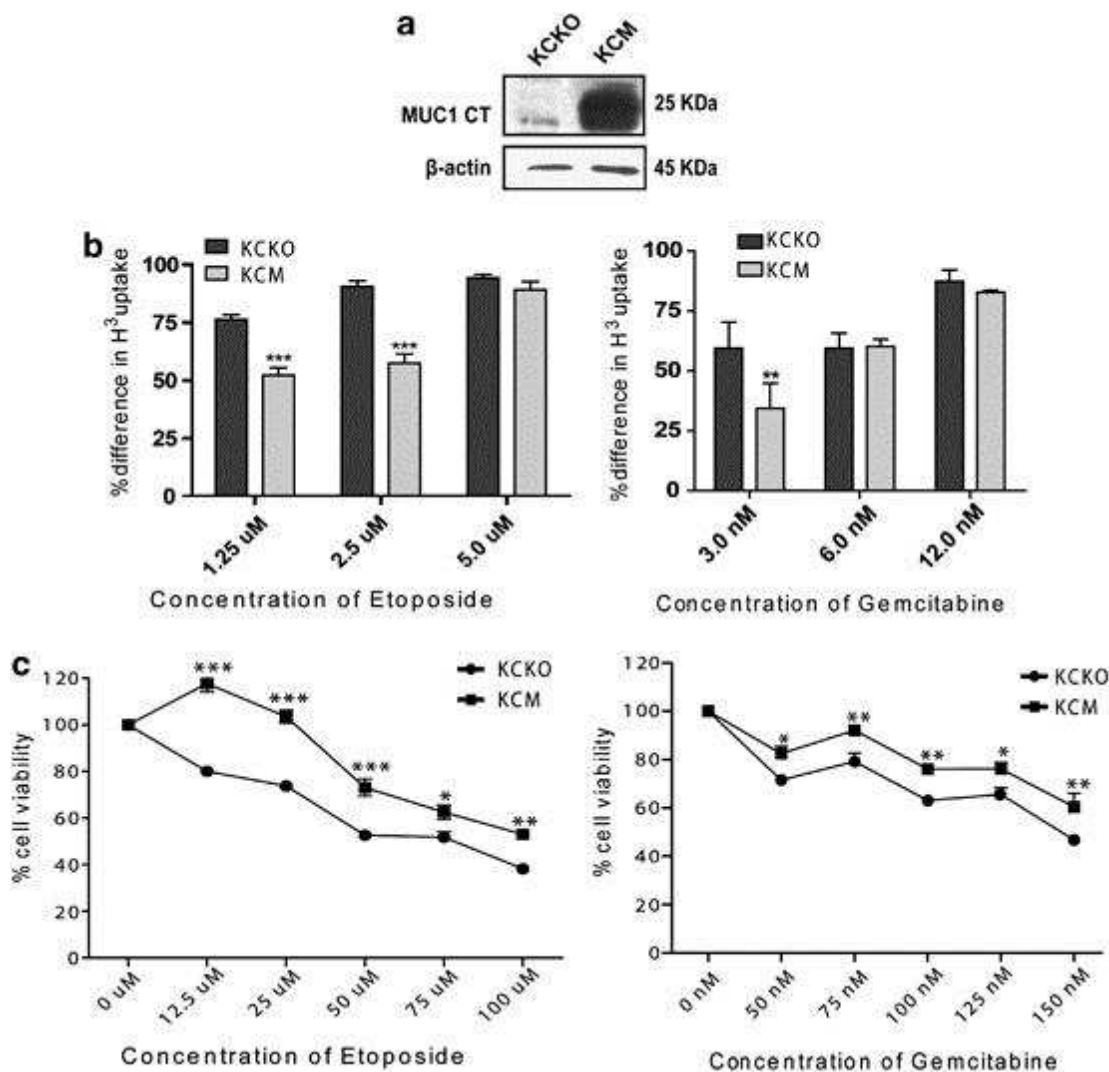
Figure 2.7: Endogenous expression of MUC1 in PDA cells confers resistance to cytotoxic drugs: (a) Western blot analysis of endogenous Muc1/MUC1 expression in mouse cells lines KCKO and KCM using CT2 antibody. Note: CT2 is the only antibody that recognizes both mouse and human Muc1/MUC1. (b) Percent difference in H^3 thymidine uptake in KCKO and KCM cells following 24 hours treatment with etoposide, and gemcitabine. Significant differences between KCKO and KCM cells at varying concentrations of the drugs is shown as p-values (n=4) (**$p<0.01$, *** $p<0.001$). (c) Cell viability in KCKO and KCM cells following 24 hours treatment with etoposide, and gemcitabine. Significant differences between KCKO and KCM cells at varying concentrations of the drugs is shown as p-values (n=6) (*$p<0.1$, **$p<0.01$, *** $p<0.001$).
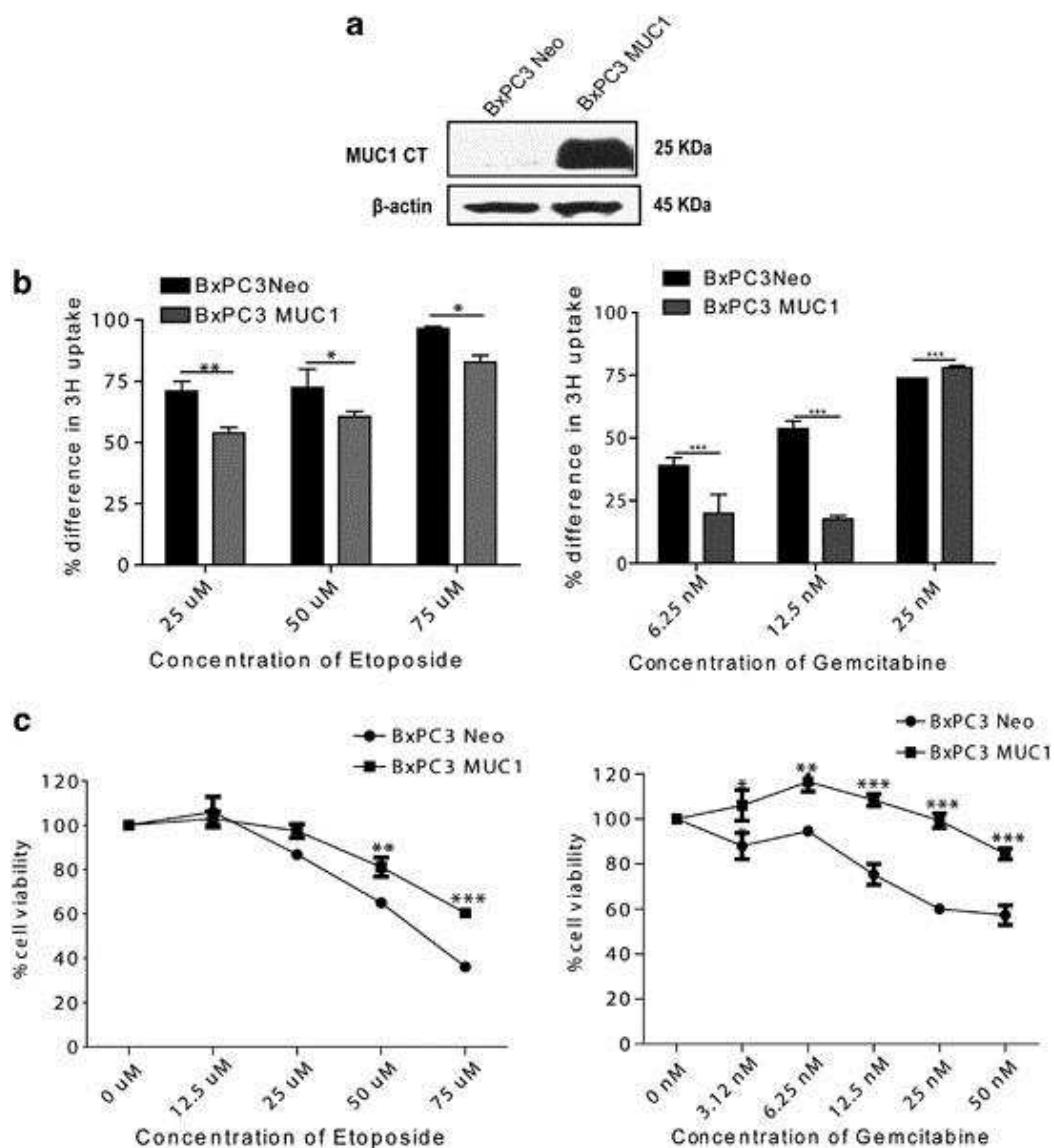
Figure 2.8: Exogenous expression of MUC1 in BxPC3 cells confers resistance to cytotoxic drugs. (a) Western blotting analysis of MUC1 expression in BxPC3 cells using CT2. (b) Percent difference in H^3 thymidine uptake of BxPC3 Neo and MUC1 cells following 24 hours treatment with etoposide and gemcitabine (n=4). Significant differences between BxPC3.Neo and MUC1 are shown (**$p<0.01$). (c). Cell viability in BxPC3 Neo and BxPC3 MUC1 cells following 24 hours treatment with etoposide, and gemcitabine. Significant differences between BxPC3 Neo and BxPC3 MUC1 cells at varying concentrations of the drugs is shown as p-values (n=6) ($p<0.1$, **$p<0.01$, *** $p<0.001$).
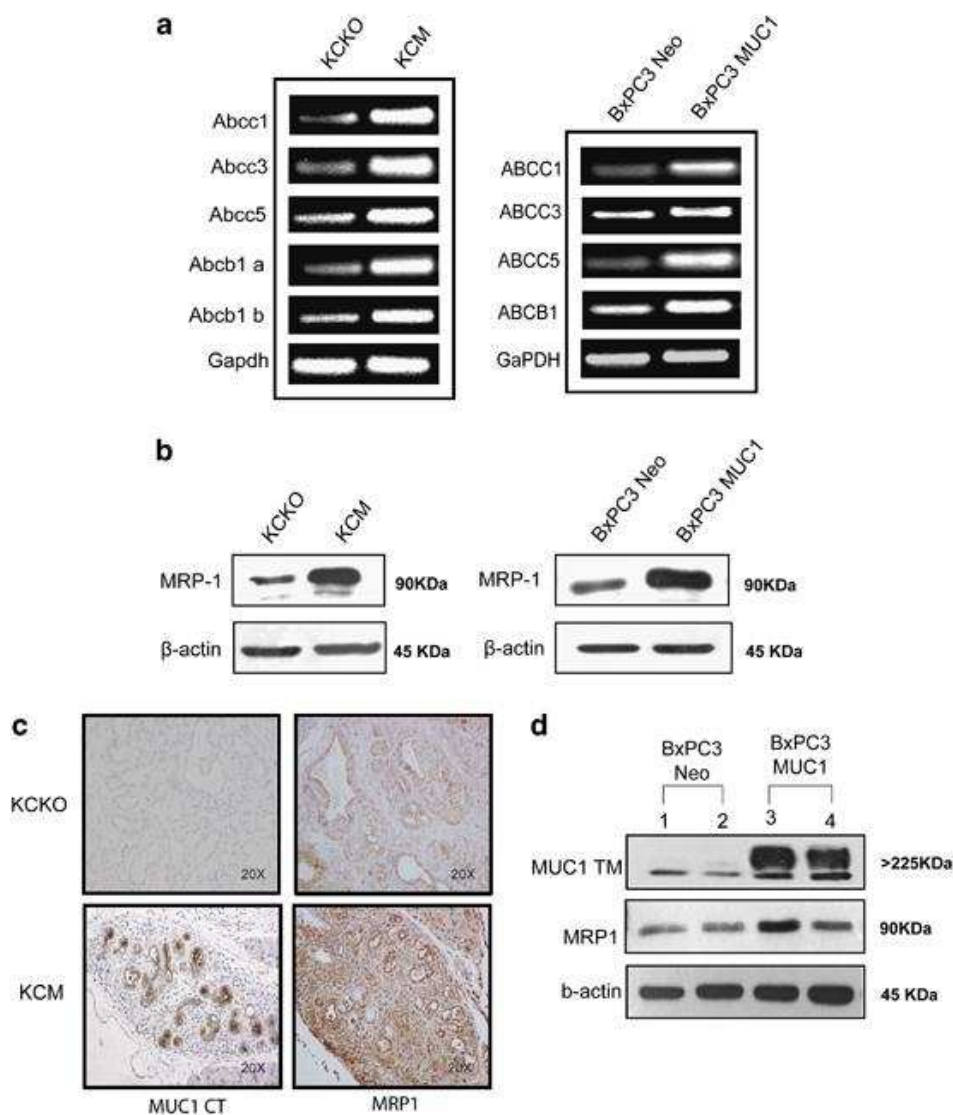
Figure 2.9: MUC1-positive PDA cells express elevated levels of MDR genes in vitro and invivo. (a) RT-PCR data showing fold changes in the m-RNA level of MDR genes that are associated with multidrug resistance. (b) Levels of MRP1 protein in BxPC3 Neo, MUC1, KCKO and KCM cell lysates analyzed by western blot. (c) IHC of MRP1 expression in the tumor sections from KCKO (24 weeks old) and KCM (16 weeks old) mice. Note: Two different time points were deliberately selected since the tumor burden in the KCKO mice at 24 weeks is equivalent to the tumor burden in 16-week old KCM mice. (d) Levels of MRP1 protein in BxPC3 Neo and MUC1 tumor lysates were determined by western blot.
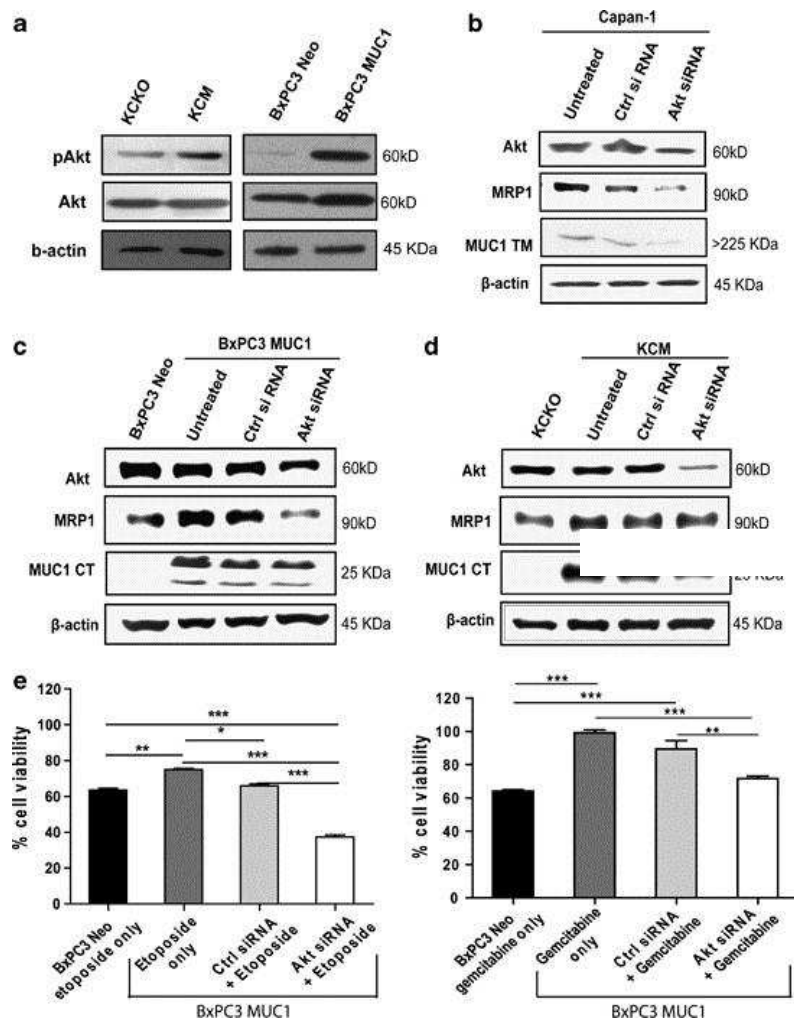
Figure 2.10: MUC1 induces MRP1 expression via Akt- dependent and -independent pathways. (a) BxPC3 Neo, MUC1, KCKO and KCM cell lysates were subjected to western blot analysis to determine phosphorylation of Akt. Level of unphosphorylated Akt served as control for phosphorylation. β-actin served as loading control. (b–d) Cells were treated with with 100 nM of Akt siRNA for 48 h, and the lysates were immunoblotted to evaluate the levels of Akt, MRP1 and MUC1. β-actin served as a loading control. (e) Cells growing in a 6-well plate were left untreated (WT) or treated with either control siRNA or Akt siRNA (100 nM). Thirty-six hours post treatment, cells were trypsinized, and equal number of cells was re-plated in a 96-well plate. The cells were allowed to adhere and, at 48 h, were left untreated or treated with 50 μM of etoposide and 25 nM of gemcitabine. MTT assay was performed to measure cytotoxicity 24 h post drug treatment.
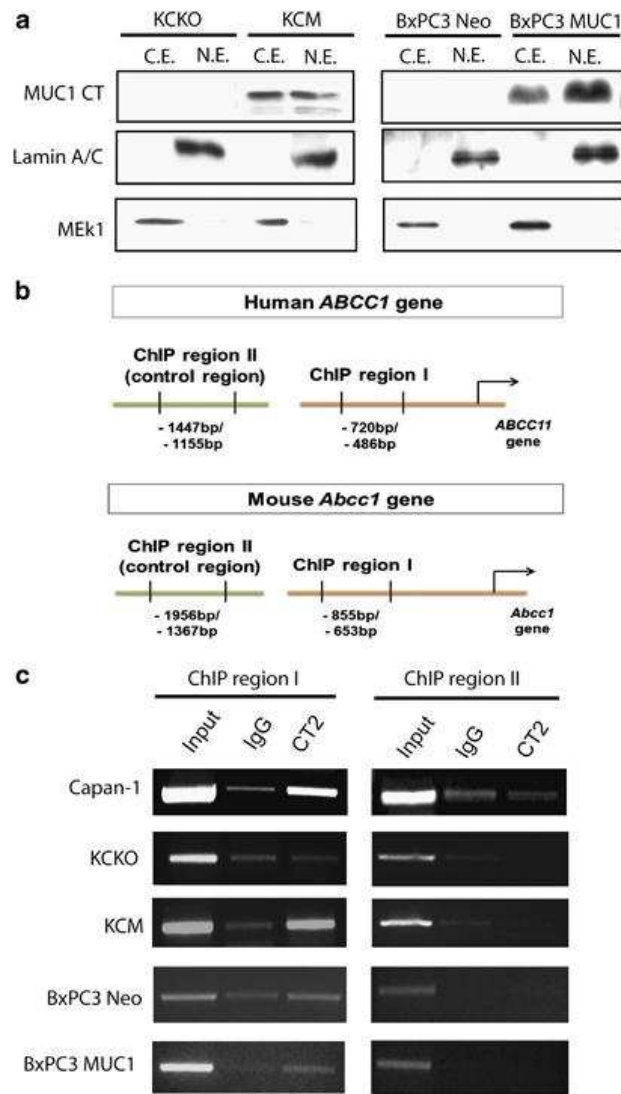
Figure 2.11: ChIP–PCR assay reveals an interaction between the MUC1 CT and the ABCC1 promoter region. (a) Nuclear lysates of KCKO, KCM, BxPC3 Neo and BxPC3 MUC1 cells were subjected to immunoblotting to determine the nuclear localization of MUC1 CT. Lamin and MEK1 were used as controls for nuclear and cytosolic fractions, respectively. (b) Schematic representation of the primers that were designed to PCR amplify the promoter region of human ABCC1 gene (top panel) and mouse Abcc1 gene (bottom panel) in ChIP assay. (c) ChIP–PCR; lanes include: Input DNA, DNA precipitated using control IgG and CT2, and amplified by PCR using Taq polymerase and separated by 2% agarose gel.
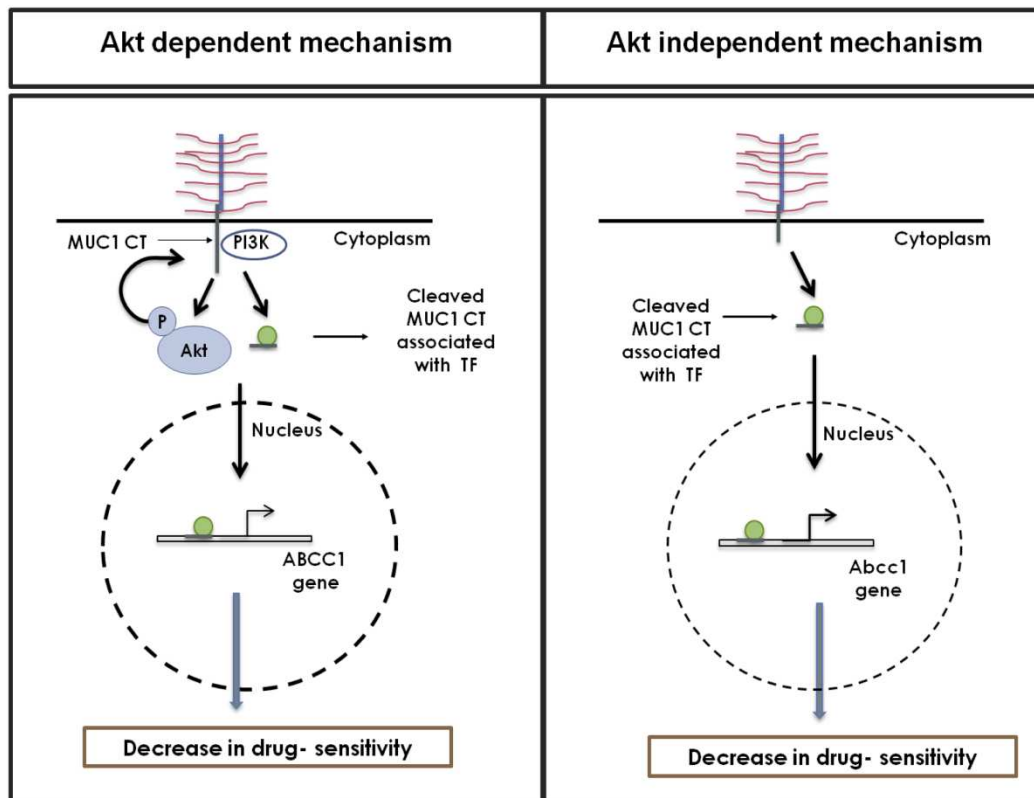
Figure 2.12: Schematic illustration of the two possible pathways by which MUC1 regulates MRP1 gene expression in PDA cells. In human PDA cell lines, Capan-1 and BxPC3 MUC1, MUC1-induced ABCC1 gene expression is dependent on PI3K/Akt pathway. The CT of MUC1 stimulates the PI3K/Akt pathway, which in turn increases MUC1 expression (left panel). In murine PDA cell line, KCM, MUC1-induced MRP1 expression is independent of the PI3K/Akt pathway (right panel). The CT of MUC1 translocates to the nucleus and binds to the promoter of ABCC1/Abcc1 gene, possibly acting as a part of the transcriptional complex that drives the expression of this gene (left and right panels).

CHAPTER 3: MUC1 POSITIVE PANCREATIC CANCER CELLS ACQUIRE GROWTH AND METASTATIC ADVANGTAGE THROUGH UPREGULATION OF COX-2 GENE.

3.1 Introduction

Cyclooxygenase (Cox) and prostaglandins (PGH):

Cyclooxygenase (Cox), also known as prostaglandin H2 synthase are a class of membrane bound bi-functional enzymes that calatyzes the rate limiting step in the conversion of arachidonic acid to prostaglandins (PGH). Prostaglandins include a large class of regulatory molecules, which mediate a wide array of crucial biological functions, such as regulation of immune function, inflammation, maintenance of gastrointestinal integrity, kidney development and reproductive biology [113]. Arachidonic acid (AA), an ω-6 polyunsaturated fatty acid (PUFA), abundantly distributed throughout the lipid bilayer is first oxidized to PGG2 by the oxygenase activity of Cox enzyme, which is further reduced to PGH2 by the endoperoxidase activity of Cox (Figure 3.1) [110]. Less commonly, Cox enzymes also catalyze conversion of Di-homo-γ-linolenic acid (DHLA) to PGH1 and eicosapentaenoic acid (EPA), a ω-3 fatty acid to PGH3. PGH2 is further converted into different isoforms by tissue specific isomerases (Figure 3.2). Prostaglandin E (PGE) isomerase is found in most cell types and PGE2 is the most abundant isoform.

Cox isoforms and their tissue expression profile:

Initially COX was thought to be a single enzyme that catalyzes the rate limiting step in the conversion of arachidonic acid to PGH. However, it soon became apparent that there are different isoforms of Cox, which have different expression profile and

physiological functions. Cox-1 is expressed constitutively in tissues such as kidney, lung, stomach, duodenum, jejunum, ileum, colon, and cecum. In contrast, Cox-2 is an inducible enzyme or early response gene. The basal level expression of Cox-2 is absent in most tissues, with the exception of CNS and kidney, which constitutively expresses Cox-2 [111]. LPS, tumor necrosis factor (TNF), interleukin (IL), interferon – γ, serum, epidermal growth factor (EGF), platelet activating factor (PAF), tumor growth factor -α (TGF-α), endothelin and arachidonic acid are some of the factors that induces Cox-2 gene and increases its expression in tissues [112]. Within a few hours of stimulation, the gene is induced, causing a spike in the levels of Cox-2 mRNA and protein, which returns to basal level within 24 hours of stimulation [111].

Cox genes, transcripts and proteins:

Cox isoforms are encoded by two different genes (PTGS1/Ptgs1 and PTGS2/Ptgs2), which are located on different chromosomes. Cox-1 is transcribed by Ptgs1 gene, located on human chromosome 11, whereas Cox-2 is transcribed by Ptgs2 gene, located on human chromosome 1. Ptgs1 gene consisting of 11 exons transcribes a 2.8kb long transcript. In contrast, Ptgs2 gene, consisting of 10 exons transcribes a 4 kb long transcript. The Cox-2 mRNA is relatively short lived due to the presence of 'Shaw Kamen instability' elements in the 3'UTR that affects its stability [111]. Inspite of substantial difference in the length and sequence of the transcripts, Cox-1 and Cox-2 proteins are very similar in length and molecular weight. Both Cox-1 and Cox-2 exits as homodimers in solution. Both Cox-1 and Cox-2 monomers are ~600 amino acids long and the molecular weight is ~71KD. Sequence homology study revealed 60%-65% sequence similarity between Cox isoforms from the same species and 85% - 90% sequence similarity between orthologs of different species[110].

General structure of Cox and the isoform specific structural differences:

The crystal structure shows significant three-dimensional structural homology between the different isoforms of Cox [113]. Broadly, the COX monomer consists of three domains: the N-terminal EGF like domain, a membrane binding domain (MBD) of about 48 amino acids, and a large C-terminal globular catalytic domain (Figure 3.4). The exact function of the EGF domain is still not known. The MBD domain comprises of β sheets which allows mototypic insertion of the enzyme into the lipid bilayer. The Cox catalytic domain constitutes bulk of the enzyme, which comprises of peroxidase (POX) catalytic site, cyclooxygenase (COX) active site and heme prosthetic group. POX active site lies in a large groove opposite to the MBD. The COX catalytic site is situated opposite to the POX site and heme prosthetic (Figure 3.4) group. A $25A^0$ long hydrophobic L shaped Cox channel extends from the MBD to the active site of COX catalytic domain. The Cox channel contains several side pockets and water channels. The Cox channel tapers to form a narrow aperture which separates the channel from the Cox catalytic site (Gly 533). 24 non-polar amino acids and only 3 polar amino acids line the hydrophobic COX active site [114]. Arg120 binds the carboxylate group of arachidonic acid (AA) at the COX active site, whereas the ω-methyl group of AA lies at the narrow terminus of the channel. This places carbon-13 of AA in close proximity to Tyr-385, which is a critical amino acid required for the COX activity. The active site of Cox-2 is 20% bigger and is of different shape in comparison to Cox-1. The cyclooxygenase active site in Cox-2 has 3 amino acids substitution. Ile 434, Ile 523 and His-513 in Cox-1 are substituted by Val-434, Val-523 and Arg-513 in Cox-2 [114]. This dramatically increases the substrate binding pocket of Cox-2 and consequently broadens its substrate specificity. Cox-1 and Cox-2 have same specificity for AA, but Cox-2 is more efficient at catalyzing

the conversion of bulkier fatty acids such as lenolenic acid and eicosapentanoic acid [111]. Another difference between Cox isoforms is that the length and sequence of amino acids vary considerably around the signal peptide in C-terminus. The signal peptide in Cox-2 consists of an 18 amino acids insert, 6 amino acids away from the end of the C-terminal. However the insert does not disrupt the last 4 amino acids in the C-terminal, which contains the ER-targeting signal. It is believed that the 18 amino acid insert in Cox-2 acts as a nuclear membrane targeting signal, which explains for the presence of Cox-2 in both ER and nuclear membrane [111].

Both Cox-1 and Cox-2 are N-glycosylated at three sites (Asn68, Asn 144 and Asn 410). Cox-2 is N-glycosylated at an additional site (Asn 588). Cox-1 is uniformly glycosylated, whereas, Cox-2 is heterogeneously glycosylated and hence the molecular weight of Cox-2 ranges from 65Kda to 80KDa [111]. Studies have shown that N-glycosylation of Cox enzymes are required for the maturation of the protein but is not essential for their catalytic activity.

Selective inhibitor of Cox-2 - Celecoxib:

The classical non-steroidal anti-inflammatory drugs (NSAID), such as aspirin and ibuprofen are competitive cyclooxygenase inhibitors and they inhibit enzyme activity of both Cox-1 and Cox-2. However, use of NSAID leads to serious side effects, such as gastric lesions and renal toxicity, as NSAID have higher specificity for Cox-1 enzyme and inhibition of Cox-1 activity leads to disruption of the cryoprotective function of Cox-1 [113]. The 2nd generation Cox inhibitors, such NS398, Celecoxib, Refecoxib etc have reduced toxicity as they are specifically designed to inhibit the Cox-2 activity. Celecoxib has 100-1000 times more specificity for Cox-2 compared to Cox-1. Celecoxib, is

approved for clinical use by FDA and is routinely used for treating symptoms of osteoarthritis and rheumatoid arthritis [115].

The Cox-1 and Cox-2 enzyme has minute structural differences around the opening of the Cox channel and catalytic site. These minute structural differences have been exploited for designing Cox-2 specific inhibitors. The last of the four helices in the MBD of Cox-2 is cantilevered upward, which creates a bigger opening of the Cox channel and allows bulkier celecoxib in accessing the catalytic site of Cox-2 (Figure 3.5)[110]. Moreover, His-513 substitution to Arg-513 alters the chemical environment in the side pocket of the cyclooxygenase active site. Positively charged Arg-513 interacts with 4-methylsulfonyl of Celecoxib (Figure 3.6).

Link between inflammation, cancer and Cox-2:

Cox-1 is important for cryoprotection and for maintaining tissue homeostasis. In contrast, Cox-2 is expressed in response to growth factors and inflammation. The link between cancer and inflammation has been long appreciated. Among a long list of proinflammatory molecules that has been closely linked to cancer, Cox-2 plays a critical role in the pathogenesis and progression of cancer. In a vast majority of malignancies, Cox-2 and its metabolite PGE2 is frequently overexpressed, and its overexpression is associated with aggressive phenotype and poor prognosis of cancer. Cox-2 is important for both the initiation and progression of cancer. Cox-2 induces production of reactive oxygen species (ROS) and reactive nitrogen intermediates (RNI), which in excess can induce oxidative DNA damage leading to genetic mutations. Cox-2 allows cancer progression by promoting proliferation, invasion, metastasis, angiogenesis, and resistance to apoptosis. Cox-2 is also known to attract and retain myeloid derived suppressor cells (MDSC), which suppress T cell activation and thereby causes profound immune

suppression around the tumor microenvironment [116], [117] . The multifaceted role of Cox-2 in cancer underscores the importance of studying the regulation of Cox-2 gene expression in malignant cells.

Previously, we reported that in PDA.MUC1 transgenic mouse, overexpression of MUC1 is detected at early stage PanIN lesions and its expression steadily increases as the cancer progresses. Similarly, a stage dependent increase in Cox-2 expression was observed in these mice (Figure 3.7) [118]. So, we asked ourselves the question, does MUC1 exert its tumorigenic effect in PDA via Cox-2/PGE2 signaling axis and if so does MUC1 directly regulates Cox-2 gene expression. In this paper, we report for the first time that MUC1 directly regulates Cox-2 gene expression via NF-kB dependent pathway and that inhibition of Cox-2 leads to a reduction in the proliferation and invasive potential of the MUC1 high PDA cells.

3.3 Materials and Methods

Cell Lines and stable transfection:

The human PDA cell lines Hs766T, Capan-2, HPAFII, HPAC and CFPAC, BxPC3, Capan-1 and Mia-Paca-2 were obtained from the ATCC (Manassas, Virginia, USA). Cells were cultured in DMEM, MEM and RPMI media supplemented with 10% fetal bovine serum (FBS), essential amino acids and antibiotic. The cells were maintained in 5% CO_2, 95% air at 37°C. BXPC3 cells, expressing low levels of endogenous MUC1, were stably transfected with empty vector or full-length MUC1 construct expressing neomycin resistance gene as selection marker to generate BxPC3 Neo and BxPC3 MUC1 respectively [62]. Cells were selected with 0.5 mg/mL G418 for 48 hours post infection and were sorted using FACS Aria to isolate MUC1+ve cells. Expression of the

constructs was stable throughout the span of experiments and the level of MUC1 expression was validated using Western blot.

Mouse model and mouse cell lines:

In our laboratory, we generated mice that spontaneous develop pancreatic ductal adenocarcinoma (PDA) by mating the P48-Cre with the LSL-KRAS^{G12D} mice. PDA mice were further mated to the MUC1.Tg mice (that express human MUC1) to generate PDA.MUC1 mice or to the Muc1 knockout mice to generate PDA.MUC1KO mice. All these mice were on the C57/B6 background. Cell lines were generated from the primary tumors of PDA.MUC1 and PDA.Muc1 KO mice and were designated as KCM and KCKO respectively. Panc02 Neo and Panc02 MUC1 cell lines were generously donated by Dr. Michael Hollingsworth.

Transient knockdown of target genes using siRNA:

Cells plated in a 6well plate in antibiotic free complete media upon reaching 30% confluence were trasfected with 100-200nM of smart pool MUC1 siRNA (DHARMACON, Thermo Fisher Sc.) and 100-200nM of scramble control siRNA (Cell Signaling) using Lipofectamine 2000 (Invitrogen) for 5–6 hours in serum-free Opti-MEM (Invitrogen). Cells were washed with PBS and replenished with media supplemented with FBS. Whole cell lysates prepared 48, 72, and 96 hours post siRNA treatment were subjected to western blot to determine the efficiency of MUC1 knockdown.

Western blots:

Cell lysates were prepared using RIPA buffer and 30-60ug of protein were subjected to denaturing SDS–PAGE and western blot. The PVDF membrane was probed with anti MUC1 antibody CT2, anti- NFkB (Cell Signaling Technology, Danvers, MA, USA), anti-Cox-2, anti- Lamin A/C and anti-β-actin (Santa Cruz, CA, USA) antibodies.

Appropriate secondary antibodies conjugated to HRP were sued and chemiluminescence kit was used for detection. All antibodies were used according to manufacturer's recommendations.

Preparation of nuclear extract:

Cells grown in 10cm plate upon reaching 85% confluence were lysed with appropriate buffers provided in the EMD Millipore nuclear extraction kit, to isolate the nuclear and the cytosolic fractions.

Serum PGEM by ELISA:

Serum PGE_2 levels were determined using a specific ELISA kit (Cayman Pharmaceuticals, Ann Arbor, MI) that measures for the PGE_2 metabolite (PGEM; 13,14-dihydro 15-keto prostaglandin A_2). The protocol was followed as recommended by the manufacturer. Results were expressed as pg/ml of PGE2 or PGEM.

Human samples:

Tissue sections of pancreatic adenocarcinoma (PDA) and normal pancreas were obtained from the NIH/NCI tissue repository (http://seer.cancer.gov/biospecimen). The serums of PC patients of different stages were also obtained from NCI.

Mouse Tumor Samples:

$1X10^6$ BxPC3 Neo and MUC1 cells were injected subcutaneously in each nude mice to grow BxPC3 Neo and MUC1 xenografted tumors. A month later, mice were sacrificed and tumors and other organs were harvested for IHC and for preparation of tumor lysate. PDA mice were sacrificed at between 16 weeks and 40 weeks to obtain KCKO and KCM tumors. Paraffin embedded blocks of formalin fixed tumor sections were made by the Histology Core at Mayo Clinic. 4 micron thick sections were prepared for immunohistochemical staining.

Immunohistochemistry:

The tumor sections were treated with Dako antigen retrieval solution at 95°C for 20-40 min followed by cooling it at RT for 20 min. To quench endogenous peroxidase, slides were rinsed, incubated for 10 minutes in methanol/2% H_2O_2 solution. Sections were washed, blocked in 5% normal bovine serum for 45 min, and incubated overnight at 4°C with primary antibodies. Sections were incubated 1 h with appropriate secondary antibody, developed with a diaminobenzidine (DAB) substrate, counterstained with hematoxylin, and mounted with Permount. Primary antibodies used were: Armenian hamster anti-MUC1 cytoplasmic tail (CT) CT2 (1:50, own), goat anti-COX-2 (1:100; Santa Cruz Inc). Secondary antibodies were anti-hamster (1:250, Jackson Labs), and anti-goat (1:100, Dako) IgGs conjugated to horseradish peroxidase. Immunopositivity was assessed using light microscopy and images taken at 20× magnification.

Chromatin Immunoprecipitation (ChIP):

Cells grown to near 80% confluence, were cross-linked with formaldehyde (Sigma) at room temperature for 10 min. Cross-linked chromatin prepared with a commercial ChIP assay kit (EZ-Magna ChIP; Millipore) was immunoprecipitated with normal Armenian hamster IgG (1:20) (Santa Cruz Biotechnology, CA, USA), anti-MUC1 CT antibody (CT2) (1:15) and anti-NF-kB (1:20) antibody. MUC1 CT binding site on Cox-2 gene promoter was amplified by PCR using the input DNA (2%) or DNA isolated from precipitated chromatin as templates and using primers flanking the promoter region -377/-175 bp upstream (ChIP region I) and +8320/+8550 bp downstream (ChIP region II) of transcription start site (TSS) of mouse Cox-2 gene (Fig. 3.11b, top panel) and -346/-118 bp upstream (ChIP region I) and -4053/3820 bp upstream (ChIP region II) of human COX-2 gene (Figure 3.11b, bottom panel). IgG was used as a

negative control for immunoprecipitation step and ChIP region II was used as a negative control for binding of MUC1 CT and NFkB to the promoter region. Sequence of the primers is available upon request.

Semi-quantitative and quantitative RT-PCR:

Total RNA was extracted from the cells by TRIzol (Invitrogen) according to the manufacturer's protocol. 1–2 μg of the extracted RNA was used as template for semi-quantitative RT-PCR reaction (Access quick RT-PCR kit, Promega, Madison, WI, USA) and real time RT- PCR (KAPA SYBR Fast One-step qRT-PCR kit). Sequence of the primers is available upon request.

Cell growth by MTT assay:

10×10^3 cells were plated in quadruplicate in normal growth medium in 96-well plates and were permitted to grow for 18 hours. Cells were left untreated or treated with Celecoxib (Pfizer, CN, USA) for 24 hours. Next, MTT (Biotium) solution was added (10 ul/well) to cells, incubated for additional 3-4 hours. In the final step, media was removed, formazan was dissolved in DMSO (200ul/well) and the absorbance was read on an ELISA plate reader.

Invasion assay:

Cells were grown on culture dish and serum-starved for 18 h before plating for the invasion assay. In a 24 well plate, 50,000 cells in serum-free media with or without Celecoxib were plated over transwell inserts (BD Biosciences, San Jose, CA, USA) precoated with reduced growth factor matrigel (BD Biosciences, San Jose, CA, USA). Cells were allowed to invade through the matrix toward the serum supplemented media contained in the bottom chamber over a period of 36 h. Percent invasion was calculated as absorbance of samples/absorbance of controls*100.

Densitometric quantification of western blot analyses: For quantification of the bands of Western blot and semi-quantitative RT-PCR, densitometric analysis was performed using image analysis software (Image J) from the National Institutes of Health (Bethesda, MD).

Statistical Analysis: Statistical analysis was performed with GraphPad software.

3.3. Results

Human PDA sections express high levels of MUC1 and Cox-2 protein:

Overexpression of Cox-2 is frequently observed in pancreatic cancer. The objective of the study was to first analyze if Cox-2 is overexpressed in PDA and if so does its expression correlate with MUC1 overexpression. We performed IHC to determine the MUC1 and Cox-2 expression in human PDA sections and compared it with adjacent normal pancreas sections. All four human PDA sections stained strongly for both MUC1 and Cox-2 in comparison to the adjacent normal pancreas indicating that MUC1 and Cox-2 are overexpressed in PDA and there is a possible link between the coexpression of these two molecules in human PDA. (Figure 3.8A) We next analyzed the PGE2 levels in serum obtained from PDA patients diagnosed with stage 0 to stage 4 of PDA. We detected 63.8 pg/ml, 118 pg/ml, 148.8 pg/ml and 210 pg/ml of PGEM/ml of serum in stage 0, stage 2, stage 3 and stage 4 samples respectively (Figure 3.8B). There was a 4 fold increase in the serum PGEM levels in stage 4 PDA patients compared to stage 0 PDA patients. Our data indicates that during the progression of human PDA, serum PGEM levels progressively increases in a stage dependent manner, implicating a possible role of Cox-2 in the progression of the disease. Similarly, there was a steady increase in levels of MUC1 in the same serum samples [119] (Appendix, figure 1).

Cox-2 is overexpressed in PDA cell lines that endogenously express high levels of MUC1:

To validate our observation of positive correlation between MUC1 and Cox-2 expression in human PDA, we examined a panel human PDA cell lines that express various levels of endogenous MUC1 and analyzed basal MUC1 and Cox-2 levels by western blot. HPAFII, HPAC, CFPAC and Capan-1 PDA cell lines express high levels of endogenous MUC1, whereas BxPC3, Hs766T, Capan-2 and MiaPaca-2 express low levels of endogenous MUC1 (Figure 3.9 A). We found that that MUC1 high HPAFII, HPAC, CFPAC and Capan-1 cells expressed higher levels of Cox-2 compared to MUC1 low Hs766T, Capan-2 and Mia-Paca-2. However, BxPC3 cell line showed significantly high levels of Cox-2 expression inspite of having low levels of endogenous MUC1 (Figure 3.9 A). This observation is similar to what has been reported before in a study where a panel of PDA cells lines were evaluated for endogenous Cox-2 levels and BxPC3 was reported to be a very high Cox-2 expressing cell line [120]. This may be due to the fact that BxPC3 is known to have a normal ras proto-oncogene while all other cell lines have mutated ras [121]. Out of the eight human PDA cell lines that were included in the study, seven cell lines exhibited a positive correlation between MUC1 and Cox-2 expression.

Overexpression of MUC1 augments Cox-2 expression and a simultaneous attenuation upon MUC1 downregulation:

We next performed a gain of function and loss of function study, to determine if Cox-2 gene expression is altered upon manipulation of MUC1 levels in the PDA cell lines. We found that BxPC3 and Panc02 cells stably transfected with full length MUC1 express 3.3 fold and 2.6 fold higher Cox-2 levels respectively in comparison to

BxPC3 and Panc02 cells stably transfected with the empty vector (Figure 3.9B, supplemental table 1). Similarly, mouse PDA cell line KCM cells that genetically express MUC1 express 3.9 fold higher Cox-2 compared to KCKO cells that are genetically null for MUC1 (Figure 3.9B, supplemental table 1). Next, we transiently knocked down MUC1 expression transiently using MUC1 specific siRNA in MUC1 high HPAFII and HPAC cell lines and evaluated the levels of Cox-2 by western blot. Following MUC1 downregulation, we observed a 3.5 fold decrease in Cox-2 expression in HPAFII cells (Figure 3.9C, supplemental table 2) and a 5.8 fold decrease in the Cox-2 expression in HPAC cells (Figure 3.9C, supplemental figure 2). Thus we observed that overexpression of MUC1 in PDA cells lines causes an increase in MUC1 expression and downregulation of MUC1 causes a decrease in MUC1 expression indicating that Cox-2 gene in PC is regulated by MUC1.

IHC was performed to compare MUC1 and Cox-2 expression between tumors from PDA mice that are null for MUC1 (KCKO) or express MUC1 (KCM). As expected, KCKO do not show any staining for MUC1 and expresses low levels of Cox-2, whereas, KCM tumors show strong membranous and cytoplasmic MUC1 staining and show abundant Cox-2 tissue expression. BxPC3 Neo and BxPC3 MUC1 xenografted tumors were also stained for MUC1 and Cox-2 expression. BxPC3.MUC1 tumors expressing high levels of MUC1 also show high Cox-2 expression in comparison to MUC1 low BxPC3 Neo tumors.

We performed IHC on mouse PDA tumors that are null for MUC1 (KCKO) or MUC1 positive (KCM) to evaluate the coexpression of MUC1 and Cox-2 insitu. KCKO tumors did not stain for MUC1 and showed low Cox-2 expression as indicated by weak brown staining. In contrast KCM tumors showed high expression of both MUC1

and Cox-2, as indicated by the strong brown staining (Figure 3.10, left panel). Staining for Cox-2 and MUC1 xenografted tumors showed similar trend. As expected, MUC1 high BxPC3MUC1 tumors showed higher expression of Cox-2 compared to MUC1 low BxPC3 Neo tumors (Figure 3.9, right panel).

MUC1 high PDA cells express high levels of Cox-2 mRNA:

We next evaluated the levels of Cox-2 mRNA in PDA cell lines expressing variable levels of MUC1. The steady state levels of Cox-2 mRNA was significantly higher in MUC1 positive Panc02 MUC1 and KCM cells compared to MUC1 low KCKO and Panc02 Neo cells (Figure 3.10A). We observed 2.14 fold higher Cox-2 mRNA in Panc02 MUC1 cells in comparison to Panc02 Neo cells by real time qPCR (Figure 3.10B). A significant decrease (13.9 fold) in Cox-2 mRNA level was observed upon transient knockdown of MUC1 in HPAFII cells (Figure 3.10A). This data suggests that Cox-2 gene is upregulated in MUC1positive PDA cell lines.

MUC1 and NFkB colocalizes and binds to the promoter of the Cox-2 gene:

We next sought to investigate the molecular mechanism of MUC1 induced Cox-2 gene regulation. The 5'UTR of human COX-2 gene contains a TATA box and several potential transcriptional regulatory elements such as CRE (59/53), NF-IL6 (-132/-124) and NF-kB (-233/-214 and -448/-439) and mouse Cox-2 gene contains CRE-2 (-438/-428), NF-kB (-400/-392), C/EBP (-136/-128) and AP-1 (-67/-62), that are essential for Cox-2 gene expression [122], [123] In colon cancer, NF-kB is important for transcriptional regulation of Cox-2 gene as indicated by attenuation of Cox-2 expression upon NFkB downregulation in colon cancer cells [124], [125]. Previously it was reported that MUC1 CT constitutively associates with NF-κB p65 subunit and prevent IkBα from binding to NF-κB p65. MUC1 also promotes the occupancy of NF-κB transcriptional

complex to the promoter of NF-κB p65 target gene Bcl-xL gene and thereby increases its expression [65]. Thus, we explored the possibility if MUC1 and NF-κB co-localizes to the promoter of the COX-2/Cox-2 gene and drives its expression.

We first evaluated the nuclear localization of MUC1 CT and NF-κB p65 in the human and mouse PDA cell lines under basal level. We observed presence of MUC1 CT in the nucleus of Panc02 MUC1, KCM, HPAFII and HPAC cells and absence of MUC1 CT in the nucleus of Panc02 Neo and KCKO cells (Figure 3.11A, top panel). We did not observe any significant difference in the levels of NF-κB p65 in the nucleus of MUC1 null KCKO, Panc02 Neo and MUC1 positive KCM and Pan02 MUC1 cells (Figure 3.11A). This data indicated that the nuclear localization of NF-κB p65 is not affected by the presence or absence of MUC1 in the cells. This observation is in contrast to what has been reported before that downregulation of MUC1 in ZR-75-1 breast cancer cells cause a decline in the nuclear accumulation of NF-κB p65. This could be possibly because of differences in tumor origin.

We performed ChIP to examine the binding of MUC1 CT and NF-kB p65 to the promoter region of mouse and human Cox-2 gene. We immunoprecipitated sheared chromatin using anti-p65 antibody and anti-MUC1 CT antibody. The immunoprecipitated chromatin was PCR amplified using primers design around the NF-kB response element in the promoter region of Cox-2 gene. In MUC1 positive KCM cells, we observed MUC1 CT and NF-kB p65 binding to ChIP region I, containing the NFkB RE in the promoter region of Cox-2 gene. In contrast, in KCKO cells, in absence of MUC1, NF-kB p65 no longer binds to ChIP region I in the promoter region of Cox-2 gene (Figure 3.11C, left panel). We observed similar trend in Panc02 Neo and Panc02 MUC1 cells (Figure 3.7.B). Further analysis of HPAFII cells showed that increased occupancy of NF-kB p65 in the

ChIP region I of Cox-2 gene is associated with MUC1 CT. As a control, there was no detectable signal in the immunoprecipitates performed with nonimmune IgG (Fig. 3B). There was also no detectable MUC1 CT and NF-nB p65 occupancy in the control region (ChIP region II) downstream of the Cox-2 promoter (Fig. 3.11C, right panels).

Blocking Cox-2 activity by Celecoxib reduces proliferation and invasion in PDA cells:

Among several factors that are known to augment proliferation and invasive phenotype of cancer cells, Cox-2 is thought to be one of the key players. In colon, breast and PDA cells, Cox-2/PGE2 signaling axis promotes proliferation, survival and invasion [126], [127], [128]. In non-small cell lung cancer (NSCLC), Cox-2 promotes invasion through decreased production of CD44, MMP-2 and EP4 receptors [129]. Another study showed that in NSCLC, Cox-2 induces invasion by suppressing E-cadherin expression via transcriptional suppressor ZEB1[130]. Previously we and others have shown that overexpression of MUC1 increases the proliferative index and invasive potential of the PDA cells [58], [61], [62], [63], [131]. So, we hypothesized that MUC1 promotes proliferation and invasiveness in cancer cells through Cox-2. In this study, we inhibited Cox-2 activity in MUC1 high PDA cells with Celecoxib and analyzed if Cox-2 inhibition negatively affects growth and invasive potential of PDA cells.

We first treated MUC1 high and low PDA cell lines HPAFII, HPAC, KCM and KCKO with increasing concentration of Celecoxib and 24 hours later performed MTT assay to evaluate the growth arrest. At 50uM, 75uM and 100uM of Celecoxib, we observed 18.9%, 42.7% and 56.4% of growth arrest in HPAFII cells (Figure 3.12A.I.), and 16%, 47.1% and 59.6% of growth arrest in HPAC cells (Figure 3.12C.I). Similarly, in KCKO and KCM cells, we observed a similar dose dependent increase in growth arrest

upon blocking Cox-2 with Celecoxib. At 25uM, 50uM, 75 uM and 100 uM of Celecoxib, 20%, 42.4%, 62.5% and 81.5% of growth arrest in KCKO cells and 15.5%, 29.7%,49.2% and 71% growth arrest in KCM cells was observed. However, in comparison to KCKO, KCM were more resistant to growth arrest, although Cox-2 was sufficiently blocked in both cell lines as indicated by the western (Figure 3.12C.II). This could be due to hyperactivation of the prosurvival pathway PI3K/Akt in KCM cells, which counteracts the growth inhibitory effect of Celecoxib [57]. Overall blocking Cox-2 activity caused a profound growth arrest in PDA cells, indicating that Cox-2 is important for the growth of these cells. However this inhibition of growth is independent of MUC1 expression as both MUC1-high and low expressing PDA cells responded to celecoxib.

We next evaluated the expression of Cox-2 and MUC1 protein upon Celecoxib treatment to a) determine the level of Cox-2 blocking and b) to analyze if MUC1 expression is affected upon inhibiting Cox-2 activity. In HPAFII, HPAC, KCKO and KCM cells, a gradual decrease in the Cox-2 protein is observed upon treatment of the cells with increasing of Celecoxib (Figure 3.12A.II, B.II and C.II). However, we did not observe the MUC1 levels to change upon blocking Cox-2 activity, indicating an absence of feedback loop between Cox-2 and MUC1. They share a unidirectional relationship, where Cox-2 gene is under MUC1 regulation and not the other way around. Interestingly in HPAC cells, we observed a moderate increase in MUC1 expression upon exposure to Celecoxib (Figure 3.12 B.II).

We next evaluated the invasive potential of a panel of human PDA cell lines that express high levels of Cox-2. Mia-Paca-2 cell line, which is null for Cox-2 was included as a negative control. We found that HPAFII, HPAC and Mia-Paca-2 cells were 13.5%, 10.85% and 11.8% invasive, whereas CFPAC was 24.6% invasive (Figure

3.13A). Thus, although HPAFII, HPAC and CFPAC cells express high endogenous MUC1 and Cox-2, their inherent invasive potential is different because the cohort of mutations in these cell lines is also different. Next we treated CFPAC cells with Celecoxib, to determine if blocking Cox-2 activity attenuates its invasive potential. We observed a 2 fold decrease in the invasive potential of CFPAC cells upon treatment with 15uM and 30 uM of Celecoxib (Figure 3.13B), indicating that Cox-2 is important the invasiveness of the cell line. KCM cells which express higher levels of Cox-2 is 82% invasive in comparison to KCKO cells which is 60% invasive. 1.6 fold (51.6%) and 4.3 fold (19.49%) decrease in the invasive potential of the KCM cells is observed upon treatment of the cells with 15uM and 30uM of Celecoxib. The invasive potential of KCM cells treated with 15uM of Celecoxib is equivalent to the invasive potential of KCKO cells, indicating that higher invasive potential in KCM cells is associated with Cox-2 activity.

3.4. Discussion

Overexpression of MUC1 in pancreatic and in other solid tumors, and its implication in malignant tumor progression, has been described by various research groups. Importantly, it was demonstrated that MUC1 overexpression promotes invasion and proliferation of PDA cells [62], [63]. Hence, MUC1 has become an attractive molecular target for cancer therapy. In pancreatic cancer Cox-2 is frequently overexpressed which is associated with increased angiogenesis, immune suppression, tumor cell proliferation and invasion. However the relationship between these two molecules has never been studied before. Our study demonstrates for the first time that MUC1 is an important regulator of Cox-2 gene expression, which promotes proliferation or invasion in the PDA cells.

We demonstrate that the levels of COX-2 protein are increased in both primary human PDA and in PDA cell lines that express high levels of MUC1 (Figure 13.8). In both human and mouse PDA sections, COX-2 was overexpressed in tumors that expressed high levels of MUC1. The relationship between MUC1 and Cox-2 was effectively recapitulated in PDA cell lines, where we demonstrate that overexpression of MUC1 in MUC1 low cell lines leads to increase in Cox-2 mRNA and protein expression. Consequently, knockdown of MUC1 in MUC1 high PDA cell lines attenuates Cox-2 mRNA and protein expression (Figure 13.9, 13.10). Interestingly, in BxPC3 cells a significant difference in Cox-2 expression was observed although there was no significant difference in the Cox-2 mRNA level, raising a possibility of post transcriptional regulation of Cox-2 by MUC1. The stability of Cox-2 mRNA is largely regulated by a complex network of Erk1/2, p38 MAPK and PI3K pathways [132]. Most of these signaling pathways are over activated in cancer cells that overexpress MUC1[57], [58], [61]. Thus the possibility that MUC1 increase Cox-2 expression posttranscriptionally in PDA cells cannot be overruled. Recently it was reported that downregulation of miR-143 in PDA cells increases the stability of Cox-2 mRNA leading to increased Cox-2 protein in PDA cells. MUC1 has been shown to induce galectin-3 expression in PDA cells via suppressing miR-322 expression and thereby stabilizing galectin-3 transcripts.

In pursuit of elucidating the mechanism by which MUC1 regulates Cox-2 expression, we analyzed occupancy of MUC1 and NF-kB to the promoter of Cox-2 (PTGS1/Ptgs1) gene by ChIP assay. We found that MUC1 CT and NFkB binding to ChIP region I (within 1000bp upstream of TSS) in the 5'UTR region of both mouse and human COX-2/Cox-2 gene. KCKO cells that are null for MUC1 did not show any binding

of MUC1 CT and NF-kB to the 5'UTR of mouse Ptgs-2 gene (Figure 13.11). These cells display low Cox-2 mRNA level indicating that loss of MUC1 attenuates binding of NFkB to the promoter of Cox-2 gene and thereby affects the transcription of Ptgs-2 gene.

Lastly, we determine the biological significance of Cox-2 in the MUC1 high PDA cells by blocking the Cox-2 activity. We observed a dose dependent decrease in growth of HPAFII, HPAC, KCKO and KCM cells upon treatment with Celecoxib underscoring the importance of Cox-2 in proliferation of PDA cells (Figure 13.12). Interestingly, although KCKO cells expressed less Cox-2 compared to KCM, they were more susceptible to growth inhibition by Celecoxib compared to KCM. This could due to the fact that Celecoxib not only inhibits Cox-2 activity, but also modulates cell survival pathways and other cellular responses. A study showed that the antitumor effect of Cox-2 is not entirely contingent upon its ability to inhibit Cox-2 activity but rather owing to its ability to initiate ER stress [133]. It could be possible that in KCKO cells Celecoxib initiates ER stress which is counteracted better in KCM cells.

On analyzing the basal level of invasive potential of HPAFII, HPAC, CFPAC and Mia-Paca-2 cell lines, we found that only CFPAC cell line was invasive and treatment with Celecoxib resulted in decrease in their invasive potential (Figure 3.13). Thus, Cox-2 is critical for proliferation of HPAFII, HPAC, KCKO and KCM cells, but not for their invasive potential. In contrast, Cox-2 is important for both invasion and proliferation of CFPAC cells. Thus, although Cox-2 is overexpressed in MUC1 high PDA cells, the biological effect of Cox-2 may not be the same in all MUC1 high cell lines. The variation in the biological effect of Cox-2 could be due to difference in the expression profile of the EP receptors in the cells lines, and the subsequent engagement of one or more of the signaling pathways downstream of Cox-2/PGE2 signaling axis. Nonetheless, the

significance of Cox-2 overexpression by the MUC1 high cells cannot be underrated as Cox-2 not only affects tumor cells but also other cellular components in the tumor microenvironment. For example, it has been reported that Cox-2 causes suppress activation of immune response against tumor by recruiting MDSC in the tumor microenvironment. Moreover, Cox-2 is known to regulate VEGF expression and promote angiogenesis [134], [135]. Previously we and others reported that MUC1 modulates expression of VEGF in pancreatic and breast cancer cells [81] [62].

In conclusion, MUC1 is an important mediator of tumor growth, metastasis and angiogenesis, and also functions as positive regulator of COX-2 expression in PDA. Hence, targeting the cytoplasmic tail of MUC1 using MUC1 inhibitor GO-203, which blocks the CQC motif and prevents MUC1 dimerization, may be a promising approach for the treatment of patients with advanced and/or metastatic pancreatic cancer.
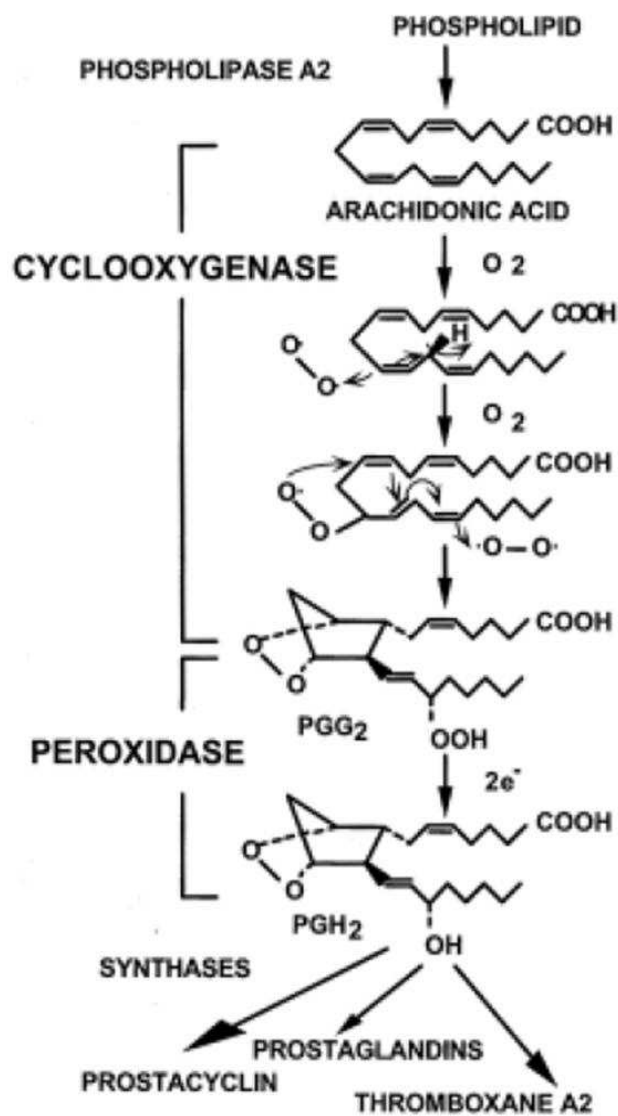
Figure 3.1. Biosynthesis of Prostaglandin from Arachidonic acid [114].
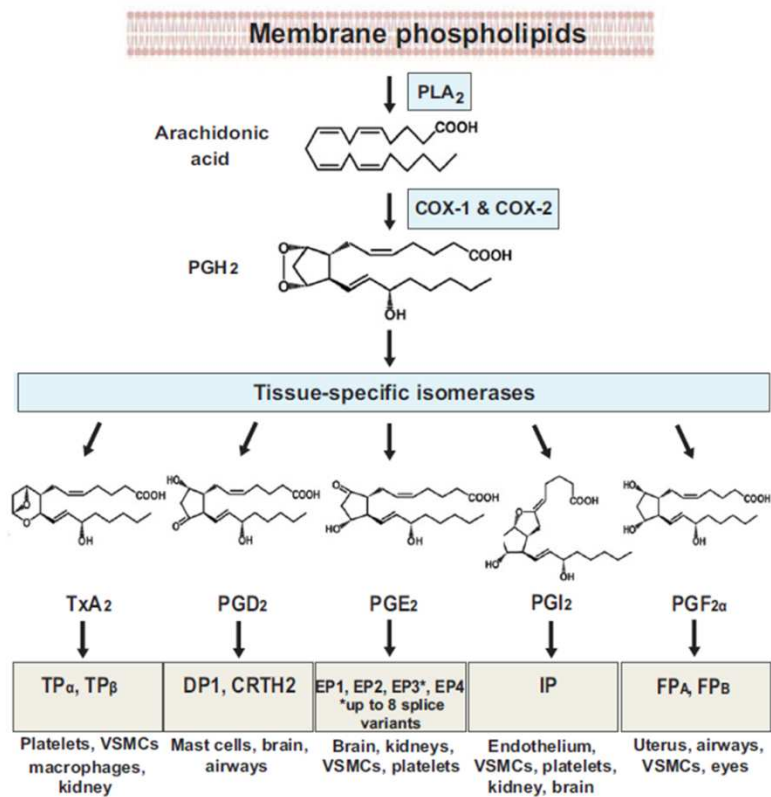
Figure 3.2.Biosynthetic pathway of prostaglandins [136].
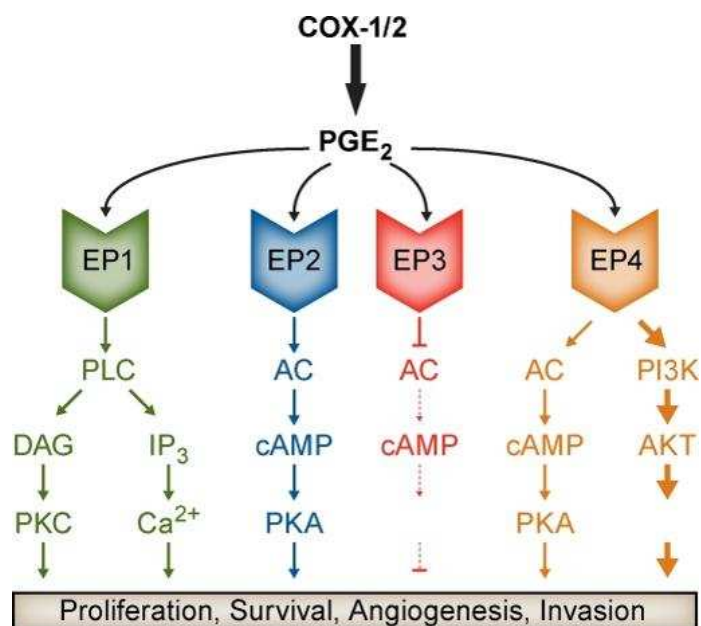
Figure 3.3: Signaling pathways activated by the EP receptors for PGE_2: PGE2 binds to G-protein couples EP receptors and activates the downstream signaling cascade. There are four types of EP receptors - EP1, EP2, EP3 and EP4.The tissue expression of the receptors are different and such the biological effect of PG is tissue specific [137].
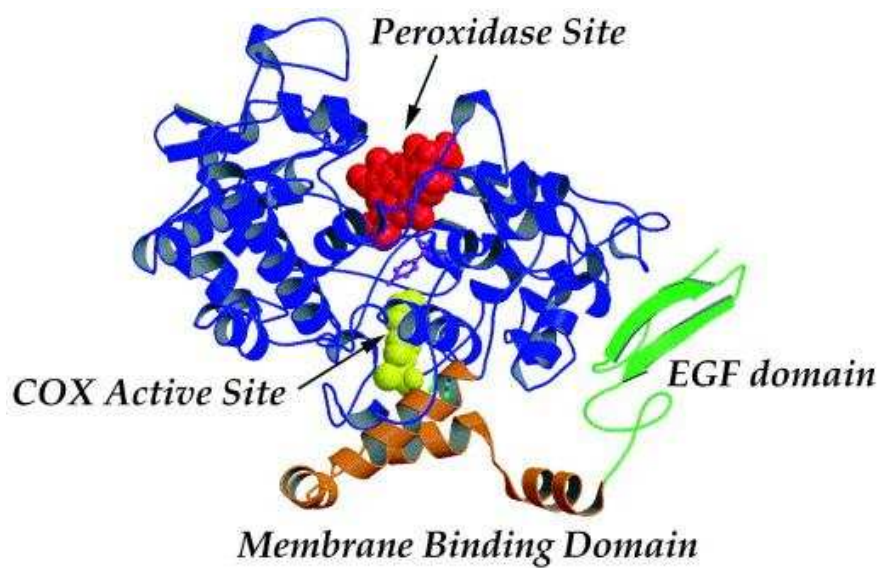
Figure 3.4: Three dimensional structure of the Cox enzyme: The Cox enzyme has 4 distinct domains, EGF like domain, membrane binding domain, peroxidase (POX) active site and cyclooxygenase (COX) active site [138].
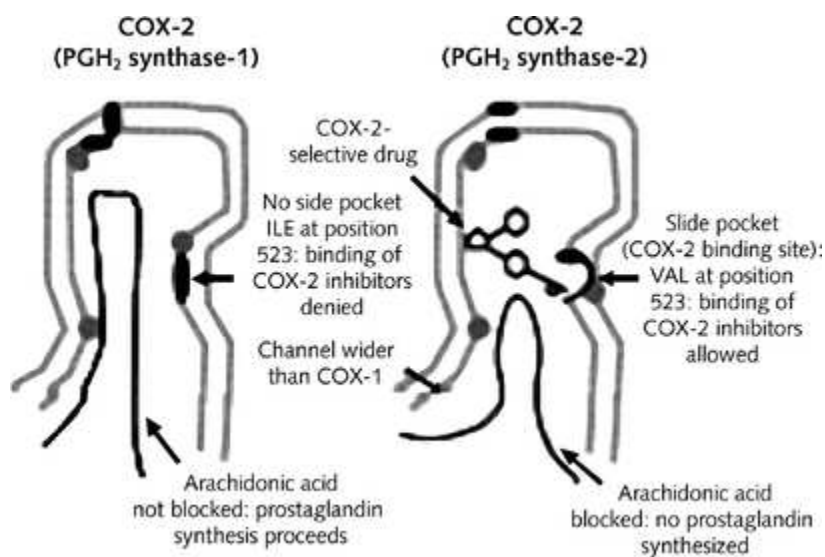
Figure 3.5: Selective binding of Celecoxib to the active site of Cox-2: The Cox channel in Cox-1 is wide enough to allow AA to access the active site of the enzyme, but excludes the entry of bulky Celecoxib. In contrast, Cox-2 has a wider Cox channel, which allows the bulky Celecoxib to enter with ease. In addition, the presence of side pocket created by Val 523 allows Celecoxib to effectively bind to the active site of Cox-2 [153]
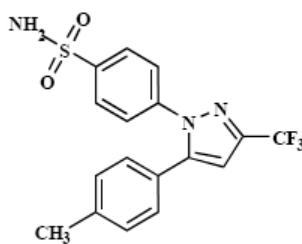
Figure 3.6: Chemical structure of Cox-2 specific inhibitor Celecoxib [139].
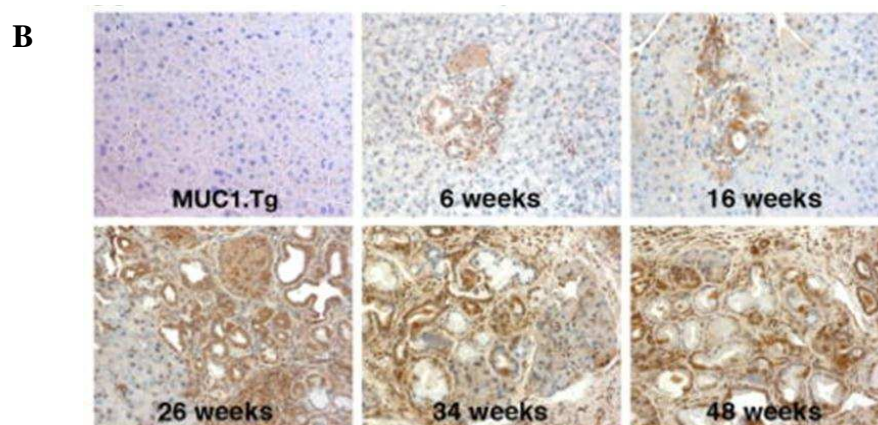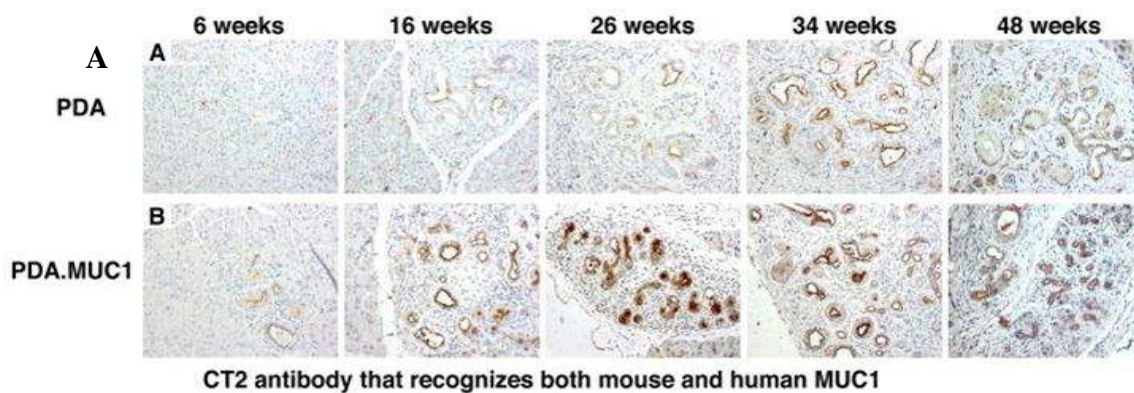
Cox-2 expression

Figure 3.7: A stage dependent increase in the MUC1 and Cox-2 expression in PDA. MUC1 mouse: Tumor sections representing different stages of PDA were obtained from PDA.MUC1 (KCM) mice and were analyzed for MUC1 expression using CT2 antibody and Cox-2 using anti-Cox-2 antibody [118].
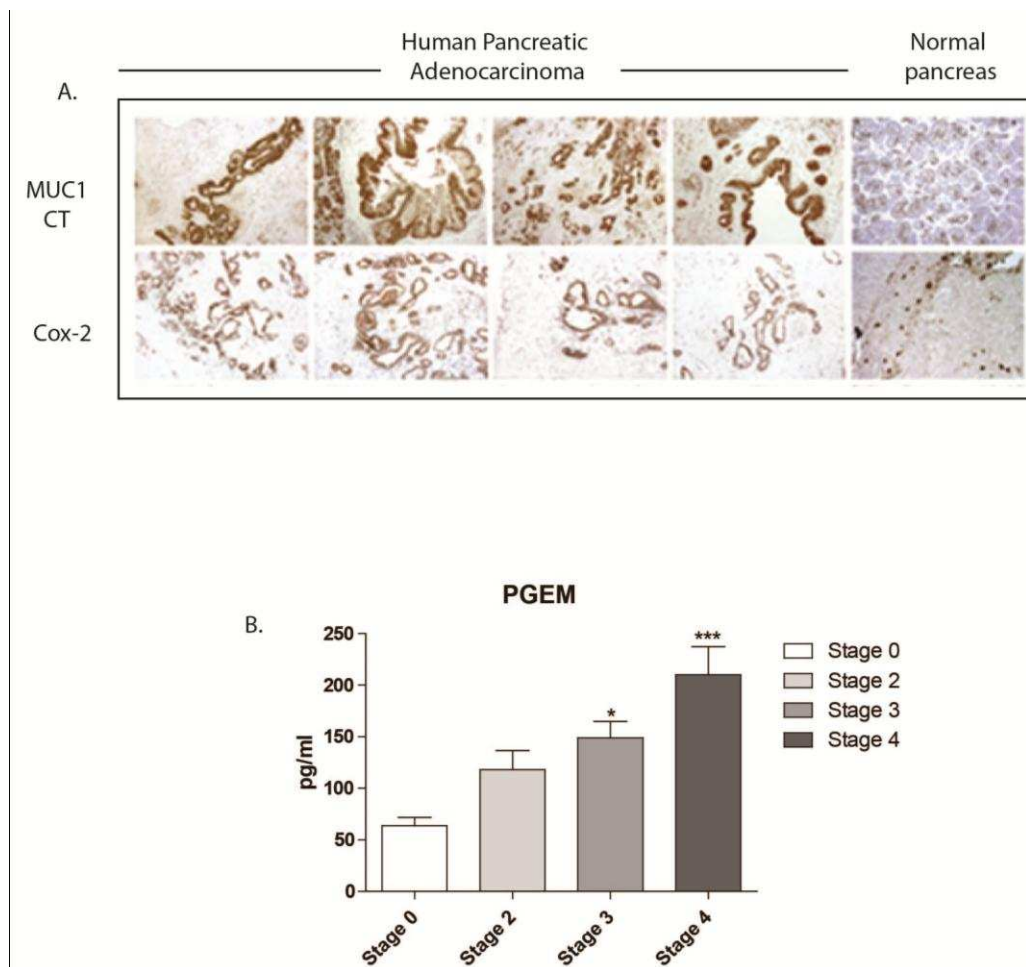
Figure 3.8: Expression of MUC1 and COX-2 in human pancreatic adenocarcinoma sections and PGE2 in the patient serum: A. IHC was performed to compare MUC1 and Cox-2 expression between the human PDA sections and its adjacent normal pancreas. Morphologically normal pancreas section shows low apical membranous MUC1 staining and lack of Cox-2 expression. Metastatic PDA samples show strong membranous and cytoplasmic MUC1 staining and show abundant Cox-2 in tumor cells. **B.** Serum PGE2 levels from pancreatic cancer patients were assessed by PGE2 metabolite (PGEM) ELISA kit. An average of 5 patient samples have been shown here. One way ANOVA was performed to determine the statistical significance between the samples, ***$p = 0.0005$.
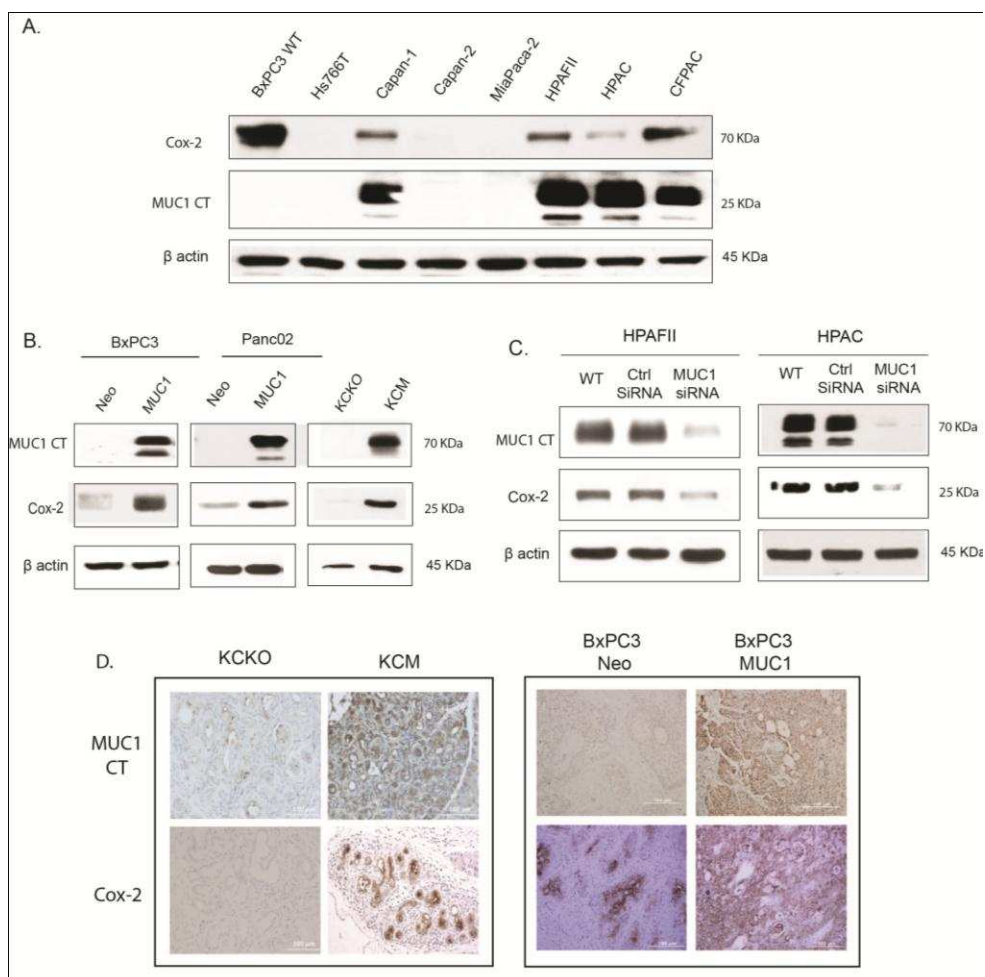
Figure 3.9: Positive correlation between MUC1 and Cox-2 expression in human cell lines (in vitro) and mouse PDA sections. A. Levels of MUC1 and Cox-2 protein in a panel of human PDA cell lines were evaluated by western blot using anti MUC1 antibody CT2 and anti-Cox-2 antibody respectively. 60ug of protein was loaded for SDS-PAGE. β-actin was used as loading control. B. Levels of MUC1 and Cox-2 protein in cell lines overexpressing MUC1was evaluated and compared with low MUC1 counterparts. 35 ug of protein was subjected to SDS-PAGE. C. Cox-2 expression was evaluated in cells following endogenous MUC1 knock down using MUC1 siRNA. Cox-2 and MUC1 levels were analyzed by western. 60ug of protein was loaded for SDS-PAGE. D. IHC was performed to compare MUC1 and Cox-2 expression between Muc1 null tumors (KCKO) and MUC1 positive tumors (KCM). BxPC3 Neo and BxPC3 MUC1 xenografted tumors were stained for MUC1 and Cox-2 expression. KCM and BxPC3.MUC1 tumors showed high levels of Cox-2 in comparison to MUC1 low KCKO and BxPC3 Neo tumors.
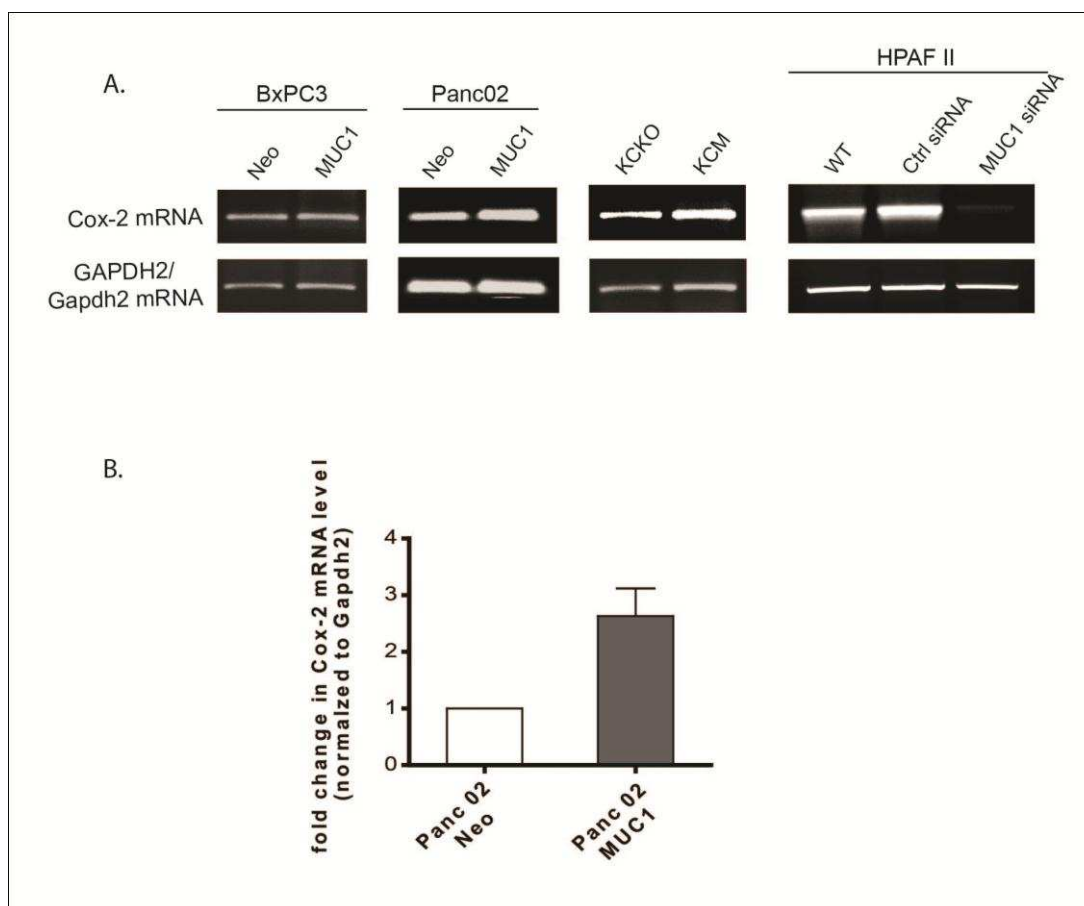
Figure 3.10: MUC1-positive PDA cell lines express elevated levels of Cox-2 gene in vitro.A. Total mRNA from PDA cell lines were isolated using TRIzol and the basal levels of Cox-2 mRNA were determined using semi-quantitative one step RT-PCR kit. B. Panc02 Neo and MUC1 Cox-2 mRNA was evaluated by real time RT-PCR.
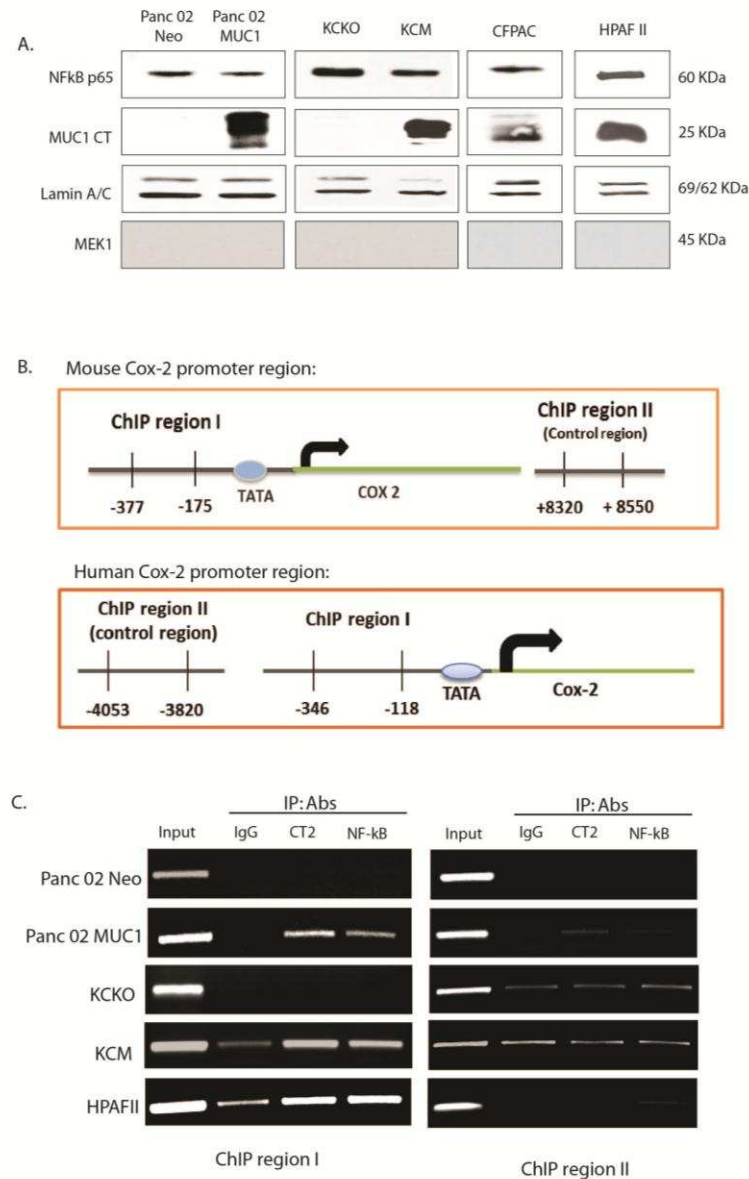
Figure 3.11: MUC1 and NF-kB binds to the upstream promoter region of Cox-2 gene: A. Whole cell lysate from a panel of human PDA cell lines were immunoblotted to determine the constitutive NFkB status. β-actin was used as a loading control for SDS-PAGE. B. Schematic representation of the promoter region with its putative DNA binding elements in mouse and human Cox-2 gene. C. Sheared chromatin was immunoprecipitated using anti-MUC1 CT antibody CT2 and anti-NFkB antibody. The immunoprecipitated chromatin was PCR amplified.
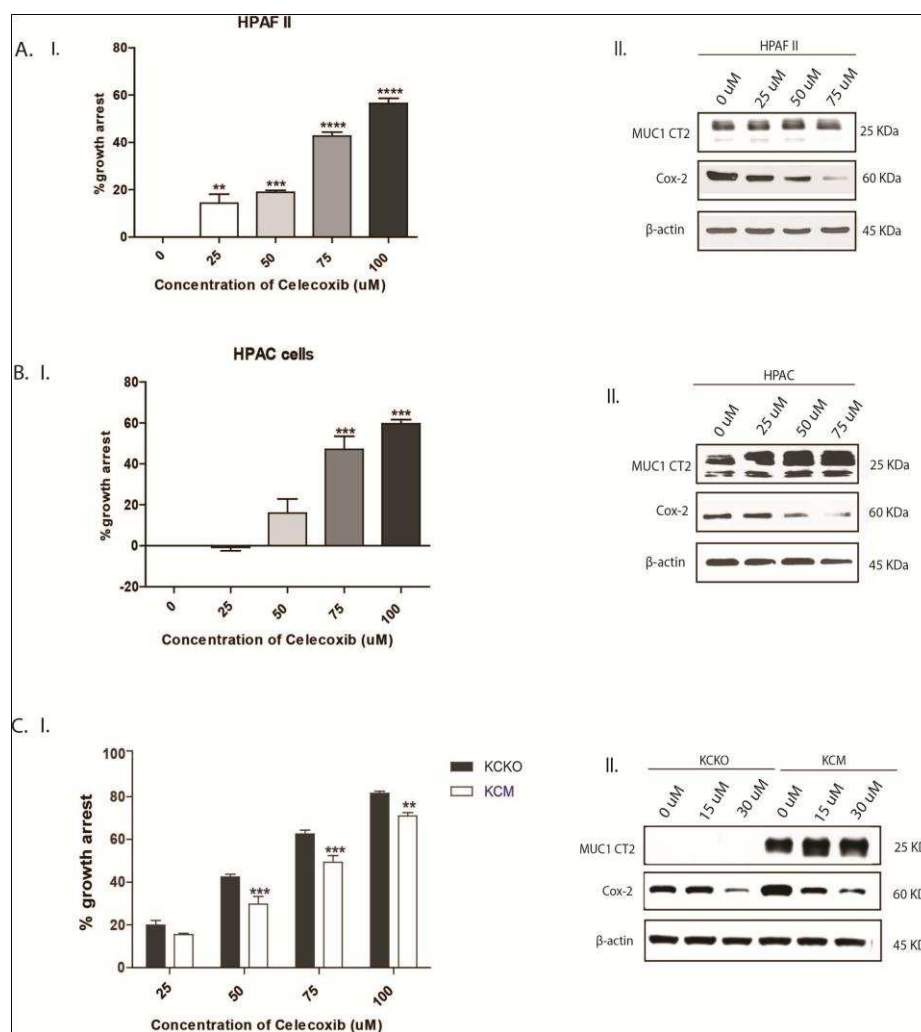
Figure 3.12: Selective inhibition of Cox-2 with Celecoxib attenuates the growth of the of PDA cell lines: AI, BI and CI: Equal number of cells (4000 - 10,000) plated in 96 well plate were grown overnight. After 18 hours, cells were treated with or without the indicated concentration of Celecoxib and control DMSO for 24 hours. MTT assay was performed to determine the growth inhibition following Celecoxib treatment. Significant differences in growth in each cell line and between KCKO and KCM at varying concentrations of the Celecoxib is shown as p-values (n=8) (*p<0.1, **p<0.01, *** p<0.001). AII, BII and CII: Cells grown overnight in a 6 well plate were left untreated or treated with indicated concentration of Celecoxib for 24 hours. Cell lysate were prepared and were subjected to immunoblotting. The membrane was probed with anti-MUC1 antibody (CT2), anti-Cox-2 and anti-β actin antibody to determine the MUC1, Cox-2 and β-actin levels respectively.
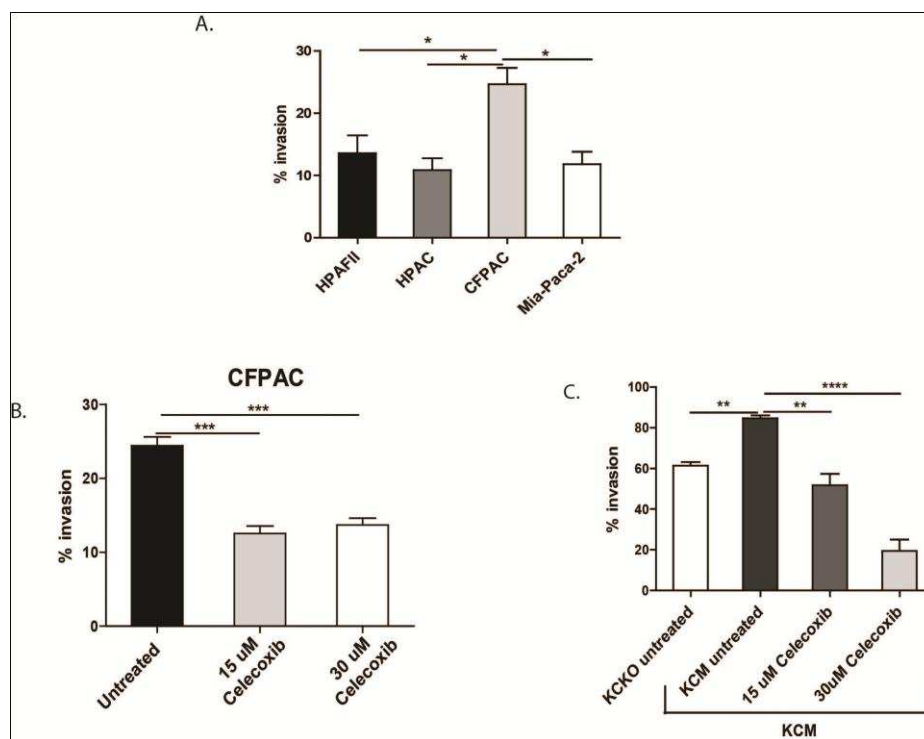
Figure 3.13: Selective inhibition of Cox-2 with Celecoxib attenuates invasive potential of the invasive PDA cell lines: Cells grown on culture dish were serum-starved for 18 h before plating for the invasion assay. In a 24 well plate, 50,000 cells in serum-free media with or without Celecoxib were plated over transwell inserts (BD Biosciences, San Jose, CA, USA) precoated with reduced growth factor matrigel (BD Biosciences, San Jose, CA, USA). Cells were allowed to invade through the matrix toward the serum supplemented media contained in the bottom chamber over a period of 36 h. Percent invasion was calculated as absorbance of samples/absorbance of controls*100.

CHAPTER 4: MUC1 REGULATES THE SWITCH IN TGF-β1 FUNCTIONING FROM TUMOR SUPPRESSOR TO TUMOR PROMOTER

4.1. Introduction

Transforming growth factor‑β (TGF-β) is a pleotropic cytokine with dual functionality. In normal epithelial cells, TGF-β causes growth arrest and apoptosis, which constitutes the tumor suppressive function of TGF-β signaling. Additionally, TGF-β can trigger proliferation and EMT (epithelial to mesenchymal transition) in normal epithelial cells, a physiological process crucial for organogenesis and development. This constitutes the tumor promoting arm of TGF-β, as in cancer cells this signaling axis of TGF-β becomes dominant and promotes invasion and metastasis of cancer [140], [141], [142]. Thus it can function both as a tumor suppressor and a tumor promoter. In normal epithelial cells, the tumor suppressive arm of TGF-β signaling is dominant. At early stages of tumorigenesis, when the tumor is still benign, it acts directly on the cancer cell to suppress tumor growth [143]. However, as the cancer progresses, the tumor suppressive arm of TGF-β signaling is lost and the tumor promoting arm of TGF-β signaling gains dominance[144], [145], [146], thus changing from a tumor suprresor to a tumor promoter. The mechanism(s) underlying the switch functional switch of TGF-β is not definitively known.

TGF-β1, TGF-β2 and TGF-β3 are the three isoforms of TGF-β. TGF-β1 is the most abundant and universally expressed isoform. Activation of TGF-βRII involves

binding of TGF-β1 to TGF-βRII and its subseuqent autophosphorylation. Activated TGF-βRII in turn phosphorylates TGF-βRI, which in turn activates a class of signaling proteins known as Smads. Smads are the principle effector molecules of the canonical TGF-β signaling pathway. TGF-βRII activates Smad2/3, which upon activation, binds to an additional protein, SMAD4 or co-Smad, and translocates to the nucleus. Within the nucleus, this complex acts as a transcription factor where the protein that binds to DNA and contributes to the activation for various genes, thus triggering apoptosis (Figure 4.1) [147]. However, in recent years, a number of additional pathways have been discovered that potentially regulate the different cellular responses to TGF-β. Some of these non-canonical signaling pathways are PI3K/Akt, Erk1/2, JNK, p38 MAPK pathways [144], [148], [149]. Integration of the canonical and non-canonical signaling pathways contributes to the paradoxical role of TGF-β1 signaling. In transformed cells, aberrations in either canonical or non-canonical signaling cascade can result in a loss of tumor suppressive but gain in the tumor promoting function of TGF-β1[150]. Some of the anomalies frequently observed in the canonical pathway are downregulation of TGF-β receptors, upregulation of I-Smads (inhibitors of TGF-β signaling cascade) and mutation or deletion of Co-Smad (Smad-4/ DPC4) [144], [150]. Overactivation of the non-canonical TGF-β signaling pathways such as PI3K/Akt, Erk1/2 and p38MAPK pathways have also been reported in transformed cells.

However, as the tumor progresses, genetic and/or biomedical changes allow TGF-β1 to stimulate tumor progression by its pleiotropic activities on the cancer cells. TGF-β1 stimulating invasion and metastasis might be of greater clinical consequence than its tumor-suppressive role, as the majority of human tumors retain a functional TGF-β1 signaling pathway [143]. TGF-β1 induces epithelial-to-mesenchymal transition (EMT), a

process by which epithelial cells lose their cell polarity and cell-cell adhesion, and gain migratory and invasive properties to become mesenchymal cells. TGF-β1-induced EMT leads to migration and invasion of local epithelial cells. This could be through the extracellular signal-regulated kinases (ERK) pathway, a chain of proteins in the cell that communicates a signal from a receptor on the surface of the cell to the nucleus of the cell. This pathway communicates by adding phosphate groups to a neighboring protein, which acts as an "on" or "off" switch. This results in an escape of apoptotic fates of these cells, and this is important for tumor metastasis [141]. Strategies for chemotherapy targeting functional TGF-β1 must consider its bifunctional action and attempt more specific targeting to inhibit tumor promoting TGF-β1 signaling pathway, thus preventing outgrowth and metastasis [143].

Previous research has shown that like TGF-β1, MUC1 plays a major role in EMT as well as drug resistance, invasion, and metastasis in pancreatic cancer [57], [62]. Therefore, the goals of this research project include determining the differential effects of TGF-β1 induced EMT in MUC1+ and MUC1- cells, and determining the differential effects of TGF-β1 induced apoptosis in MUC1+ and MUC1-. It is hypothesized that upregulation of MUC1 and signaling through its cytoplasmic tail supports TGF-β1-induced EMT and invasion and inhibits TGF-β1-induced apoptosis (Figure. 4.2).

4.2 Materials and Methods

Cell Culture:

All experiments were performed in vitro with a panel of human (CFPAC, HPAC, HPAF II, Capan 1, Panc 1, Mia Paca 2, SU86.86, BxPC3 MUC1, BxPC3 Neo) and mouse (KCM, KCKO, Panc o2 MUC1, Panc o2 Neo) PDA cell lines. All cells lines are established cell lines from the American Type Culture Collection (ATCC) and derive

from pancreatic ductal adenocarcinoma. All cells were cultured in 10 cm plates in an incubator at 37^0C. Cells were split and fed with C-DMEM media every other day or when the cells became, at most, eighty percent confluent.

Western blots:

Equal quantities (determined from BCA Assay) of cell lysates were loaded on SDS-PAGE gels. When developing the loading buffer and gel for the Western Blotting, 8%, 10%, and 12% gels were used. These gels consisted of various amounts of DI H20, 30% Acrylamide, 1.5M Tris pH 8.8, 10% SDS, 10% APS, and TEMED. After pouring the gel, the samples were added to the gel, and the protein was transferred through the 6 processes of gel electrophoresis, a method for separation and analysis of macromolecules and their fragments, based on their size and charge (AbCam, 2012). The molecular weights of TGF-βR1 (56 kDa), TGF-β R2 (64 kDA), and β-actin (42 kDa) were taken not of, and they were analyzed using various primary antibodies (1:1000 dilution) and secondary antibodies (1:2000 dilution).

Invasion assay:

Cells were serum starved for 18 hours before plati8ng for invasion assay. 30,000 cells were plated on growth factor reduced matrigel coated inserts and were left untreated or treated with 10ng/ml of TGFβ1. The cells were allowed to invade through the matrix towards the serum containing media in the bottom chamber for 48 hours.

Annexin – V staining:

Serum starved cells were treated with 10ng/ml of TGF-β1 for 48hours. Apoptosis was measured by via Annexin V / 7AAD flow cytometry staining. Annexin V binds with high affinity to membrane phospholipid phospha-tidylserine (PS) which translocates from the inner to the outer leaflet of the plasma membrane in apoptotic cells. Staining with

Annexin V-FITC is typically used in conjunction with a live/dead dye 7-Amino-Actinomycin (7-AAD) to allow the identification of early apoptotic cells (7-AAD negative, Annexin V-FITC positive) from dead cells (7-AAD positive, AnnexinV-FITC positive). Viable cells with intact membranes exclude 7-AAD, whereas the membranes of dead and damaged cells are permeable to 7-AAD.

4.3. Results

We wanted to first investigate if there is any correlation between expression of MUC1, TGF-β receptors and TGFβ1 in human PDA cell lines. We analyzed the levels of MUC1, TGF-β RI and TGF-β RII in a panel of human PDA cell lines expressing variable levels of MUC1 by western blot. Panc1, MiaPaca2, and SU86.86 cells, which express low levels of endogenous MUC1 also express high levels of TGF-β RI and negligible levels of TGF-βRII (Figure 4.3a). Whereas, CFPAC, HPAC and HPAF II cells, which express high levels of endogenous MUC1 express high levels of TGF-β RII and low levels of TGF-βRI (Figure 4.3a). Similarly we observed that BxPC3 MUC1 cells which express high levels of MUC1 also express higher levels of TGF-βRII but lower levels of TGF-β RI in comparison to BxPC3 Neo cells. The data is indicative of a positive relationship between MUC1 and TGF-βII expression and an inverse relationship between MUC1 and TGF-βRI expression.

TGF-β1 is a known inducer of EMT and invasion in pancreatic cancer and since MUC1-expressing PDA cells undergo EMT and are highly invasive as compared to MUC1-null cells, we first examined if TGF-β1-induced invasion is dependent upon MUC1 expression. We found that MUC1-positive cells became more invasive upon TGF-β1 stimulation compared to MUC1-null cells. This suggests that MUC1 facilities TGF-β1 mediated EMT and signaling (Figure. 4.4a). Whether this is due to the

differential expression of the TGF-βRI and TGF-βRII levels in these cells is not yet known.

In normal epithelial cells, TGF-β1 induces apoptosis. However, in transformed cells, the TGF-β1 mediated apoptosis is abrogated. It has also been demonstrated that MUC1 expression abrogates the intrinsic apoptotic pathway. Therefore, we wanted to know if MUC1 has the ability to modulate TGF-β1 mediated apoptosis in MUC1 expressing PDA cells. To determine the effect of MUC1 expression on TGF-β1 induced apoptosis, we performed Annexin V/7AAD staining and flow cytometry. We found that MUC1-positive cells resisted apoptosis upon TGF-β1 stimulation compared to MUC1-null cells (Figure 4.4b). To further validate that the differences are indeed due to MUC1 expression, we first examined the basal level production of TGF-β1 by ELISA. We observed elevated levels of TGFβ1 in the culture supernatants of BxPC3 MUC1 cells in comparison to BxPC3 Neo cells at 6, 12 and 24 hour time points. However, at 48 hours, no significant difference in the levels of TGF-β1 was noted between BxPC3 Neo and MUC1 cells (Figure 4.4c). This could be due to accumulation of TGF-β1in the media of BxPC3 Neo cells that are not internalized for signaling purposes.

We next wanted to investigate if the differential effect of TGF-β1 on MUC1 positive and negative PDA cells stemmed from the differential activation of the TGFβ signaling pathways, especially since the TGF-βRI and TGF-βRII levels were significantly altered in MUC1 high and low cells. We analyzed the activation of Erk1/2 and Smad2/3pathways which represents the respective non-canonical and canonical signaling axis of TGFβ signaling pathways. We assessed the kinase activity of the receptors by evaluating the phosphorylation of Smads and Erk1/2 following TGF-β1 stimulation. We observed significant phosphorylation of Smad2/3 at 30 minutes following TGF-β1

stimulation in both BxPC3 MUC1 and BxPC3 Neo cells. However, there was no difference in the levels of the phosphorylated Smad2/3 between the MUC1-positive and MUC1-null BxPC3 cell lines (Figure 4.5a). Interestingly, we observed elevated levels of phosphorylated Erk1/2 at 15 minutes and the consecutive time points following TGF-β1 stimulation in MUC1 positive PDA cells compared to MUC1 null PDA cells (Figure 4.5b). Note that BxPC3 MUC1 cells have inherently higher phospho Erk1/2 levels compared to Neo cells. Together, these data indicates that the difference in invasiveness and apoptotic response of MUC1 positive and negative PDA cells could be caused due to the difference in the expression of the TGF-β receptors and activation of the downstream Erk1/2 signaling cascades.

4.4. Discussion

So far data indicates that MUC1 plays a role in switch of TGF-β1 function from a tumor suppressor to a tumor promoter. The negative correlation between MUC1 and TGF-β1 RI levels underscores that MUC1 could play a role in blocking TGF-β1-induced apoptosis because the phosphorylation of TGF-β1 RI leads to activation of proapototic pathway via Smad. Based on these results, if MUC1 is up regulated, then TGF-β1 RI is down regulated, thus the apoptotic signaling pathway is not initiated. Also, the positive correlation between MUC1 and TGF-β1 RII with CFPAC, HPAC, and HPAF II is significant because the up regulation of TGF-β1 RII and down regulation of TGF-β1 RI indicates that TGF-β1-induced EMT may be occurring.

This study gives us the basis of a screening tool to predict whether inhibition of TGF-β1 would be an effective treatment for a particular patient with pancreatic adenocarcinoma. This tool can be used to prevent patients from getting false treatment. If MUC1 is not expressed, then TGF-β1 inhibition would not be suggested because it would

be blocking TGF-β1 functioning as a tumor suppressor. If MUC1 is expressed, then TGF-β1 inhibition would be suggested because this this expression leads to TGF-β1-induced-EMT, which needs to be blocked. Not only does this study open up a whole new field of study using TGF-β1 targeting as an effective treatment, but this study can also take us one step closer to understanding pancreatic cancer and cancers in general.

Figures 4.5
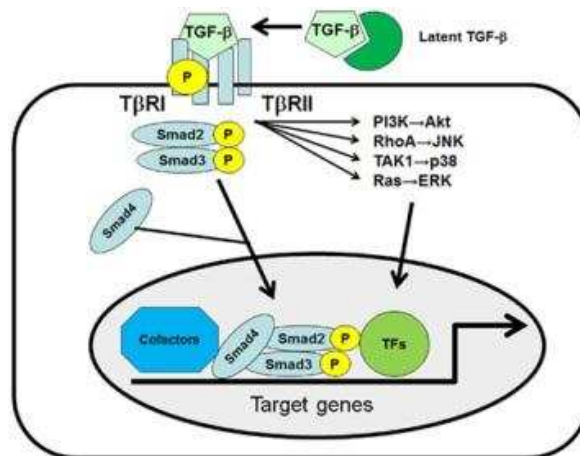
Figure 4.1: Canonical and non-canonical signaling pathways of TGF-β: Divergent TGF-β signaling pathways induce transcriptional regulation through SMAD pathway and induce invasion and metastasis through epithelial-to-mesenchymal transition (EMT) pathway [151].
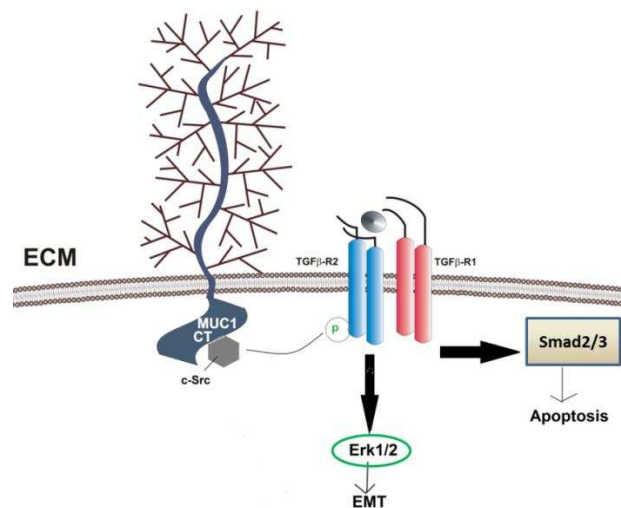
Figure 4.2: Hypothesis: The cytoplasmic tail of MUC1 supports TGF-β1- induced EMT and invasion and inhibits TGF-β1-induced apoptosis

.
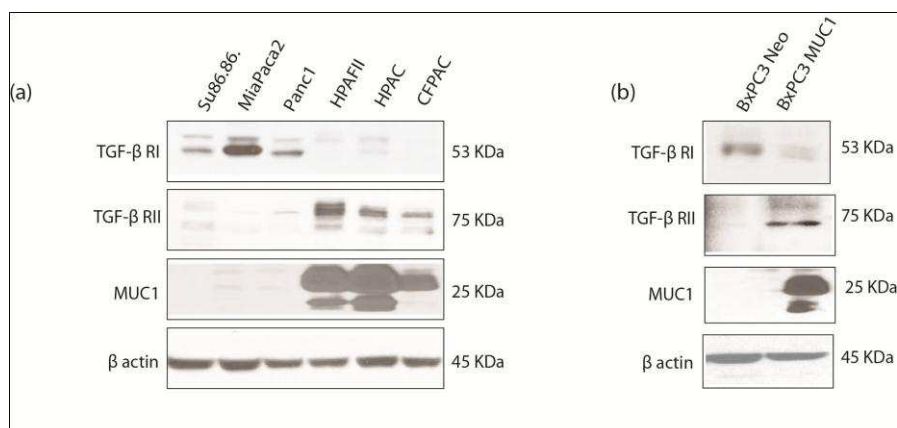
Figure.4.3: Expression of TGF-β receptors in PDA cell lines: (a) A panel of human cell lines were tested for TGF-β RI, TGF-β RII, MUC1 expression by western blot. (b) BxPC3 Neo, MUC1 and Y0 cell lines were tested for expression of TGF-β RI, TGF-β RII, MUC1 by western blot. B-acting was used as a loading control. (c) $0.25*10^6$ $0.4*10^6$, $0.55*10^6$ and $0.7*10^6$ cells were plated in 6 well plates for the supernatant to be collected at 48hours, 24 hours,12 hours and 6 hours respectively. Whole cell lysates were prepared from the cells for BCA assay. The level of TGF-β1 secreted by BxPC3 Neo, MUC1 and Y0 cells were determined by analyzing the cell culture supernatant by ELISA. The results are represented as pg of TGF-β1 per ml of the cell culture supernatant. The levels of TGF-β1 were normalized to the whole cell lysates.
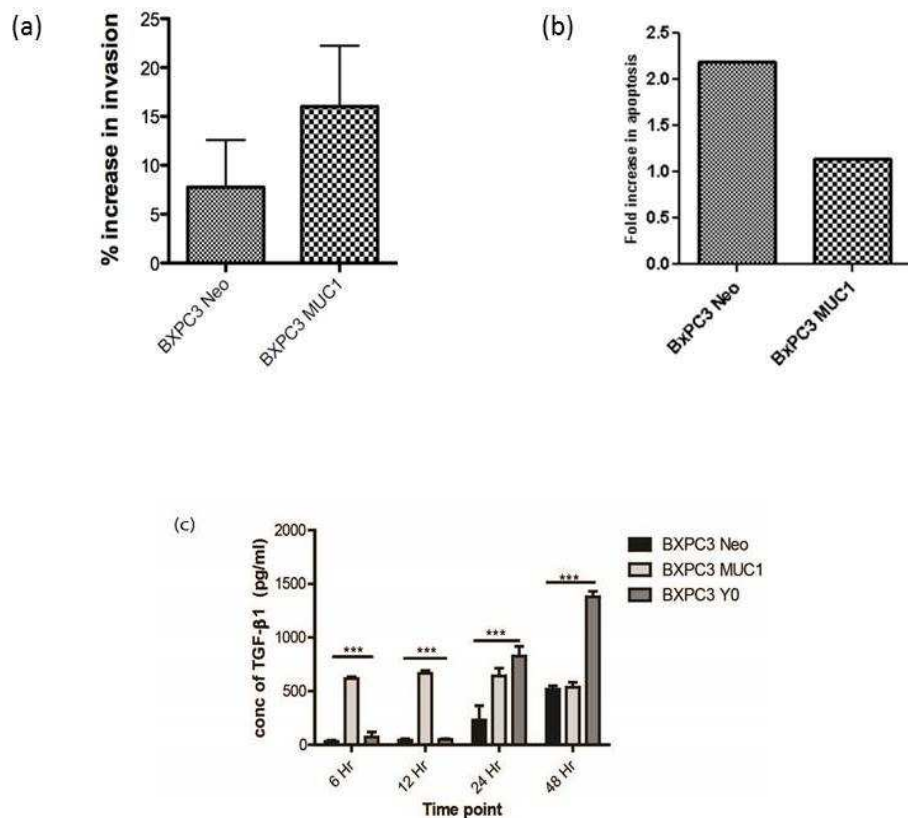
Figure 4.4: Differential effect of TGF-β1 on the human PDA cell line BxPC3 in absence and presence of MUC1: (a) Cells were serum starved for 18 hours before plati8ng for invasion assay. 30,000 cells were plated on growth factor reduced matrigel coated inserts and were left untreated or treated with 10ng/ml of TGFβ1. The cells were allowed to invade through the matrix towards the serum containing media in the bottom chamber for 48 hours. (b) 30,000 cells were plated in a 24 well plate and were serum starved overnight. Next day, cells were treated with 10ng/ml of TGF-β1 for 48 hours and were stained with Annexin V apoptosis kit to determine the level of apoptosis.
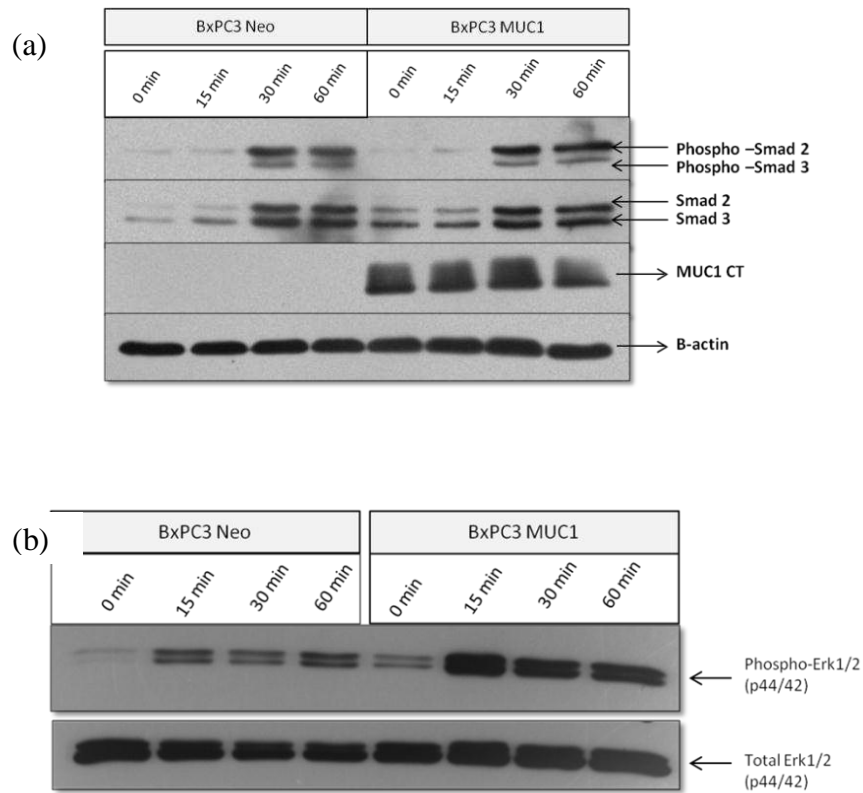
Figure 4.5: Preferential activation of the non-canonical TGF-β pathway-Erk1/2 in response to TGF-β1 in BxPC3 MUC1 cells: (a) $0.5*10^6$ cells were plated in a 24 well plate and were serum starved for 6 hours. Cells were treated with 10ng/ml of TGF-β1 for indicated time points and were harvested following treatment to prepare whole cell lysates. Phosphor-Smad2/3, total Smad, phosphor Erk1/2 and total Erk1/2 were determined by western blot.

CHAPTER 5: OVERALL CONCLUSION AND FUTURE DIRECTIONS

The aim of my PhD dissertation was to study the mechanistic role of MUC1 in conferring drug resistance, invasion and proliferation in PDA cells. Chapter 2 of my dissertation illustrates MUC1 induced drug resistance in PDA cells due to upregulation of ABC transporters. Previously, MUC1 has been implicated for attenuated sensitivity to chemotherapeutic drug cisplatin in colon cancer cells. The report stated that the cytoplasmic tail of MUC1 translocates to mitochondria where it interferes with the release of pro-apoptogenic factors and prevents induction of apoptosis. This accounts for the reduced sensitivity of the colon cancer cells to cisplatin [106]. Pancreatic cancer is a lethal disease and responds poorly to the chemotherapeutic drugs. Here, we demonstrate that MUC1 upregulates MDR genes, which encodes for ABC transporters and it leads to reduced sensitivity of the PDA cells to anticancer drugs etoposide and gemcitabine. We observed overexpression of four ABC transporters, MRP1, MRP3, MRP5 and P-gp in MUC1 high PDA cells, and our investigation further focused on the ABC transporter MRP1. The mechanism of regulation of MRP3, MRP-5 and P-gp gene expression and their contribution towards increased drug resistance in PDA cells remains to be evaluated. Further, it would also be interesting to determine if MUC1 downregulates the nucleotide transporters (NTs) in PDA cells, the lack of which has largely been implicated for reduced uptake of gemcitabine by cancer cells and hence reduced sensitivity to the drug [152].

In recent years, cancer stem cells have gained considerable attention, as the cancer stem cells contribute partly to the high drug resistance and metastasis associated with pancreatic cancer. Thus, an understanding of the molecular mechanism of drug resistance and metastasis with respect to cancer stem cells is of utmost importance. Studies have shown that cancer stem cells display overexpression of ABC transporters, especially P-gp, MRP1 and ABCG2 [153]. Our research group demonstrated recently that MUC1 is expressed in pancreatic cancer stem cells [119]. It would be interesting to determine if MUC1 similarly upregulates the ABC transporters and contributes to the drug resistant phenotype in cancer stem cells. The insights gained from such studies can be used for designing therapies to combat the ABC transporters mediated drug resistance in cancer cells, including the highly resistant pancreatic cancer stem cell population, with an overall aim to improve the chemotherapy outcomes in pancreatic cancer patients.

The second section of my dissertation aimed to investigate if MUC1 in PDA regulates a pro-inflammatory enzyme Cox-2, since high Cox-2 expression in cancer cells is known to be associated with increased drug resistance, angiogenesis, and invasion. Previously our research group demonstrated a stage dependent increase in Cox-2 expression in PDA.MUC1 tumors (KCM) which was absent in MUC1-null tumors. This was the first report which provided a direct correlation between MUC1 and Cox-2 expression in PC. However, it was not studied in depth and it was not known if indeed MUC1 regulates Cox-2 expression and function in PC, and if so how. So, in the second part of my PhD thesis work, I addressed these questions. I studied the correlation between MUC1 and Cox-2 gene expression and also investigated the mechanism by which MUC1 regulates Cox-2 gene expression in PDA cells. Here, we report that MUC1 increases Cox-2 expression in PDA cells, which bestows the cancer cells with growth and invasion

advantage. The study mainly focused on the transcriptional regulation of Cox-2 gene expression by MUC1. We demonstrate that MUC1 cytoplasmic tail promotes the occupancy of NFkB in the promoter of Cox-2 gene and thereby increases Cox-2 gene expression. The expression of Cox-2 gene is also largely regulated by a post-transcriptional mechanism. A recent report demonstrated that downregulation of miR-143 reduces stability of Cox-2 mRNA which leads to overexpression of Cox-2 in PDA cells [154]. Another report stated that miR-301 is upregulated in PDA cells which causes constitutive activation of NFkB via downregulating the expression of NFkB repressing factor (Nkrf), causing augmentation in expression of several NF-kB target genes, including Cox-2 [155]. It would be interesting to determine if MUC1 regulates expression of these miRNAs or yet some newly undiscovered ones that regulate Cox-2 gene expression in cancer cells by a post-transcription mechanism. To date only one research article has been published that demonstrates the potential role of MUC1 as a post-transcriptional regulator of its target gene [156]. A whole new exciting path remains unexplored which will unveil the role of MUC1 in post-transcriptional regulation of its target genes.

The third part of my thesis involved studying the effect of MUC1 on TGF-β1 signaling cascade. We have preliminary data which indicates that the presence or absence of MUC1 in the PDA cells acts as a decisive factor that governs TGF-β1 functions as a tumor promoter or tumor suppressor, respectively. We observed increased TGF-βRII expression in MUC1 positive BxPC3 cells and also increased activation of Erk1/2 pathway. Currently, the causes of TGF-β1 functioning switch remains to be established. We speculate it could be caused by differential expression of TGFβ receptors and the downstream signaling cascade. A study showed that in breast cancer cells, intergrinβ

physically interacts with TGF-βRII via c-Src, which phosphorylates Y284 of TGF-βRII both in vitro and in vivo, and causes activation of p38 MAPK pathway. MUC1 CT has been shown to physically associate with c-Src at YEKV motif (6th tyrosine residue). Thus, it would be interesting to determine if MUC1 activates TGF-βRII and downstream signaling cascades p38 MAPK or Erk1/2 pathway via c-Src. We have preliminary data that suggests that c-Src is important for TGF-β1 mediated activation of Erk1/2 pathway, as blocking c-Src with the c-Src inhibitor PP2 failed to activate Erk1/2 pathway upon TGF-β1 stimulation. However, whether TGF-βRII is at all required for c-Src mediated Erk1/2 activation remains unclear. Another intriguing aspect was the equal activation of the canonical Smad pathway in both MUC1 null and MUC1 positive cells. Although the expression profile of TGF-βRI and TGF-βRII is opposite in MUC1 null and MUC1 positive cells, the activation status of the Smad pathway seems to be independent of the receptor expression profile. Thus, MUC1 may interfere with TGFβ signaling downstream of the receptors in such a way that it blocks Smad proteins mediated apoptosis but promotes Erk1/2 pathway mediated invasion.

Several scientific studies have demonstrated that the tyrosine residues of MUC1 CT possess critical signaling roles that augment proliferation, invasion and resistance to apoptosis in cancer cells. Our research group demonstrated that MUC1 overexpression induces EMT in PDA cells and removal of all seven tyrosine residues of MUC1 CT (MUC1 Y0) abates the invasive potential of the PDA cells. However, absence of the tyrosine residues in MUC1 CT (MUC1 Y0) does not diminish MUC1 induced mdr genes expression or chemoresistance of the PDA cells, indicating that the tyrosine residues of MUC1 CT are important with respect to EMT, but not for the chemotherapeutic resistance against anti-cancer drugs (Figure 5.1a,b). In MUC1 Y0, although all the

tyrosine residues are missing, it still retains the CQC motif, which is critical for MUC1 dimerization and nuclear translocation [157]. Thus, in MUC1 Y0, we observe MUC1 CT to translocate to the nucleus, bind to the promoter of ABCC1 gene and upregulates its expression (Figure 5.1c).

Interestingly, when we investigated the importance of the tyrosine residues of MUC1 CT on the Cox-2 gene expression, we found that BxPC3 cells expressing MUC1 Y0 expressed lower level of Cox-2 protein in comparison to BxPC3 MUC1. However, there was no significant difference in the Cox-2 mRNA levels between BxPC3 MUC1 and BxPC3 Y0. Ekr1/2, p38 MAPK pathways have been implicated in the post transcriptional regulation of Cox-2 gene. We and others have observed that MUC1 overexpression causes hyperactivation of the Erk1/2 pathway which is reversed upon removal of the tyrosine residues (MUC1 Y0). Thus, the decreased Cox-2 levels in BxPC3 Y0 cells might be due to reduced activation of Erk1/2 pathway in MUC1 Y0 cells. Therefore, the manifestations of oncogenic properties of MUC1 are not just restricted to signaling through its tyrosine residues, but also through other yet unidentified motifs which regulates its transcriptional ability.

Based on the current knowledge about MUC1 and its oncogenic role in pancreatic cancer, the cytoplasmic tail of MUC1 presents an attractive drugable target. Small molecule inhibitors targeting MUC1 CT can be used in combination with chemotherapy to increase the sensitivity of PDA cells to chemotherapeutic drugs. In addition, proliferation and invasion of PDA cells can also be counteracted upon targeting MUC1 CT. A peptide based inhibitor GO-203, has been designed against the CQC motif of MUC1, which prevents MUC1 dimerization and nuclear translocation [158]. Currently

GO-203 is at phase I clinical trial, where the inhibitor is being tested for optimal dosage, toxicity, route of administration and its effect on tumor regression [159].

(a)

(b)

(c)
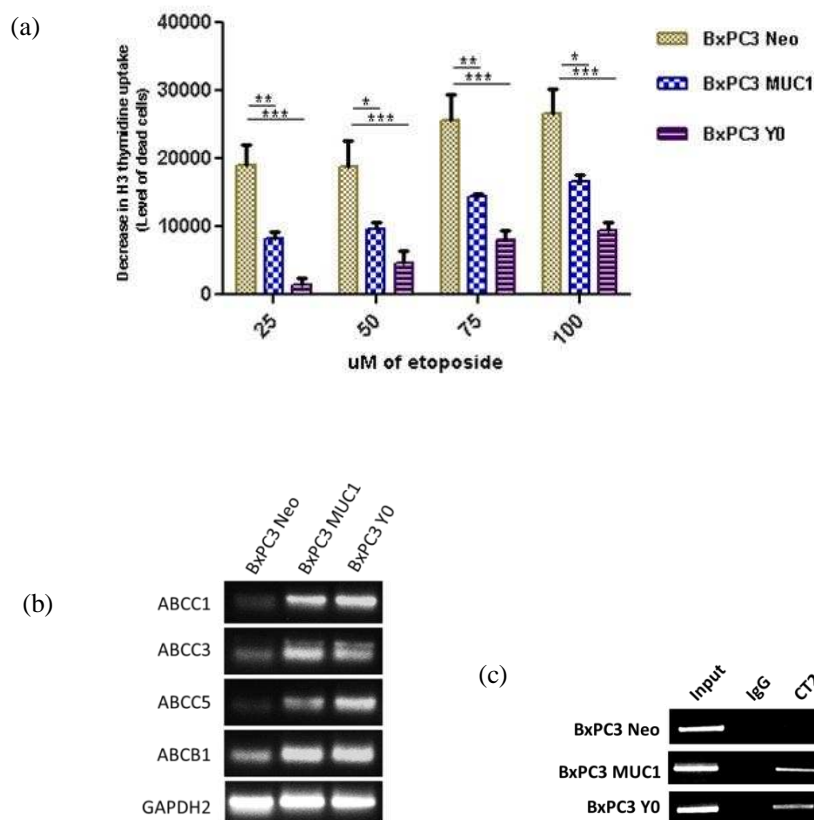
Figure 5.1. The functional role of full length MUC1 in coxtemt of drug resistance is not attenuated upon removal of the tyrosine residues.(a) Difference in H^3 thymidine uptake in BxPC3 Neo, MUC1 and Y0 cells following 24 hours treatment with etoposide. Significant differences in H^3 uptake between Neo, MUC1 and Y0 at varying concentrations of the drugs is shown as p-values (n=4) (**p<0.01, *** p<0.001). (b) RT-PCR data showing fold changes in the m-RNA level of MDR genes that are associated with multidrug resistance. (c) ChIP–PCR assay reveals an interaction between full length MUC1 CT and MUC1 YO with the promoter region of the ABCC1 gene. ChIP–PCR; lanes include: Input DNA, DNA precipitated using control IgG and CT2, and amplified by PCR using Taq polymerase and separated by 2% agarose gel.

REFERENCES

[1]   C. Facts, "Cancer Facts & Figures," 2013.

[2]   C. K. (eds). Howlader N, Noone AM, Krapcho M, Garshell J, Neyman N, Altekruse SF, Kosary CL, Yu M, Ruhl J, Tatalovich Z, Cho H, Mariotto A, Lewis DR, Chen HS, Feuer EJ, "SEER Cancer statistics review 1975-2010," 2013.

[3]   N. Bardeesy and R. a DePinho, "Pancreatic cancer biology and genetics.," Nature reviews. Cancer, vol. 2, no. 12, pp. 897–909, Dec. 2002.

[4]   L. Liszka, J. Pająk, S. Mrowiec, E. Zielińska-Pająk, D. Gołka, and P. Lampe, "Precursor lesions of early onset pancreatic cancer.," *Virchows Archiv : an* international journal of pathology, vol. 458, no. 4, pp. 439–51, Apr. 2011.

[5]   A. Maitra, S. E. Kern, and R. H. Hruban, "Molecular pathogenesis of pancreatic cancer.," Best practice & research. Clinical gastroenterology, vol. 20, no. 2, pp. 211–26, May 2006.

[6]   E. Tsiambas, A. Karameris, C. Dervenis, and A. C. Lazaris, "HER2 / neu Expression and Gene Alterations in Pancreatic Ductal Adenocarcinoma : A Comparative Immunohistochemistry and Chromogenic in Situ Hybridization Study Based on Tissue Microarrays and Computerized Image Analysis," vol. 7, no. 3, pp. 283–294, 2006.

[7]   M. Goggins, M. Schutte, J. Lu, C. A. Moskaluk, C. L. Weinstein, G. M. Petersen, C. J. Yeo, C. E. Jackson, H. T. Lynch, R. H. Hruban, and S. E. Kern, "Germline BRCA2 Gene Mutations in Patients with Apparently Sporadic Pancreatic Carcinomas Advances in Brief Germline BRCA2 Gene Mutations in Patients with Apparently Sporadic Pancreatic Carcinomas '," pp. 5360–5364, 1996.

[8]   S. Jones, X. Zhang, D. W. Parsons, J. C.-H. Lin, R. J. Leary, P. Angenendt, P. Mankoo, H. Carter, H. Kamiyama, A. Jimeno, S.-M. Hong, B. Fu, M.-T. Lin, E. S. Calhoun, M. Kamiyama, K. Walter, T. Nikolskaya, Y. Nikolsky, J. Hartigan, D. R. Smith, M. Hidalgo, S. D. Leach, A. P. Klein, E. M. Jaffee, M. Goggins, A. Maitra, C. Iacobuzio-Donahue, J. R. Eshleman, S. E. Kern, R. H. Hruban, R. Karchin, N. Papadopoulos, G. Parmigiani, B. Vogelstein, V. E. Velculescu, and K. W. Kinzler, "Core signaling pathways in human pancreatic cancers revealed by global genomic analyses.," Science (New York, N.Y.), vol. 321, no. 5897, pp. 1801–6, Sep. 2008.

[9]   N. Jonckheere, N. Skrypek, and I. Van Seuningen, "Mucins and Pancreatic Cancer," Cancers, vol. 2, no. 4, pp. 1794–1812, Oct. 2010.

[10]   A. Vonlaufen1, S. Joshi1, C. Qu1, P. A. Phillips1, Z. Xu1, N. R. Parker1, C. S. Toi1, R. C. Pirola1, J. S. Wilson1, A. David Goldstein2, and M. V. Apte1, "Pancreatic Stellate Cells: Partners in Crime with Pancreatic Cancer Cells," Cancer research, vol. 68, no. 7, pp. 2085–93, 2008.

[11] 2 and Ralph H. Hruban1 Anirban Maitra1, "Pancreatic cancer," Annual review of pathology, 2008.

[12] M. Hidalgo, "Pancreatic cancer," The New England Journal of Medicine, vol. 362, no. 17, pp. 1605–1617, 2008.

[13] M. Goggins, "Markers of Pancreatic Cancer: Working Toward Early Detection," Clinical Cancer Research, vol. 17, 2011.

[14] N. M. Takezako Y, Okusaka T, Ueno H, Ikeda M, Morizane C, "Tumor markers for pancreatic and biliary tract cancer.," Gan To Kagaku Ryoho, vol. 31, no. 9, pp. 1443–1460, 2004.

[15] Z. K. Szajda SD, Waszkiewicz N, Chojnowska S, "Carbohydrate markers of pancreatic cancer.," Biochemical Society transactions, vol. 39, no. 1, pp. 340–343, 2011.

[16] H. B. | F. G. | G. L. HG, "Pancreatic cancer: Who benefits from curative resection?," Canadian Journal of Gastroenterology, vol. 16, 2002.

[17] V. H. D. Burris HA 3rd, Moore MJ, Andersen J, Green MR, Rothenberg ML, Modiano MR, Cripps MC, Portenoy RK, Storniolo AM, Tarassoff P, Nelson R, Dorr FA, Stephens CD, "Improvements in survival and clinical benefit with gemcitabine as first-line therapy for patients with advanced pancreas cancer," *Journal of clinical oncology : official journal of the American Society of Clinical* Oncology, no. 15, pp. 2403–13, 1997.

[18] F. N. Squadroni M, "Chemotherapy in pancreatic adenocarcinoma.," European review medical pharmacological sciences, vol. 14, no. 4, pp. 386–394, 2010.

[19] V. E. Kindler HL, Karrison TG, Gandara DR, Lu C, Krug LM, Stevenson JP, Jänne PA, Quinn DI, Koczywas MN, Brahmer JR, Albain KS, Taber DA, Armato SG 3rd, Vogelzang NJ, Chen HX, Stadler WM, "Multicenter, double-blind, placebo-controlled, randomized phase II trial of gemcitabine/cisplatin plus bevacizumab or placebo in patients with malignant mesothelioma.," Journal of Clinical Oncology, vol. 30, no. 20, pp. 2509–2515, 2012.

[20] L. C. Heinemann V, Boeck S, Hinke A, Labianca R, "Meta-analysis of randomized trials: evaluation of benefit from gemcitabine-based combination chemotherapy applied in advanced pancreatic cancer.," BMC cancer, vol. 8, no. 82, 2008.

[21] B. A. 3rd. Poplin E, Feng Y, Berlin J, Rothenberg ML, Hochster H, Mitchell E, Alberts S, O'Dwyer P, Haller D, Catalano P, Cella D, "Phase III, randomized study of gemcitabine and oxaliplatin versus gemcitabine (fixed-dose rate infusion) compared with gemcitabine (30-minute infusion) in patients with pancreatic carcinoma E6201: a trial of the Eastern Cooperative Oncology Group.," Journal of Clinical Oncology, vol. 27, no. 23, pp. 3778–3785, 2009.

[22] G. R. Kindler HL, Niedzwiecki D, Hollis D, Sutherland S, Schrag D, Hurwitz H, Innocenti F, Mulcahy MF, O'Reilly E, Wozniak TF, Picus J, Bhargava P, Mayer RJ, Schilsky RL, "Gemcitabine plus bevacizumab compared with gemcitabine plus placebo in patients with advanced pancreatic cancer: phase III trial of the Cancer and Leukemia Group B (CALGB 80303).," Journal of Clinical Oncology, vol. 28, no. 22, pp. 3617–3622, 2010.

[23]
  "http://www.fda.gov/NewsEvents/Newsroom/PressAnnouncements/ucm367442.htm," 2013. .

[24] C. L. Hattrup and S. J. Gendler, "Structure and function of the cell surface (tethered) mucins.," Annual review of physiology, vol. 70, pp. 431–57, Jan. 2008.

[25] N. Jonckheere, N. Skrypek, F. Frénois, and I. Van Seuningen, "Membrane-bound mucin modular domains: from structure to function.," Biochimie, vol. 95, no. 6, pp. 1077–86, Jul. 2013.

[26] G. Theodoropoulos and K. L. Carraway, "Molecular signaling in the regulation of mucins.," Journal of cellular biochemistry, vol. 102, no. 5, pp. 1103–16, Dec. 2007.

[27] N. Jonckheere and I. Van Seuningen, "The membrane-bound mucins: From cell signalling to transcriptional regulation and expression in epithelial cancers.," Biochimie, vol. 92, no. 1, pp. 1–11, Jan. 2010.

[28] D. W. Kufe, "Mucins in cancer: function, prognosis and therapy.," Nature reviews. Cancer, vol. 9, no. 12, pp. 874–85, Dec. 2009.

[29] M. C. Rose, "Mucins: structure, function, and role in pulmonary diseases.," The American journal of physiology, vol. 263, no. 4 Pt 1, pp. L413–29, Oct. 1992.

[30] I. V. S. N. Jonckheere, "The Epithelial Mucins: Structure/Function. Roles in Cancer and Inflammatory Diseases.," Research Signpost, pp. 17–38, 2008.

[31] B. Macao, D. G. a Johansson, G. C. Hansson, and T. Härd, "Autoproteolysis coupled to protein folding in the SEA domain of the membrane-bound MUC1 mucin.," Nature structural & molecular biology, vol. 13, no. 1, pp. 71–6, Jan. 2006.

[32] P. J. Cullen, "Post-Translational Regulation of Signaling Mucins," Current opinion structural biology, vol. 21, no. 5, pp. 590–596, 2011.

[33] S. Röttger, J. White, H. H. Wandall, J. C. Olivo, a Stark, E. P. Bennett, C. Whitehouse, E. G. Berger, H. Clausen, and T. Nilsson, "Localization of three human polypeptide GalNAc-transferases in HeLa cells suggests initiation of O-

linked glycosylation throughout the Golgi apparatus.," Journal of cell science, vol. 111 (Pt 1, pp. 45–60, Jan. 1998.

[34]   S. Parry, F. G. Hanisch, S.-H. Leir, M. Sutton-Smith, H. R. Morris, A. Dell, and A. Harris, "N-Glycosylation of the MUC1 mucin in epithelial cells and secretions.," Glycobiology, vol. 16, no. 7, pp. 623–34, Jul. 2006.

[35]   Thomas A. Gerken, L. Revoredo, J. J. C. Thome, L. A. Tabak, M. B. Vester-Christensen, H. Clausen, G. K. Gahlay, D. L. Jarvis, R. W. Johnson, H. A. M. And, and K. Moremen, "Glycosylation in an N- or C-terminal Direction, Further Controlling Mucin Type O-Glycosylation.," The Journal of biological chemistry, vol. 288, pp. 19900–19914, 2013.

[36]   Y. Altschuler, C. L. Kinlough, P. A. Poland, J. B. Bruns, G. Apodaca, O. A. Weisz, and R. P. Hughey, "Clathrin-mediated Endocytosis of MUC1 Is Modulated by Its Glycosylation State," vol. 11, no. March, pp. 819–831, 2000.

[37]   K. Engelmann, C. L. Kinlough, S. Müller, H. Razawi, S. E. Baldus, R. P. Hughey, and F.-G. Hanisch, "Transmembrane and secreted MUC1 probes show trafficking-dependent changes in O-glycan core profiles.," Glycobiology, vol. 15, no. 11, pp. 1111–24, Nov. 2005.

[38]   J. Litvinov, S.V. and Hilkens, "The epithelial sialomucin, episialin, is sialylated during recycling," The Journal of biological chemistry, vol. 268, pp. 21364–21371, 1993.

[39]   M. a Hollingsworth and B. J. Swanson, "Mucins in cancer: protection and control of the cell surface.," Nature reviews. Cancer, vol. 4, no. 1, pp. 45–60, Jan. 2004.

[40]   S. J. Gendler, "MUC1, the renaissance molecule.," Journal of mammary gland biology and neoplasia, vol. 6, no. 3, pp. 339–53, Jul. 2001.

[41]   J. F. Chang, H. L. Zhao, J. Phillips, and G. Greenburg, "The epithelial mucin, MUC1, is expressed on resting T lymphocytes and can function as a negative regulator of T cell activation.," Cellular immunology, vol. 201, no. 2, pp. 83–8, May 2000.

[42]   A. Baruch, M. Hartmann, M. Yoeli, Y. Adereth, S. Greenstein, Y. Stadler, and Y. Skornik, "The Breast Cancer-associated MUC1 Gene Generates Both a Receptor and Its Cognate Binding Protein The Breast Cancer-associated MUC1 Gene Generates Both a Receptor and Its," pp. 1552–1561, 1999.

[43]   D. W. Kufe, "MUC1-C oncoprotein as a target in breast cancer: activation of signaling pathways and therapeutic approaches.," Oncogene, vol. 32, no. 9, pp. 1073–81, Mar. 2013.

[44] F. Levitin‡, O. Stern‡, M. Weiss§, C. Gil-Henn‡, R. Ziv‡, Z. Prokocimer‡, N. I. Smorodinsky‡¶, D. B. R. And, and 1 Daniel H. Wreschner‡, "The MUC1 SEA Module Is a Self-cleaving Domain*," Journal of Biological Chemistry, vol. 280, no. 8, pp. 33374–33386., 2005.

[45] a P. Spicer, G. Parry, S. Patton, and S. J. Gendler, "Molecular cloning and analysis of the mouse homologue of the tumor-associated mucin, MUC1, reveals conservation of potential O-glycosylation sites, transmembrane, and cytoplasmic domains and a loss of minisatellite-like polymorphism.," The Journal of biological chemistry, vol. 266, no. 23, pp. 15099–109, Aug. 1991.

[46] I. Brockhausen, J. M. Yang, J. Burchell, C. Whitehouse, and J. Taylor-Papadimitriou, "Mechanisms underlying aberrant glycosylation of MUC1 mucin in breast cancer cells.," European journal of biochemistry / FEBS, vol. 233, no. 2, pp. 607–17, Oct. 1995.

[47] D. D. Carson, "The cytoplasmic tail of MUC1: a very busy place.," Science signaling, vol. 1, no. 27, p. pe35, Jan. 2008.

[48] C. L. Kinlough, R. J. McMahan, P. A. Poland, J. B. Bruns, K. L. Harkleroad, R. J. Stremple, O. B. Kashlan, K. M. Weixel1, O. A. W. And, and R. P. Hughey2, "Recycling of MUC1 Is Dependent on Its Palmitoylation," Journal of Biological Chemistry, vol. 281, no. 4, pp. 12112–12122., 2006.

[49] C. L. Kinlough, P. a Poland, J. B. Bruns, K. L. Harkleroad, and R. P. Hughey, "MUC1 membrane trafficking is modulated by multiple interactions.," The Journal of biological chemistry, vol. 279, no. 51, pp. 53071–7, Dec. 2004.

[50] H. Razawi2, 5 Carol L Kinlough4, S. Staubach2, 5 Paul A Poland4, Y. Rbaibi4, O. A. Weisz4, 5 and Rebecca P Hughey1, 4, and 3 Franz-Georg Hanisch1, 2, "Evidence for core 2 to core 1 O-glycan remodeling during the recycling of MUC1," Glycobiology, 2013.

[51] F. G. Hanisch and S. Müller, "MUC1: the polymorphic appearance of a human mucin.," Glycobiology, vol. 10, no. 5, pp. 439–49, May 2000.

[52] B. C. Schut IC, Waterfall PM, Ross M, O'Sullivan C, Miller WR, Habib FK, "MUC1 expression, splice variant and short form transcription (MUC1/Z, MUC1/Y) in prostate cell lines and tissue," Bju International, vol. 91, pp. 278–283, 2003.

[53] W. D. Baruch A, Hartmann M, Zrihan-Licht S, Greenstein S, Burstein M, Keydar I, Weiss M, Smorodinsky N, "Preferential expression of novel MUC1 tumor antigen isoforms in human epithelial tumors and their tumor-potentiating function.," International Journal of Cancer, vol. 71, no. 741–749, 1997.

[54] L. K. Bast RC Jr, Badgwell D, Lu Z, Marquez R, Rosen D, Liu J, Baggerly KA, Atkinson EN, Skates S, Zhang Z, Lokshin A, Menon U, Jacobs I, "New tumor markers:CA125 and beyond," International journal of gynecological cancer, vol. 15, pp. 274–281, 2005.

[55] A. M. Lacunza E, Baudis M, Colussi AG, Segal-Eiras A, Croce MV, "MUC1 oncogene amplification correlates with protein overexpression in invasive breast carcinoma cells.," Cancer genetics and cytogenetics, vol. 201, no. 2, pp. 102–110, 2010.

[56] A. Thathiah, M. Brayman, N. Dharmaraj, J. J. Julian, E. L. Lagow, and D. D. Carson, "Tumor necrosis factor alpha stimulates MUC1 synthesis and ectodomain release in a human uterine epithelial cell line.," Endocrinology, vol. 145, no. 9, pp. 4192–203, Sep. 2004.

[57] S. Nath, K. Daneshvar, L. D. Roy, P. Grover, A. Kidiyoor, L. Mosley, M. Sahraei, and P. Mukherjee, "MUC1 induces drug resistance in pancreatic cancer cells via upregulation of multidrug resistance genes," Oncogenesis, vol. 2, no. 6, pp. e51–9, 2013.

[58] D. M. Besmer, J. M. Curry, L. D. Roy, T. L. Tinder, M. Sahraei, J. Schettini, S.-I. Hwang, Y. Y. Lee, S. J. Gendler, and P. Mukherjee, "Pancreatic ductal adenocarcinoma mice lacking mucin 1 have a profound defect in tumor growth and metastasis.," Cancer research, vol. 71, no. 13, pp. 4432–42, Jul. 2011.

[59] K. Kato, W. Lu, H. Kai, and K. C. Kim, "Phosphoinositide 3-kinase is activated by MUC1 but not responsible for MUC1-induced suppression of Toll-like receptor 5 signaling.," American journal of physiology. Lung cellular and molecular physiology, vol. 293, no. 3, pp. L686–92, Sep. 2007.

[60] E. J. Thompson, K. Shanmugam, C. L. Hattrup, K. L. Kotlarczyk, A. Gutierrez, J. M. Bradley, P. Mukherjee, and S. J. Gendler, "Tyrosines in the MUC1 cytoplasmic tail modulate transcription via the extracellular signal-regulated kinase 1/2 and nuclear factor-kappaB pathways.," *Molecular cancer research : MCR*, vol. 4, no. 7, pp. 489–97, Jul. 2006.

[61] C. L. Hattrup and S. J. Gendler, "MUC1 alters oncogenic events and transcription in human breast cancer cells.," *Breast cancer research : BCR*, vol. 8, no. 4, p. R37, Jan. 2006.

[62] L. D. Roy, M. Sahraei, D. B. Subramani, D. Besmer, S. Nath, T. L. Tinder, E. Bajaj, K. Shanmugam, Y. Y. Lee, S. I. L. Hwang, S. J. Gendler, and P. Mukherjee, "MUC1 enhances invasiveness of pancreatic cancer cells by inducing epithelial to mesenchymal transition.," Oncogene, vol. 30, no. 12, pp. 1449–59, Mar. 2011.

[63] M. P. Sahraei M, Roy LD, Curry JM, Teresa TL, Nath S, Besmer D, Kidiyoor A, Dalia R, Gendler SJ, "MUC1 regulates PDGFA expression during pancreatic cancer progression.," Oncogene, vol. 31, no. 47, pp. 4935–45, 2012.

[64] M. E. Behrens, P. M. Grandgenett, J. M. Bailey, P. K. Singh, C.-H. Yi, F. Yu, and M. a Hollingsworth, "The reactive tumor microenvironment: MUC1 signaling directly reprograms transcription of CTGF.," Oncogene, vol. 29, no. 42, pp. 5667–77, Oct. 2010.

[65] R. Ahmad, D. Raina, M. D. Joshi, T. Kawano, J. Ren, S. Kharbanda, and D. Kufe, "MUC1-C oncoprotein functions as a direct activator of the nuclear factor-kappaB p65 transcription factor.," Cancer research, vol. 69, no. 17, pp. 7013–21, Sep. 2009.

[66] F. O. Cascio S, Zhang L, "MUC1 protein expression in tumor cells regulates transcription of proinflammatory cytokines by forming a complex with nuclear factor-κB p65 and binding to cytokine promoters: importance of extracellular domain.," Cancer research, vol. 286, no. 49, pp. 42248–56, 2011.

[67] G. J. Rowse, "Delayed Mammary Tumor Progression in Muc-1 Null Mice," Journal of Biological Chemistry, vol. 270, no. 50, pp. 30093–30101, Dec. 1995.

[68] D. Raina, S. Kharbanda, and D. Kufe, "The MUC1 oncoprotein activates the anti-apoptotic phosphoinositide 3-kinase/Akt and Bcl-xL pathways in rat 3Y1 fibroblasts.," The Journal of biological chemistry, vol. 279, no. 20, pp. 20607–12, May 2004.

[69] S. J. Bitler BG, Goverdhan A, "MUC1 regulates nuclear localization and function of the epidermal growth factor receptor.," Journal of cell science, vol. 123, pp. 1716–23, 2010.

[70] T. Brabletz, "To differentiate or not--routes towards metastasis.," Nature reviews. Cancer, vol. 12, no. 6, pp. 425–36, Jul. 2012.

[71] R. Kalluri and R. A. Weinberg, "Review series The basics of epithelial-mesenchymal transition," Journal of Clinical Investigation, vol. 119, no. 6, 2009.

[72] K. Kondo, N. Kohno, A. Yokoyama, B. Cancer, C. Lines, and K. Hiwada, "Decreased MUC1 Expression Induces E-Cadherin-mediated Cell Adhesion of Breast Cancer Cell Lines Decreased MUC1 Expression Induces E-Cadherin-mediated Cell Adhesion of," pp. 2014–2019, 2014.

[73] 2 Pankaj K. Singh1, 2 Yunfei Wen1, B. J. Swanson1, K. Shanmugam3, A. Kazlauskas4, R. L. Cerny5, A. Sandra J. Gendler3, and 2 Michael A. Hollingsworth1, "Platelet-Derived Growth Factor Receptor β–Mediated Phosphorylation of MUC1 Enhances Invasiveness in Pancreatic Adenocarcinoma Cells," Cancer Research, vol. 67, 2007.

[74] K. G. Lüttges J, Feyerabend B, Buchelt T, Pacena M, "The mucin profile of noninvasive and invasive mucinous cystic neoplasms of the pancreas," American Journal of Surgical Pathology, vol. 26, no. 4, pp. 466–71, 2002.

[75] "MUC1 mucin expression as a marker of progression and metastasis of human colorectal carcinoma.," Gastroenterology, vol. 106, pp. 353–361, 1994.

[76] M. H. Kashiwagi H, Kijima H, Dowaki S, Ohtani Y, Tobita K, Tsukui M, Tanaka Y, Matsubayasi H, Tsuchida T, Yamazaki H, Nakamura M, Ueyama Y, Tanaka M, Tajima T, "DF3 expression in human gallbladder carcinoma: significance for lymphatic invasion," International Journal of Oncology, vol. 16, no. 3, pp. 455–9, 2000.

[77] N. S. Chandel, D. S. McClintock, C. E. Feliciano, T. M. Wood, J. a Melendez, a M. Rodriguez, and P. T. Schumacker, "Reactive oxygen species generated at mitochondrial complex III stabilize hypoxia-inducible factor-1alpha during hypoxia: a mechanism of O2 sensing.," The Journal of biological chemistry, vol. 275, no. 33, pp. 25130–8, Aug. 2000.

[78] G. L. Semenza, "Targeting HIF-1 for cancer therapy.," Nature reviews. Cancer, vol. 3, no. 10, pp. 721–32, Oct. 2003.

[79] J. P. Fruehauf and F. L. Meyskens, "Reactive oxygen species: a breath of life or death?," *Clinical cancer research : an official journal of the American Association* for Cancer Research, vol. 13, no. 3, pp. 789–94, Feb. 2007.

[80] S. Kitamoto, S. Yokoyama, M. Higashi, N. Yamada, S. Takao, and S. Yonezawa, "MUC1 enhances hypoxia-driven angiogenesis through the regulation of multiple proangiogenic factors.," Oncogene, no. May, pp. 1–8, Oct. 2012.

[81] J. K. Woo, Y. Choi, S.-H. Oh, J.-H. Jeong, D.-H. Choi, H.-S. Seo, and C.-W. Kim, "Mucin 1 enhances the tumor angiogenic response by activation of the AKT signaling pathway.," Oncogene, vol. 31, no. 17, pp. 2187–98, Apr. 2012.

[82] S. Kitamoto, S. Yokoyama, M. Higashi, N. Yamada, S. Takao, S. Yonezawa, and Y. S. Kitamoto S, Yokoyama S, Higashi M, Yamada N, Takao S, "MUC1 enhances hypoxia-driven angiogenesis through the regulation of multiple proangiogenic factors.," Oncogene, no. May, pp. 1–8, Oct. 2012.

[83] P. M. Aubert S, Fauquette V, Hémon B, Lepoivre R, Briez N, Bernard D, Van Seuningen I, Leroy X, S. Aubert, V. Fauquette, B. Hémon, R. Lepoivre, N. Briez, D. Bernard, I. Van Seuningen, X. Leroy, and M. Perrais, "MUC1, a new hypoxia inducible factor target gene, is an actor in clear renal cell carcinoma tumor progression.," Cancer research, vol. 69, no. 14, pp. 5707–5715, Jul. 2009.

[84] L. Yin, S. Kharbanda, and D. Kufe, "Mucin 1 oncoprotein blocks hypoxia-inducible factor 1alpha activation in a survival response to hypoxia.," The Journal of biological chemistry, vol. 282, no. 1, pp. 257–66, Jan. 2007.

[85] "Pancreatic cancer treatment." .

[86] D. G. a Johansson, B. Macao, A. Sandberg, and T. Härd, "SEA domain autoproteolysis accelerated by conformational strain: mechanistic aspects.," Journal of molecular biology, vol. 377, no. 4, pp. 1130–43, Apr. 2008.

[87] "http://www.genusoncology.com/technology.php." .

[88] C. M. Niessen, "Tight junctions/adherens junctions: basic structure and function.," The Journal of investigative dermatology, vol. 127, no. 11, pp. 2525–32, Nov. 2007.

[89] W. Jäeger, "Classical resistance mechanisms.," International journal of clinical pharmacology and therapeutics, vol. 47, no. 1, pp. 46–8, Jan. 2009.

[90] Z. Wang, Y. Li, A. Ahmad, S. Banerjee, A. S. Azmi, D. Kong, and F. H. Sarkar, "Pancreatic cancer: understanding and overcoming chemoresistance.," Nature reviews. Gastroenterology & hepatology, vol. 8, no. 1. pp. 27–33, Jan-2011.

[91] M. M. Gottesman, T. Fojo, and S. E. Bates, "Multidrug resistance in cancer: role of ATP-dependent transporters.," Nature reviews. Cancer, vol. 2, no. 1, pp. 48–58, Jan. 2002.

[92] S. Misra, S. Ghatak, and B. P. Toole, "Regulation of MDR1 expression and drug resistance by a positive feedback loop involving hyaluronan, phosphoinositide 3-kinase, and ErbB2.," The Journal of biological chemistry, vol. 280, no. 21, pp. 20310–5, May 2005.

[93] A. Persidis, "Cancer multidrug resistance," Nature biotechnology, vol. 17, pp. 94–95, 1999.

[94] P. Borst, "Multidrug resistance: A solvable problem?," Annals of oncology, pp. 162–164, 1999.

[95] C. F. Higgins, "ABC transporters: physiology, structure and mechanism--an overview.," Research in microbiology, vol. 152, no. 3–4, pp. 205–10, 2001.

[96] J.-T. Zhang, "Use of arrays to investigate the contribution of ATP-binding cassette transporters to drug resistance in cancer chemotherapy and prediction of chemosensitivity.," Cell research, vol. 17, no. 4, pp. 311–23, Apr. 2007.

[97] F. J. Sharom, "ABC multidrug transporters: structure, function and role in chemoresistance.," Pharmacogenomics, vol. 9, no. 1, pp. 105–27, Jan. 2008.

[98] W. S. O. L. O'DRISCOLL1*, N. WALSH1*, A. LARKIN1, J. BALLOT2 and 2** and S. KENNEDY2** G. GULLO2, R. O'CONNOR1, M. CLYNES1, J. CROWN1, "MDR1/P-glycoprotein and MRP-1 Drug Efflux Pumps in Pancreatic Carcinoma.," Anticancer research, vol. 27, pp. 2115–2120, 2007.

[99] J. König, M. Hartel, A. T. Nies, M. E. Martignoni, J. Guo, M. W. Büchler, H. Friess, and D. Keppler, "Expression and localization of human multidrug resistance protein (ABCC) family members in pancreatic carcinoma.," International journal of cancer. Journal international du cancer, vol. 115, no. 3, pp. 359–67, Jun. 2005.

[100] G. A. and C. A. Kruh GD, Gaughan KT, "Expression pattern of MRP in human tissues and adult solid tumor cell lines," J Natl Cancer Inst, vol. 87, pp. 1256–1258, 1995.

[101] J. A. Fresno Vara, E. Casado, J. de Castro, P. Cejas, C. Belda-Iniesta, and M. González-Barón, "PI3K/Akt signalling pathway and cancer.," Cancer treatment reviews, vol. 30, no. 2, pp. 193–204, Apr. 2004.

[102] M. Siragusa, M. Zerilli, F. Iovino, M. G. Francipane, Y. Lombardo, L. Ricci-Vitiani, G. Di Gesù, M. Todaro, R. De Maria, and G. Stassi, "MUC1 oncoprotein promotes refractoriness to chemotherapy in thyroid cancer cells.," Cancer research, vol. 67, no. 11, pp. 5522–30, Jun. 2007.

[103] J. T. Lee, L. S. Steelman, and J. a McCubrey, "Phosphatidylinositol 3'-kinase activation leads to multidrug resistance protein-1 expression and subsequent chemoresistance in advanced prostate cancer cells.," Cancer research, vol. 64, no. 22, pp. 8397–404, Nov. 2004.

[104] S. R. Hingorani, E. F. Petricoin, A. Maitra, V. Rajapakse, C. King, M. a Jacobetz, S. Ross, T. P. Conrads, T. D. Veenstra, B. a Hitt, Y. Kawaguchi, D. Johann, L. a Liotta, H. C. Crawford, M. E. Putt, T. Jacks, C. V. E. Wright, R. H. Hruban, A. M. Lowy, and D. a Tuveson, "Preinvasive and invasive ductal pancreatic cancer and its early detection in the mouse.," Cancer cell, vol. 4, no. 6, pp. 437–50, Dec. 2003.

[105] T. L. Tinder, D. B. Subramani, G. D. Basu, J. M. Bradley, J. Schettini, A. Million, T. Skaar, and P. Mukherjee, "MUC1 enhances tumor progression and contributes toward immunosuppression in a mouse model of spontaneous pancreatic adenocarcinoma.," *Journal of immunology (Baltimore, Md. : 1950)*, vol. 181, no. 5, pp. 3116–25, Sep. 2008.

[106] J. Ren, N. Agata, D. Chen, Y. Li, W. Yu, L. Huang, D. Raina, W. Chen, S. Kharbanda, and D. Kufe, "Human MUC1 carcinoma-associated protein confers resistance to genotoxic anticancer agents.," Cancer cell, vol. 5, no. 2, pp. 163–75, Feb. 2004.

[107] K. W. Scotto, "Transcriptional regulation of ABC drug transporters.," Oncogene, vol. 22, no. 47, pp. 7496–511, Oct. 2003.

[108] E. U. Kurz, S. P. Cole, and R. G. Deeley, "Identification of DNA-protein interactions in the 5' flanking and 5' untranslated regions of the human multidrug resistance protein (MRP1) gene: evaluation of a putative antioxidant response element/AP-1 binding site.," Biochemical and biophysical research communications, vol. 285, no. 4, pp. 981–90, Jul. 2001.

[109] H. Zahreddine and K. L. B. Borden, "Mechanisms and insights into drug resistance in cancer.," Frontiers in pharmacology, vol. 4, no. March, p. 28, Jan. 2013.

[110] R. M. Garavito and A. M. Mulichak, "The structure of mammalian cyclooxygenases.," Annual review of biophysics and biomolecular structure, vol. 32, pp. 183–206, Jan. 2003.

[111] S. Zha, V. Yegnasubramanian, W. G. Nelson, W. B. Isaacs, and A. M. De Marzo, "Cyclooxygenases in cancer: progress and perspective.," Cancer letters, vol. 215, no. 1, pp. 1–20, Nov. 2004.

[112] C. S. Williams, M. Mann, and R. N. DuBois, "The role of cyclooxygenases in inflammation, cancer, and development.," Oncogene, vol. 18, no. 55, pp. 7908–16, Dec. 1999.

[113] S. W. Kurumbail RG, Stevens AM, Gierse JK, McDonald JJ, Stegeman RA, Pak JY, Gildehaus D, Miyashiro JM, Penning TD, Seibert K, Isakson PC, "Structural basis for selective inhibition of cyclooxygenase-2 by antiinflammatory drugs."

[114] W. L. Smith, D. L. DeWitt, and R. M. Garavito, "Cyclooxygenases: structural, cellular, and molecular biology.," Annual review of biochemistry, vol. 69, pp. 145–82, Jan. 2000.

[115] H. T. Everts B, Währborg P, "COX-2-Specific inhibitors--the emergence of a new class of analgesic and anti-inflammatory drugs," Clinical Rheumatology, vol. 19, no. 5, pp. 331–43, 2000.

[116] P. Sinha, V. K. Clements, A. M. Fulton, and S. Ostrand-Rosenberg, "Prostaglandin E2 promotes tumor progression by inducing myeloid-derived suppressor cells.," Cancer research, vol. 67, no. 9, pp. 4507–13, May 2007.

[117] B. B. Aggarwal, S. Shishodia, S. K. Sandur, M. K. Pandey, and G. Sethi, "Inflammation and cancer: how hot is the link?," Biochemical pharmacology, vol. 72, no. 11, pp. 1605–21, Nov. 2006.

[118] T. L. Tinder, D. B. Subramani, G. D. Basu, J. M. Bradley, A. Million, T. Skaar, and P. Mukherjee, "MUC1 enhances tumor progression and contributes towards

immunosuppression in a mouse model of spontaneous pancreatic adenocarcinoma," vol. 181, no. 5, pp. 3116–3125, 2009.

[119] J. M. Curry, K. J. Thompson, S. G. Rao, D. M. Besmer, A. M. Murphy, V. Z. Grdzelishvili, W. a Ahrens, I. H. McKillop, D. Sindram, D. a Iannitti, J. B. Martinie, and P. Mukherjee, "The use of a novel MUC1 antibody to identify cancer stem cells and circulating MUC1 in mice and patients with pancreatic cancer.," Journal of surgical oncology, vol. 107, no. 7, pp. 713–22, Jun. 2013.

[120] M. T. Yip-schneider, D. S. Barnard, S. D. Billings, L. Cheng, D. K. Heilman, A. Lin, S. J. Marshall, P. L. Crowell, M. S. Marshall, and C. J. Sweeney, "Cyclooxygenase-2 expression in human pancreatic adenocarcinomas treatment of pancreatic cancer .," vol. 21, no. 2, pp. 139–146, 2000.

[121] N. M. Ura H, Obara T, Nishino N, Tanno S, Okamura K, "Cytotoxicity of simvastatin to pancreatic adenocarcinoma cells containing mutant ras gene," Japanese journal of cancer research, vol. 85, no. 6, pp. 633–8, 1994.

[122] Y.-J. Kang, B. a Wingerd, T. Arakawa, and W. L. Smith, "Cyclooxygenase-2 gene transcription in a macrophage model of inflammation.," Journal of immunology (Baltimore, Md. : 1950), vol. 177, no. 11, pp. 8111–22, Dec. 2006.

[123] H. Inoue, T. Nanayama, S. Hara, C. Yokoyama, and T. Tanabe, "The cyclic AMP response element plays an essential role in the expression of the human prostaglandin-endoperoxide synthase 2 gene in differentiated U937 monocytic cells.," FEBS letters, vol. 350, no. 1, pp. 51–4, Aug. 1994.

[124] H. L. Plummer SM, Holloway KA, Manson MM, Munks RJ, Kaptein A, Farrow S, "Inhibition of cyclo-oxygenase 2 expression in colon cells by the chemopreventive agent curcumin involves inhibition of NF-kappaB activation via the NIK/IKK signalling complex," Oncogene, vol. 19, pp. 6013–6020, 1999.

[125] G. N. Charalambous MP, Lightfoot T, Speirs V, Horgan K, "Expression of COX-2, NF-kappaB-p65, NF-kappaB-p50 and IKKalpha in malignant and adjacent normal human colorectal tissue.," British journal of cancer, vol. 101, no. 1, pp. 106–115, 2009.

[126] A. TE Ding XZ, Hennig R, "Lipoxygenase and cyclooxygenase metabolism: new insights in treatment and chemoprevention of pancreatic cancer," Molecular cancer, vol. 2, no. 10, 2003.

[127] L. R. Howe, "Inflammation and breast cancer. Cyclooxygenase/ prostaglandin signaling and breast cancer," Breast cancer research : BCR, vol. 9, no. 4, p. 210, 2007.

[128] M. Zhu1, 2 Y. Zhu1, and P. Lance1, "TNFα-activated stromal COX-2 signalling promotes proliferative and invasive potential of colon cancer epithelial cells," Cell Proliferation, vol. 46, no. 4, pp. 374–381, 2013.

[129] M. Dohadwala, R. K. Batra, J. Luo, Y. Lin, K. Krysan, M. Pold, S. Sharma, and S. M. Dubinett, "Autocrine/paracrine prostaglandin E2 production by non-small cell lung cancer cells regulates matrix metalloproteinase-2 and CD44 in cyclooxygenase-2-dependent invasion.," The Journal of biological chemistry, vol. 277, no. 52, pp. 50828–33, Dec. 2002.

[130] M. Dohadwala, S.-C. Yang, J. Luo, S. Sharma, R. K. Batra, M. Huang, Y. Lin, L. Goodglick, K. Krysan, M. C. Fishbein, L. Hong, C. Lai, R. B. Cameron, R. M. Gemmill, H. a Drabkin, and S. M. Dubinett, "Cyclooxygenase-2-dependent regulation of E-cadherin: prostaglandin E(2) induces transcriptional repressors ZEB1 and snail in non-small cell lung cancer.," Cancer research, vol. 66, no. 10, pp. 5338–45, May 2006.

[131] R. A. and D. K. H Rajabi, M Alam, H Takahashi, A Kharbanda, M Guha, "MUC1-C oncoprotein activates ZEB1/miR-200c regulatory loop and epithelial-mesenchymal transition," Oncogene, 2013.

[132] D. Dixon, "Dysregulated post-transcriptional control of COX-2 gene expression in cancer," Current pharmaceutical design, pp. 635–646, 2004.

[133] N. A. P. and Huan-Ching Chuang1, Adel Kardosh2, Kevin J Gaffney3, A. H. Schönthal*2, H.-C. Chuang, A. Kardosh, K. J. Gaffney, N. a Petasis, and A. H. Schönthal, "COX-2 inhibition is neither necessary nor sufficient for celecoxib to suppress tumor cell proliferation and focus formation in vitro," Molecular cancer, vol. 38, no. 7, p. 38, Jan. 2008.

[134] M. M. Yoshida S, Amano H, Hayashi I, Kitasato H, Kamata M, Inukai M, Yoshimura H, "COX-2/VEGF-dependent facilitation of tumor-associated angiogenesis and tumor growth in vivo.," Laboratory investigation; a journal of technical methods and pathology, vol. 83, no. 10, pp. 1385–94., 2003.

[135] H. Liu, Y. Yang, J. Xiao, and Y. Lv, "COX-2-Mediated Regulation of VEGF-C in Association With Lymphangiogenesis and Lymph Node Metastasis in Lung Cancer," The Anatomical …, vol. 1846, no. July, pp. 1838–1846, 2010.

[136] E. R. and G. A. FitzGerald, "Prostaglandins and Inflammation," Arteriosclerosis, thrombosis and vascular biology, vol. 31, pp. 986–1000, 2011.

[137] F. S. Rundhaug JE, Simper MS, Surh I, "The role of the EP receptors for prostaglandin E2 in skin and skin cancer.," Cancer metastasis reviews, vol. 30, pp. 465–480, 2011.

[138] R. M. Garavito and D. L. , DeWitt, "The cyclooxygenase isoforms: structural insights into the conversion of arachidonic acid to prostaglandins," Biochemica et Biophysica Acta, vol. 1441, no. 2, pp. 278–287, 1999.

[139] "http://dailymed.nlm.nih.gov/dailymed/archives/fdaDrugInfo.cfm?archiveid=6868. ".

[140] L. . Rahimi RA, "A tale of two responses," ournal of Cellular Biochemistry, vol. 102, pp. 593–608.

[141] J. Song, "EMT or apoptosis: a decision for TGF-beta.," Cell research, vol. 17, no. 4, pp. 289–90, Apr. 2007.

[142] carl-H. H. and A. M. Ulrich Valcourt, M.K., Hideki Niimi, "TGF-β and the Smad signaling pathway support transcription reprogramming during epithelial-mesenchymal cell transition," Molecular Biology of Cell, vol. 16, no. 4, pp. 1987–2002, 2005.

[143] and R. D. Akhurst, Rosemary J., "TGF-B Signaling in Cancer- a Double-edged Sword," Trends in Cell Biology, vol. 11, no. 11, pp. 44–51, 2001.

[144] "TGFβ signalling: a complex web in cancer progression," Nature reviews. Cancer, vol. 10, no. 6, pp. 415–424, 2010.

[145] B. E. Zavadil J, "TGFβ and epithelial-to-mesenchymal transitions," Oncogene, vol. 24, no. 37, pp. 5764–74, 2005.

[146] L. E. Rahimi RA, "TGF-beta signaling: a tale of two responses.," Journal of cellular biochemistry, vol. 102, no. 3, pp. 593–608, 2007.

[147] L. J. KLEINSMITH, PRINCIPLES OF CANCER BIOLOGY. 2005.

[148] Y. E. Zhang, "Non-Smad pathways in TGF-beta signaling.," Cell research, vol. 19, no. 1, pp. 128–39, Jan. 2009.

[149] X.-F. W. Xing Guo, "Signaling cross-talk between TGF-β/BMP and other pathways," Cell Research, vol. 19, pp. 71–88, 2009.

[150] J. Massagué, "TGFβ in Cancer," Cell, vol. 134, no. 2, pp. 215–30, 2008.

[151] S. M. and T. M. Iwata Ozaki1, Hiroshi Hamajima, "Regulation of TGF-β1-induced pro-apoptotic signaling by growth factor receptors and extracellular matrix receptor integrins in the liver," Frontiers in physiology, vol. 2, 2011.

[152] C. C. Mackey JR, Mani RS, Selner M, Mowles D, Young JD, Belt JA, Crawford CR, "Functional nucleoside transporters are required for gemcitabine influx and

manifestation of toxicity in cancer cell lines.," Cancer research, vol. 58, no. 19, pp. 4349–57, 1998.

[153] M. Dean, T. Fojo, and S. Bates, "Tumour stem cells and drug resistance.," Nature reviews. Cancer, vol. 5, no. 4, pp. 275–84, May 2005.

[154] E. G. Pham H, Ekaterina Rodriguez C, Donald GW, Hertzer KM, Jung XS, Chang HH, Moro A, Reber HA, Hines OJ, "miR-143 decreases COX-2 mRNA stability and expression in pancreatic cancer cells.," Biochemical Biochemical research communication, vol. 439, no. 1, pp. 6–11, 2013.

[155] A. T. Zhongxin Lu, Yan Li,, J. Z. Benhui Li, K. H. Y. Daniel J Conklin, and R. M. and Y. Li1, "miR-301a as an NF-jB activator in pancreatic cancer cells," The EMBO Journal, vol. 30, pp. 57–67, 2011.

[156] S. Ramasamy, S. Duraisamy, S. Barbashov, T. Kawano, S. Kharbanda, and D. Kufe, "The MUC1 and galectin-3 oncoproteins function in a microRNA-dependent regulatory loop.," Molecular cell, vol. 27, no. 6, pp. 992–1004, Sep. 2007.

[157] K. D. Raina D, Ahmad R, Rajabi H, Panchamoorthy G, Kharbanda S, "Targeting cysteine-mediated dimerization of the MUC1-C oncoprotein in human cancer cells.," Oncology, International Journal of, vol. 40, no. 5, pp. 1643–9, 2012.

[158] L. Y. and D. Kufe, "MUC1-C Oncoprotein Blocks Terminal Differentiation of Chronic Myelogenous Leukemia Cells by a ROS-Mediated Mechanism," Genes and Cancer, vol. 2, no. 1, pp. 56–64, 2011.

[159] "http://clinicaltrials.gov/show/NCT01279603," 2013.
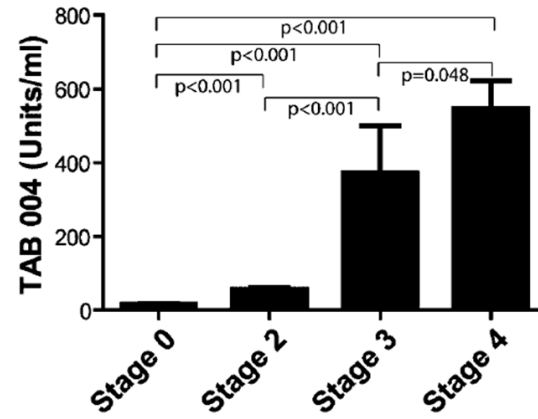
APPENDIX A: FIGURE

Figure1: MUC1 ELISA showing levels of MUC1 in the serum of PC patients at different stages of the disease.

APPENDIX B: DENSITOMETRIC ANALYSIS

Supplemental Table 1. Densitometric analysis of MUC1 and β-actin levels in MUC1 siRNA treated Capan-1 cell line using Image J software (Figure 1C).						
Samples	**MUC1**			**β-actin**		
	Area	**Mean**	**Adjusted mean**	**Area**	**Mean**	**Adjusted mean**
Capan-1 WT	0.08	35.09	35.09	0.03	119.16	1.00
Capan-1 Ctrl siRNA	0.08	40.10	46.26	0.03	103.31	1.15
Capan-1 MUC1 siRNA	0.08	3.63	3.66	0.03	118.16	1.01
% expression after knockdown			10.43			

Supplemental Table 2. Densitometric analysis of MUC1 and β-actin levels in KCKO and KCM cell lines using Image J software (Figure 2A).						
Samples	**MUC1**			**β-actin**		
	Area	**Mean**	**Adjusted mean**	**Area**	**Mean**	**Adjusted mean**
KCKO	0.11	15.36	19.40	0.02	98.10	1.26
KCM	0.11	141.88	141.88	0.02	123.94	1.00

Supplemental Table 3. Densitometric analysis of MUC1 and β-actin levels in BxPC3 Neo and BxPC3 MUC1 cell lines using Image J software (Figure 3A).						
Samples	**MUC1**			**β-actin**		
	Area	**Mean**	**Adjusted mean**	**Area**	**Mean**	**Adjusted mean**
BxPC3 Neo	0.11	0.00	0.00	0.04	119.80	1.1
BxPC3 MUC1	0.11	97.01	97.01	0.04	129.61	1.0

Supplemental Table 4. Densitometric analysis of MRP1 and β-actin levels in BxPC3 Neo and BxPC3 MUC1 tumor lysate using Image J software (Figure 4B).						
Samples	**MRP1**			**β-actin**		
	Area	**Mean**	**Adjusted mean**	**Area**	**Mean**	**Adjusted mean**
KCKO	0.08	42.01	42.01	0.06	110.39	1.00
KCM	0.08	124.33	125.39	0.06	109.46	1.01
BxPC3 Neo	0.09	54.00	58.96	0.06	96.57	1.09
BxPC3 MUC1	0.09	144.24	144.24	0.06	105.44	1.00

Supplemental Table 5. Densitometric analysis of MUC1 expression in BxPC3 Neo and BxPC3 MUC1 tumor lysate using Image J software (Figure 4D).

Samples	MUC1			MRP1			β-actin		
	Area	Mean	Adjusted mean	Area	Mean	Adjusted mean	Area	Mean	Adjusted mean
BxPC3 Neo sample #1	0.224	62.521	76.3	0.061	80.36	98.07	0.061	127.1	1.22
BxPC3 Neo sample #2	0.224	70.731	73.2	0.061	81.45	84.26	0.061	149.9	1.03
BxPC3 MUC1 sample #4	0.224	141.456	141.5	0.061	99.34	99.34	0.061	155.1	1.00

Supplemental Table 6. Densitometric analysis of phospho Akt and total Akt levels in cell lines using image J software (Figure 5A).

Samples	phospho-Akt			Akt			β-actin				MUC1+ve/MUC1 -ve
	Area	Mean	Adjusted mean	Area	Mean	Adjusted mean	Area	Mean	Adjusted mean	phospho Akt/total Akt	phospho Akt/total Akt
KCKO	0.03	66.8	70.2	0.0	117.9	124.0	0.0	158.3	1.1	0.6	
KCM	0.03	120.5	120.5	0.0	113.2	113.2	0.0	166.4	1.0	1.1	1.9
BxPC3 Neo	0.04	72.5	77.3	0.0	145.2	154.8	0.0	141.6	1.1	0.5	
BxPC3 MUC1	0.04	154.0	156.8	0.0	164.3	167.3	0.0	148.3	1.0	0.9	1.9

Supplemental Table 7. Densitometric analysis of total Akt, MRP1, MUC1 and β-actin levels in Akt siRNA treated Capan-1 cells using image J software (Figure 5 B).

Samples	Akt		MRP1		MUC1		β-actin	
	Mean	Adjusted mean	Mean	Adjusted mean	Mean	Adjusted mean	Mean	Adjusted mean
Capan-1 WT	131.4	131.4	194.8	194.8	75.7	75.7	161.1	1.0
Capan-1 Ctrl siRNA	133.6	139.5	100.4	104.9	65.0	67.9	154.3	1.0
Capan-1 Akt siRNA	94.3	80.1	35.6	35.9	23.4	23.5	160.1	1.0
% expression after kncokdown		61.0						
Fold change				5.4		3.2		

Supplemental Table 8. Densitometric analysis of total Akt, MRP1, MUC1 and β-actin levels in Akt siRNA treated BxPC3 cells using image J (Figure 5 C).

Samples	Akt		MRP1		MUC1		β-actin	
	Mean	Adjusted mean	Mean	Adjusted mean	Mean	Adjusted mean	Mean	Adjusted mean
BxPC3 Neo WT	149.0	166.4	83.943	93.7	4.998	5.6	90.157	1.1
BxPC3 MUC1 WT	125.6	176.5	137.408	193.1	124.328	174.7	71.64	1.4
BxPC3 MUC1 Ctrl siRNA	114.2	139.9	112.779	138.2	87.616	107.4	82.154	1.2

BxPC3 MUC1 Akt siRNA	86.5	86.5	41.376	41.4	71.432	71.4	100.667	1.0
% expression after kncokdown		49.02						
Fold change				4.67		2.45		

Supplemental Table 9. Densitometric analysis of total Akt, MRP1, MUC1 and β-actin levels in KCKO cells and Akt siRNA treated KCM cells using image J (Figure 5D).

Samples	Akt		MRP1		MUC1		β-actin	
	Mean	Adjusted mean	Mean	Adjusted mean	Mean	Adjusted mean	Mean	Adjusted mean
KCKO WT	93.9	117.3	56.9	71.0	0.0	0.0	82.5	1.2
KCM WT	79.2	81.4	93.6	96.3	132.1	135.8	100.3	1.0
KCM Ctrl siRNA	80.2	89.0	84.8	94.1	135.6	150.5	92.9	1.1
KCM Akt siRNA	22.9	22.9	81.6	81.6	115.9	115.9	103.1	1.0
% expression after kncokdown		28.159						
Fold change				1.18		1.17		

Supplemental Table 10. Densitometric analysis of the PCR product following ChIP assay in Capan-1 cells (Figure 6C).

ChIP region I	Area	Arbitary units	Fold enrichment (CT2 DNA/ IgG DNA)
Capan-1 Input	5472	242	
Capan-1 IgG	5472	19	
Capan-1 CT2	5472	124	6.5
ChIP region II	**Area**	**Arbitary units**	**Fold enrichment (CT2 DNA/ IgG DNA)**
Capan-1 Input	4300	240	
Capan-1 IgG	4300	46	
Capan-1 CT2	4300	16	0.3

Supplemental Table 11. Densitometric analysis of the PCR product following ChIP assay in KCKO and KCM cells (Figure 6C).

ChIP region I	Area	Arbitary units	Fold enrichment (CT2 DNA/ IgG DNA)
KCKO Input	840	185	
KCKO IgG	840	43	
KCKO CT2	840	29	0.7

KCM Input	0.11	152	
KCM IgG	0.11	40	
KCM CT2	0.11	128	3.2
ChIP region II	**Area**	**Arbitary units**	**Fold enrichment (CT2 DNA/ IgG DNA)**
KCKO Input	406	85	
KCKO IgG	406	27	
KCKO CT2	406	20	0.7
KCM Input	0.08	141	
KCM IgG	0.08	35	
KCM CT2	0.08	25	0.7

Supplemental Table 12. Densitometric analysis of the PCR product following ChIP assay in BxPC3 Neo and BxPC3 MUC1 cells (Figure 6C).			
ChIP region I	**Area**	**Arbitary units**	**Fold enrichment (CT2 DNA/ IgG DNA)**
BxPC3 Input	0.03	123.3	
BxPC3 IgG	0.03	96.1	
BxPC3 CT2	0.03	108.4	1.1
BxPC3 Input	0.03	212.6	
BxPC3 IgG	0.03	93.3	
BxPC3 CT2	0.03	101.7	1.1
ChIP region II	**Area**	**Arbitary units**	**Fold enrichment (Chip/Input DNA)**
BxPC3 Input	0.03	95.1	
BxPC3 IgG	0.03	83.9	
BxPC3 CT2	0.03	85.3	1.0
BxPC3 Input	0.03	98.6	
BxPC3 IgG	0.03	80.5	
BxPC3 CT2	0.03	79.7	1.0

Supplemental table 13: Densitomectric analysis of figure 3.9B. Cox-2 expression following MUC1 overexpression in BxPC3 and Panc02 cells and MUC1 knockdown in KCKO cells.									
	MUC1			**Cox-2**			**b-actin**		
	Area	Mean	Adjusted mean	Area	Mean	Adjusted mean	Area	Mean	Adjusted mean
BxPC3 Neo	0.1	2.9	2.9	0.1	27.4	27.4	0.0	85.6	1.0
BxPC3 MUC1	0.1	87.5	90.4	0.1	87.4	90.3	0.0	82.8	1.0
Fold increase			31.0			3.3			
Panc02 Neo	0.1	15.3	19.1	0.0	21.9	27.4	0.0	95.9	1.2
Panc02 MUC1	0.1	91.8	91.8	0.0	71.5	71.5	0.0	119.7	1.0
Fold increase			4.8			2.6			
KCKO	0.1	5.2	8.6	0.0	11.5	19.3	0.0	57.1	1.7

KCM	0.1	88.3	88.3	0.0	74.4	74.4	0.0	95.4	1.0
Fold increase			10.2			3.9			

Supplemental table 14: Densitomectric analysis of figure 3.9C. Cox-2 expression following MUC1 knockdown in HPAFII and HPAC cells									
	MUC1			**Cox-2**			**b-actin**		
	Area	**Mean**	**Adjusted mean**	**Area**	**Mean**	**Adjusted mean**	**Area**	**Mean**	**Adjusted mean**
HPAFII WT	0.1	106.3	116.4	0.0	60.2	65.9	0.1	103.4	1.1
HPAFII Ctrl siRNA	0.1	100.3	128.2	0.0	64.0	81.8	0.1	88.6	1.3
HPAFII MUC1 siRNA	0.1	10.7	10.7	0.0	18.9	18.8	0.1	113.2	1.0
Fold decrease			10.9			3.5			
HPAC WT	0.1	121.0	121.0	0.0	76.4	76.4	0.1	107.3	1.0
HPAC Ctrl siRNA	0.1	98.3	102.0	0.0	72.6	75.4	0.1	103.4	1.0
HPAC MUC1 siRNA	0.1	19.3	20.7	0.0	12.2	13.1	0.1	99.8	1.1
Fold decrease			5.8			5.8			

Supplemental table 15: Densitometric analysis of figure 3.10 A. Level of Cox-2 mRNA evaluated by semi-quantitative RT-PCR.						
	Cox-2 mRNA			**GAPDH2/Gapdh2**		
Cell Lines	**Area**	**Mean**	**Adjusted mean**	**Area**	**Mean**	**Adjusted mean**
BxPC3 Neo	0.02	125.6	143.1	0.02	112.6	1.1
BxPC3 MUC1	0.02	135.2	135.2	0.02	128.2	1.0
Fold difference			1.06			
Panc02 Neo	0.021	151.7	160.96	0.025	205.1	1.1
Panc02 MUC1	0.021	189.2	189.21	0.025	217.6	1.0
Fold difference			1.2			
KCKO	1326	92.08	119.38	1030	154.4	1.30
KCM	1326	178.9	178.93	1030	200.2	1.00
Fold difference			1.5			
HPAF WT	0.085	197.9	204.1	0.147	206.1	1.0
HPAC Ctrl siRNA	0.085	235.3	235.3	0.147	212.6	1.0
HPAC MUC1 siRNA	0.085	12.35	14.7	0.147	178.8	1.2
Fold difference			13.9			

Supplemental table 16: Densitometric analysis of figure 3.11A. Nuclear localization of MUC1 CT and NF-kB in cells.									
	NFkB			**MUC1 CT**			**Lamin A/c**		
Cell Lines	**Area**	**Mean**	**Adjusted mean**	**Area**	**Mean**	**Adjusted mean**	**Area**	**Mean**	**Adjusted mean**
Panc02 Neo	0.03	78.9	78.8	0.14	0.1	0.1	0.1	43.0	1.0
Panc02 MUC1	0.03	55.8	68.6	0.14	121.4	149.2	0.1	35.0	1.2
Fold difference			1.1			1254			
KCKO	0.024	222.2	222.2	0.14	2.1	2.1	0.155	63.572	1.0
KCM	0.024	170.8	234.7	0.14	69.9	96.1	0.155	46.262	1.4
Fold difference			0.9			45.4			

Supplemental table 17: Densitometric analysis of figure 3.11C. ChIP data			
Cell Lines	**Area**	**Mean**	**Fold enrichment**
Panc02 Neo Input	0.04	107	
Panc02 Neo IgG	0.04	0	
Panc02 Neo CT2	0.04	0	
Panc02 Neo NF-kB	0.04	1	
Panc02 MUC1 Input	0.04	177.4	
Panc02 MUC1 IgG	0.04	0	
Panc02 MUC1 CT2	0.04	97.8	
Panc02 MUC1 NF-kB	0.04	59.6	
KCKO Input	1290	197.3	
KCKO IgG	1290	1.527	
KCKO CT2	1290	0.626	
KCKO NF-kB	1290	0.153	
KCM Input	0.243	176.4	
KCM IgG	0.243	18.52	
KCM CT2	0.243	135.9	7.34
KCM NF-kB	0.243	109.6	5.92
HPAFII Input	1672	191.5	
HPAFII IgG	1672	57.01	
HPAFII CT2	1672	125.6	2.2
HPAFII NFkB	1672	129.8	2.3